Alma Mater Studiorum – Università di Bologna

DOTTORATO DI RICERCA IN

ONCOLOGIA E PATOLOGIA SPERIMENTALE

XXIX Ciclo

Settore Concorsuale di afferenza: 06/A2
Settore Scientifico disciplinare: MED/04

DEVELOPMENT OF PRECLINICAL MODELS OF MAMMARY CARCINOGENESIS: FUNCTIONAL ROLE OF HER2 AND ITS ISOFORMS IN TUMOR PROGRESSION AND IN DRUG RESISTANCE

Presentata da Dott.ssa Roberta Laranga

Coordinatore Dottorato	Relatore
Chiar.mo Prof. Pier-Luigi Lollini	Chiar.mo Prof. Pier-Luigi Lollini

Esame finale anno 2017

CONTENTS

INTRODUCTION

1. Breast Cancer: Clinical, Pathological and Molecular aspects

Breast cancer is the most common cancer and the second leading cause of cancer death in women (Siegel et al., 2015) despite significant improvements in survival over the past 25 years. It is estimated that in 2016, close to 246.000 new cases will be diagnosed and over 40.000 women will die from the disease in the USA (Siegel et al., 2015). One of the greatest challenges faced by clinicians and researchers in this field is that breast cancer is not a single entity, but rather a heterogeneous group of several subtypes displaying distinct differences in biological and clinical behavior (Dawson et al., 2013). This heterogeneity is visible at the histological, clinical, genetic and genomic level.

1.1 Classification of breast cancer

The classification of invasive breast cancer currently involves the assessment of histological criteria including both morphology-based and immunohistochemical (IHC) analysis. The vast majority of breast carcinomas (~70–80%) are described as "invasive ductal carcinomas not otherwise specified" (IDC-NOS) based on architectural patterns and cytological features. In contrast, around 15% of breast cancers are lobular (Ellis., 2003). In addition to histological tumor type, tumor grade is the other important intrinsic characteristic that can be assessed by histopathological analysis. Tumor grade is an assessment of differentiation (tubule formation and nuclear pleomorphism) and proliferative activity (mitotic index), allowing tumors to be further stratified and providing key prognostic information (Rakha et al., 2010).

Traditional pathological parameters such as histological type, tumor size, histological grade and axillary lymph-node involvement have been shown to correlate with clinical outcome and provide the basis for prognostic evaluation (Elston et al., 1999). IHC markers such as the expression of hormone receptors (estrogen (ER) and progesterone receptors (PR)) and the overexpression and/or amplification of the human epidermal growth factor receptor 2 (HER2) provide additional therapeutic predictive value and are of key importance in guiding treatment selection (Harris et al., 2007). Hormone receptor-positive breast cancers account for around 75–80% of all cases. Standardized IHC assays for the routine testing of ER and PR are

used to guide the selection of patients for hormonal-based therapies. HER2 represents the only additional predictive marker currently in routine use. Approximately 10–15% of breast cancers displays HER2 overexpression and/or amplification with around half of these tumors co-expressing hormone receptors (Konecny et al., 2003). The remaining 10–15% of breast cancers are defined by hormone receptor and HER2 negativity (i.e., triple negative cancers), which represent a key clinical entity given their lack of therapeutic options (Dawson et al., 2009).

While the current classification of human breast tumors has been fundamental for prognostic and predictive evaluation, a number of important limitations remains. First, considerable variation in response to therapy and clinical outcome still exists, even for tumors with apparent similarities in clinical and pathological characteristics. Second, this classification continues to provide limited insight into the complex underlying biology and the molecular pathways driving the disease in different subtypes. Recently, rapid progress has been made in understanding the genomic diversity of breast cancer. These advances led to the characterization of a new genome-driven integrated classification of breast cancer, which substantially refines the existing classification systems currently used. Genomic studies identified five intrinsic subtypes of breast cancer: luminal A, luminal B, basal like, HER2-enriched and triple positive.

Luminal tumors are the most common subtypes among breast cancer, with luminal A being the majority, representing the 50%-60% of all breast cancer (Yersal and Barutca, 2014). At the RNA and protein level, Luminal A and B subtypes are largely distinguished by the expression of two main biological processes: proliferation/cell cycle-related and luminal/hormone regulated pathways. Luminal A subtype is defined as ER-positive and/or PR-positive tumors with negative HER2 and low Ki67 (proliferating cell nuclear antigen) index by immunohistochemistry (Carey et al., 2006). Luminal B tumors comprise 15%-20% of breast cancers (Creighton et al., 2012). From the immunohistochemical point of view are defined as ER-positive, HER2-negative and Ki67 high or ER and HER-2 positive tumors (Yersal and Barutca, 2014). This subtype has a higher recurrence rate and lower survival rates after relapse compared to Luminal A subtype (Ellis et al., 2008).

Luminal tumors respond well to hormone therapy but poorly to conventional chemotherapy (Brenton et al., 2005). Treatment response differs between luminal subtypes. Thus, Luminal A tumors could be adequately treated with endocrine therapy, while Luminal B tumors which

are more proliferative may benefit more from the combination of chemotherapy and hormonal treatment. Other targeted approaches such as anti-angiogenic strategies were suggested to be effective for luminal tumors as well. For example, the anti-VEGF antibody, bevacizumab, was shown to improve progression free survival when combined with neoadiuvant chemotherapy in metastatic breast cancer (Makhoul et al., 2015).

HER2-positive cancer accounts for 15-20% of breast tumors. HER2 positivity confers more aggressive biological and clinical behavior. These tumors are characterized by high expression of the HER2 gene and other genes associated with the HER2 pathway and/or HER2 amplicon located in the 17q12 chromosome. Morphologically, these tumors are highly proliferative, 75% have a high histological and nuclear grade and more than 40% have p53 mutations (Yersal and Barutca, 2014). Nearly half of HER2-positive breast cancers are positive for ER but they generally express low ER levels. In the absence of treatment, HER2-positive tumors have a poor prognosis. They have increased sensitivity to certain cytotoxic agents such as doxorubicin, relative resistance to hormonal agents and a propensity to metastasize to the brain and visceral organs. Advances in translational science have led to the development of a large spectrum of HER2 directed therapies, e.g. trastuzumab (Prat et al., 2014; Vici et al., 2015).

Overall, ER-positive breast cancers are classified as luminal cancers, but these cancers are further subclassified based on their HER2 status and proliferation rate into the ER positive/PgR positive/HER2 positive (‘‘triple positive’’) and ER positive/PgR positive/HER2 negative subtypes. HER2 triple positive comprise 10% of breast cancers and have a worst prognosis compared to the ER positive/PgR positive/HER2 negative subtype (Dowsett et al., 2008; De Laurentiis et al., 2005; Lipton et al., 2002). Preclinical evidence seems to confirm that cross-talks between HER2 and ER signalling pathways may contribute to resistance to endocrine therapy (Osborne et al., 2004; Vici et al., 2015).

The basal subtype is composed of triple negative (ER-PR-HER2-) tumors with expression profiles mimicking that of the basal epithelial cells of other parts of the body and normal breast myoepithelial cells (Perou et al., 2000). Such expression patterns include lacking or low expression of hormone receptors and HER2, and high expression of basal markers (such as keratins 5, 6, 14, 17, EGFR) and proliferation related genes (Perou et al., 2000). These tumors are of particular interest because they follow aggressive clinical course and currently lack any form of standard targeted systemic therapy. Basal tumors are

associated with a lower disease-specific survival and a higher risk of local and regional relapse. The metastasis pattern also separates basal tumors from the other breast cancers, with a tendency towards visceral organs (excluding bone) and less likely to lymph nodes (Ho-Yen et al., 2012).

1.2 HER2-positive breast cancer

1.2.1 Role and function of EGFR/Erb-B receptors

The Erbb family consists of four closely related type 1 transmembrane tyrosine kinase receptors: epidermal growth factor receptor (EGFR; also known as HER1), ERBB2 (HER2), ERBB3 (HER3) and ERBB4 (HER4) (Figure 1). Each receptor comprises an extracellular domain at which ligand binding occurs, an α-helical transmembrane segment and an intracellular protein tyrosine kinase domain (Olayioye et al. 2000). Receptor dimerization is an essential requirement for Erbb function and for the signalling activity of these receptors (Olayioye et al., 2000; Ferguson et al. 2003). Dimerization can occur between two different Erbb receptors (heterodimerization) or between two molecules of the same receptor (homodimerization) (Cho et al., 2002; Burgess et al. 2003) (Figure 1). The ERBB receptors are expressed in various tissues of epithelial, mesenchymal and neuronal origin. Under normal physiological conditions, activation of the ERBB receptors is controlled by the spatial and temporal expression of their ligands, which are members of the epidermal growth factor (EGF) family of growth factors (Hynes & Lane 2005). EGF is the prototype of a family of ligands that include the transforming growth factor-alpha (TGF-α), which binds to HER1, and heregulin (HRG), which binds to HER3 and HER4. None of the EGF family peptides bind HER2, which is present in a constitutive active form. Ligand binding to the extracellular domain initiates a conformational rearrangement, exposing the dimerization domain that forms the core of the dimer interface with another receptor (Figure 1) (Ogiso et al., 2002). After receptor dimerization, transactivation of the tyrosine kinase portion of the dimer occurs as each receptor activates its partner by phosphorylation. The phosphorylation event allows the recruitment and activation of downstream proteins and a signalling cascade is initiated (Mendelsohn & Baselga, 2003; Baselga & Swine, 2009).

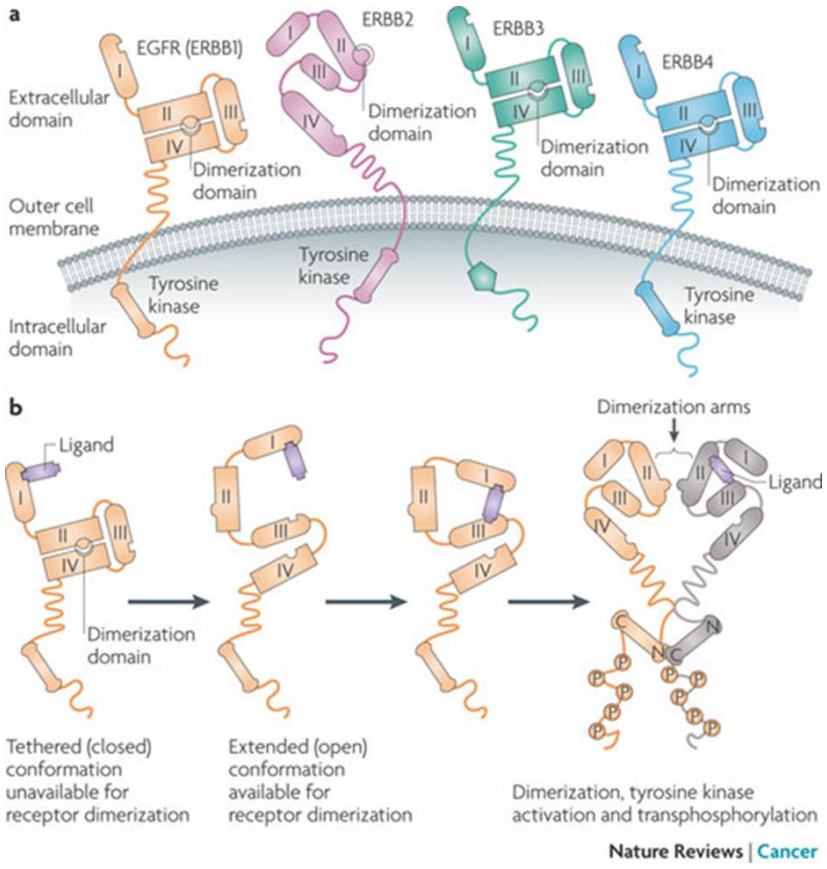

Figure 1: EGFR/Erb-B receptors: a) the four members of the Erbb family with their three functional domains. b) Ligand binding to Erbb receptors conformational change and activation of the molecule. Image from Baselga & Swain, Nat Rev Cancer 2009.

Activated ERBBs stimulate many intracellular signalling pathways and, despite extensive overlap in the molecules that are recruited to the different active receptors, different ERBBs preferentially modulate certain signalling pathways, owing to the ability of individual ERBBs to bind specific effector proteins (Hynes & Lane 2005). Two of the main pathways activated by the receptors are the mitogen-activated protein kinase (MAPK) and the phosphatidylinositol 3-kinase (PI3K–AKT) pathways (Yarden & Sliwkowski, 2001, Schlessinger, 2004). Other important ERBB signalling effectors are the signal transducer and activator of transcription proteins (Yu & Jove, 2004), which, in cancer, have often been associated with EGFR activation; SRC tyrosine kinase, the activity of which is increased in response to EGFR and ERBB2 signalling (Ishizawar & Parsons, 2004); and mammalian target of rapamycin (mTOR), a serine/threonine kinase activated downstream of PI3K–AKT and other growth regulators (Bjornsti & Houghton, 2004) (Figure 2).

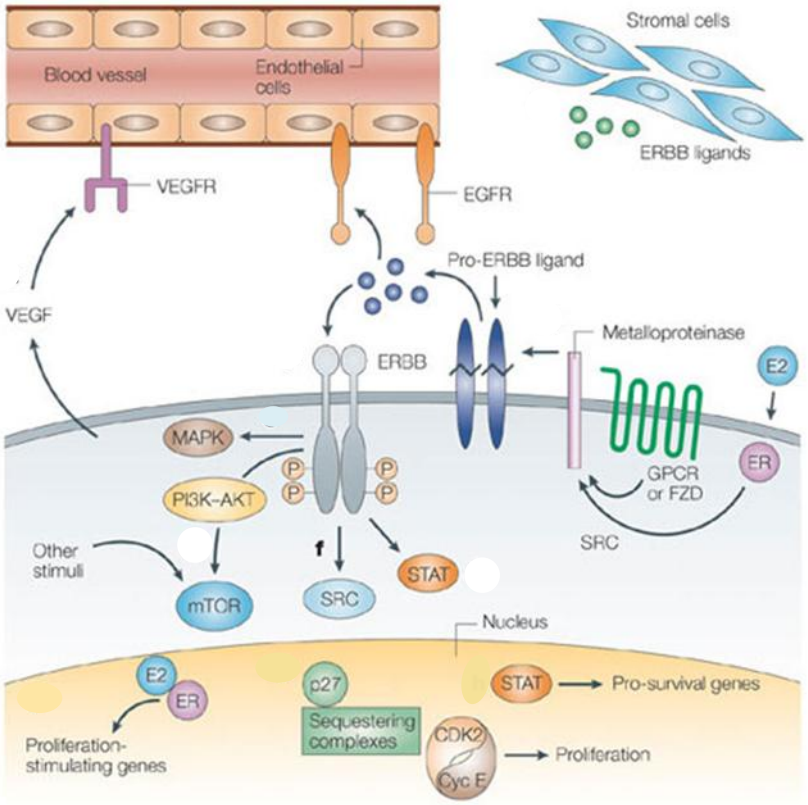

Figure 2: Active ERBB receptors and downstream signalling pathways in a tumor setting. Figure adapted from Hynes & Lane 2005.

The specificity and potency of this multi-layered signalling network depend on the composition of ligands (at least 12) and monomers (input layer), along with the variety of intracellular effectors and regulators (signal-processing layers). The physiological outputs consist of cell division, migration, adhesion, differentiation and apoptosis. Ligand-mediated receptor endocytosis allows the turning off of the signalling network (Yarden and Sliwkowski, 2001).

1.2.2 HER2-driven neoplastic transformation

Deregulation of Erbb signalling pathways has been described in many cancers, including breast, linked to a multiplicity of molecular and epigenetic mechanisms, activating mutations of the receptors themselves or activation induced by autocrine/paracrine ligands (Eccles 2011).

HER2 is a 185 kDa transmembrane receptor tyrosine kinase, codificated by the proto-oncogene ERBB2 located on chromosome 17q12. Although HER2 does not bind any ligand, because of the

constitutive exposure of its dimerization domain, it is the preferred partner for heterodimerization. In fact, some authors consider HER2 as an amplifier of the HER receptor pathway rather than a bona fide receptor (Citri and Yarden 2006).

Overexpression of the HER2 protein, either through gene amplification or through transcriptional deregulation, has been reported in 15-20% of human breast cancers (Wolf et al., 2013), as well as in subsets of patients with ovarian cancers (Marinas et al., 2012; English et al., 2013), gastric carcinoma (Ahmadi et al., 2011) and salivary gland tumours (Cornolti et al., 2007). In addition, other potential mechanisms might be responsible for increased HER2 levels, e.g. the absence or mutation of FOXP3, an X-linked tumor suppressor gene that maintains low levels of HER2 (Zuo et al., 2007). HER2 might also be aberrantly activated by acquired mutations, similarly to EGFR, in a small proportion of non-small cell lung tumours (Cappuzzo et al. 2006; Wang et al. 2006, Swanton et al, 2006; Yamamoto et al, 2014). Regardless of the causative mechanism, HER2 overexpression in conditions in which the number of HER2 molecules expressed on the surface of tumor cells far exceeds that on normal cells, facilitates the formation of heterodimers and the spontaneous formation of HER2 homodimers (Yarden & Sliwkowsk, 2001; Lv et al., 2016).

Breast cancers can have up to 25-50 copies of the HER2 gene and up to 40-100 fold increase in HER2 protein expression resulting in up to 2 million receptors expressed at the tumor cell surface (Kallioniemi et al. 1992; Wolff et al., 2013); consequently, an excess of HER2-mediated signalling occurs driving oncogenic cell survival and proliferation.

To further complicate this signalling network, other membrane receptors, such as insulin-like growth factor 1 receptor (IGF-1R) (Nahta et al., 2005) and MET (Maroun & Rowlands, 2014), have been shown to dimerize with HER2 receptor and activate the phosphorylation cascade. In addition, ER can activate HER2 signalling when bound by estrogen (Schiff et al., 2004). Finally, alterations in signalling molecules downstream of the receptors can activate the pathway, including reduced levels of the tumor suppressor genes INPP4-B (for inositol polyphosphate-4-phosphatase, type II) and PTEN (phosphatase and tensin homolog) which normally inactivate PI3K, or activating mutations in PIK3CA (for phosphatidylinositor-4,5-bisphosphate 3-kinase), the gene that encodes the catalytic subunit of PI3K (The Cancer Genome Atlas Network, 2012; Berns et al., 2007).

With four receptors, multiple ligands, several feedback loops in the MAPK and PI3K pathways, and multiple levels of control, the Erbb network, like a robust electronic circuit, is

complex, redundant, capable of fine tuning, adaptable, and difficult to block completely (Citri & Yarden, 2006).

2. Therapies targeting HER2-positive breast cancer

HER2 crucial role in tumor growth and progression makes HER2 a prototypic oncoantigen, the targeting of which may be critical for the development of effective anticancer therapies (Lollini et al., 2006).

First, HER2 overexpression has been defined by immunohistochemistry as being high (reported as 3+) when receptor levels approach 2 million, or of medium intensity (2+) when receptor levels are approximately 500.000, compared to normal levels of HER2 membrane-bound receptor, reported to be 20.000 per cell (Ross JS et al., 2004). Second, elevated HER2 levels strongly correlate with the pathogenesis and prognosis of breast cancer (Slamon DJ et al., 1987; Slamon DJ et al., 1989) Third, the level of HER2 gene amplification in human cancer cells is much higher than in normal adult tissues; thus, targeting the HER2 protein with HER2-targeted drugs could reduce the pathogenicity caused by HER2 overexpression. Fourth, HER2 protein levels are relatively homogeneous between HER2-overexpressing tumor cells (Eccles, 2001). Tumors with high expression of HER2 (i.e. an IHC score of 3+) often show uniform and intense IHC staining, (Paik et al., 1990) suggesting that anti-HER2 therapy would target most cancer cells in a given patient. Fifth, overexpression of the HER2 protein is found both in the primary tumor and in metastatic sites (Niehans et al., 1993), indicating that anti-HER2 therapy could be effective in all disease locations (Nahta et al., 2006).

2.1 Clinically approved anti-HER2 agents

Growing understanding of the biology and complexity of the HER2 signalling network and of potential resistance mechanisms has guided the development of new HER2-targeted agents. Combination of these drugs to more completely inhibit the HER receptor layer, or combined HER2-targeted agents with compounds that target downstream signalling, alternative pathways, or component of the host immune system, are being vigorously investigated in the preclinical and clinical settings

Trastuzumab

Trastuzumab was the first approved targeted therapy for HER2 positive breast cancer (Herceptin, Genetech Inc., San Francisco). It is a humanized immunoglobulin G1 antibody that binds to an epitope in the juxtamembrane region IV of HER2. The mechanisms by which trastuzumab induces regression of HER2-overexpressing tumors are incompletely defined, but several molecular and cellular effects have been observed in experimental *in vitro* and *in vivo* models (Nahta and Esteva, 2003; Nahta and Esteva, 2006).

Diminished receptor signalling might result from trastuzumab-mediated internalization and degradation of HER2 (Baselga et al. 2001; Sliwkowski et al. 1999). In addition it inhibits basal and activated HER2 extracellular domain cleavage (Molina et al. 2001), and uncouples ligand-independent HER2-containing dimers leading to partial inhibition of downstream signalling (Junttila et al., 2009). Data from *in vivo* experiments and clinical trials indicate that the efficacy of trastuzumab could be partly related to its induction of an immune response. HER2-targeted antibodies, including trastuzumab, have been shown to induce apoptosis in multiple breast cancer cell lines via antibody-dependent cellular cytotoxicity (ADCC) (Gennari et al. 2004; Carter et al. 1992; Cooley et al. 1999; Lewis et al. 1993; Stockmeyer et al. 2003). Natural killer cells, a principal immune cell type involved in ADCC, express the Fc gamma receptor, to which the Fc domain of the trastuzumab IgG1 binds, activating natural-killer-cell-mediated lysis.

HER2-targeted therapy using the humanized monoclonal antibody trastuzumab has significantly improved disease-free and overall survival (DFS and OS) in early stage HER2-positive breast cancer (Slamon, et al., 2001). The efficacy of Trastuzumab was first studied as monotherapy in unselected patients with heavily pretreated metastatic breast cancer. Response rates were not impressive, with 10-15% of patients having a partial response and rare patients with a complete response. On the other hand, a later single-agent trial on untreated patient showed better results (26% of patients with a complete response) (Rimawi et al., 2015). The next generation studies of Trastuzumab in metastatic disease were based on preclinical data showing a synergistic or additive effect with several classes of cytotoxic chemotherapies (Pegram et al., 1999; Pietras et al., 1998). With longer follow-up of these large adjuvant studies, adjuvant trastuzumab treatment continues to make statistically significant improvements in DFS and OS (Goldhirsch et al. 2013).

Pertuzumab

Pertuzumab is a monoclonal antibody, discovered and developed by Genentech, approved in 2012. It can recognize an epitope in the heterodimerization domain II of HER2, thus blocking ligand-induced HER2-HER3 dimerization, resulting in partial inhibition of PI3K/AKT signalling (Agus et al., 2002). Due to the different epitopes targeted by pertuzumab and trastuzumab (Franklin et al., 2004), their combination showed to be effective in preclinical studies (Scheuer et al., 2009) and clinical trials (Baselga et al., 2012; Gianni et al., 2012) and is currently approved for the treatment of patients with HER2 positive breast cancer (Arteaga and Engelman, 2014). Indeed, pertuzumab is administered as an intravenous infusion in combination with trastuzumab and docetaxel as a first line treatment for HER2-positive metastatic breast cancer or as a neoadjuvant therapy (Giordano et al., 2014).

Trastuzumab-derivative of emtansine 1 (T-DM1)

T-DM1 is an antibody-drug conjugate consisting of the monoclonal antibody trastuzumab linked to the cytotoxic agent emtansine (DM1). A molecule of trastuzumab and 3.5 molecules of the compound are linked together by a covalent non-reducible thioether bond. T-DM1 combines trastuzumab mechanism of action to the cytotoxic microtubule-depolymerizing ability of DM1. Hence, after trastuzumab-mediated HER2 binding, the conjugate is internalized and degraded by lysosomes. Then, DM-1 is released in the cytoplasm, causing lysis of HER2-positive cancer cells (Arteaga and Engelman, 2014).

T-DM1 was approved in 2013 specifically for treatment of HER2-positive metastatic breast cancer (mBC) in patients previously treated with trastuzumab and a taxane (Giordano et al., 2014).

Lapatinib

Lapatinib, an orally available small molecule, is a reversible dual inhibitor of EGFR and HER2 (Cameron et al., 2008). Lapatinib binds to the ATP-binding pocket of HER2, thus preventing receptor phosphorylation and subsequent activation of downstream pathways, including PI3K-AKT and MAPK pathways (Arteaga and Engelman, 2014). It is approved in combination with capecitabine for the treatment of advanced HER2 positive breast cancer. Lapatinib greatly improved BC prognosis in recent years after the initial introduction of trastuzumab.

Table 1: Clinically approved anti-HER-2 agents (modified from Arteaga and Engelman, 2014)

Drug	Type of molecule	Mechanism of action	FDA approval
Trastuzumab	humanized IgG_1, binds juxtamembrane domain IV	inhibits ectodomain cleavage and ligand-independent HER-2-containing dimers; ADCC and adaptive immunity to HER-2	1998 (metastatic breast) 2006 (adjuvant early breast) 2010 (advanced gastric)
Lapatinib	small molecule	reversible, ATP-competitive TKI	2006 (advanced breast)
Pertuzumab	humanized IgG1, binds heterodimerization domain II	inhibits ligand-induced HER-2-containing dimers	2012 (metastatic breast) 2013 (neoadjuvant breast)
T-DM1	antibody-drug conjugate	same as Trastuzumab plus inhibition of microtubules and cell lysis (DM-1)	2013 (advanced breast)

2.2 Resistance to current anti-HER2 therapies

HER2-targeted therapies altered the natural history of HER2-positive BC and metastatic BC (MBC) (Cobleigh et al., 1999; Swain et al., 2013). Despite this significant progress, up to 62% of patients treated with neoadjuvant trastuzumab experience disease progression or de novo resistance (Petrelli et al., 2011). BC patients who initially respond to treatment with trastuzumab plus chemotherapy achieve an increase in response of 18% compared with chemotherapy alone; however, acquired resistance will be developed after one year (Slamon et al., 2001).

The underlying mechanisms of resistance to anti-HER2 therapies are not entirely clear, but several mechanisms have been proposed, including heterodimerization between HER2 and other Erbb receptors (Robinson et al., 2006), increased expression of HER and non-HER receptor ligands (Wang et al., 2008; Straussman et al., 2012), a more active signalling through the SRC family kinase (Wheeler et al., 2012). Moreover, molecular heterogeneity could underlie the unresponsiveness to target therapies and foster the development of resistance. Changes in HER2 interactions with trastuzumab or other HER receptor family members often result in (re)activation of the HER receptor layer and consequent potential intrinsic or acquired resistance

to trastuzumab. These changes include genetic and epigenetic alterations in HER2 receptor itself, which have the following results:

1. Truncated forms of HER2 that lack the trastuzumab-binding epitope (p95-HER2 (Arribas et al., 2011);

2. more constitutively activated receptors, like the HER2 extracellular-domain splice variant Delta16 (Castiglioni et al., 2006), or activating mutations in the kinase and the extracellular domains of HER2 (recently described in HER2 negative tumors and in some primary and metastatic HER2+ breast cancers) (Herter-Sprie et al., 2013, The Cancer Genome Atlas Network, 2012, Bose et al., 2013; Prempree and Wongpaksa 2006);

3. loss or increased expression of HER2 (Arteaga et al. 2012).

In addition, increased expression of HER1 (Rimm et al., 2012; Nahta et al. 2009) and HER3 (Nahta et al., 2009), or excess ligands for these receptors (Rexer and Arteaga, 2012), have also been described in the context of trastuzumab resistance.

Resistance to trastuzumab or other single anti-HER2 agents may commonly arise from incomplete inhibition of the HER receptor layer, allowing compensatory activation of the pathway by other Erbb members (Citri & Yarden, 2006). Indeed, a combination of two or three agents with different mechanisms of action that together block all HER1–3 dimers results in a more effective inhibition of the HER pathway and in the eradication of HER2 positive xenografts in mice (Arpino et al 2007; Wang et al., 2011).

Most of these mechanisms of resistance stem from the tumor cells themselves, but studies also highlight a role for the host and tumor microenvironment in resistance. Multiple signalling molecules and pathways implicated in resistance have been thoroughly reviewed recently (Herter-Sprie et al., 2013).

2.2.1 HER2 isoforms

Subgroups of HER2-positive breast tumors express a series of carboxy-terminal fragments of HER2 collectively known as HER2 CTFs or p95HER2 (Arribas et al., 2001). They originate by proteolytic cleavage of the extracellular domain of full-length HER2 or by traduction of HER2 mRNA from internal initiation codons. p95HER2 fragments are able to homodimerize on cell membrane, leading to a much more rapid and acute signal transduction than that driven by HER2-containing dimers. Compared with tumors with undetectable levels of these fragments,

p95HER2-positive tumors have a worse prognosis and tend to be resistant to the treatment with trastuzumab (Scaltriti et al., 2007). However, two recent studies connected CTF expression in human samples of HER2-positive breast cancer to a good trastuzumab response (Scaltriti et al., 2014; Parra-Palau et al., 2014). One of the fragments, 100–115 kDa p95HER2 (also known as 611-CTF), is a constitutively active form of HER2 because of its ability to form dimers maintained by intermolecular disulfide bonds (Pedersen et al., 2009).

During the characterization of the HER2 species recognized by the anti-p95HER2 antibodies under denaturing conditions, Morancho and colleagues observed the existence of the N-terminal fragment of HER2 (H2NTF), expressed at variable levels in 60% of the breast cancer samples analyzed. Characterization of H2NTF showed that even if it lacks the intracellular tyrosine kinase domain it readily interacts with full-length HER2 and other HER receptors. As a consequence, H2NTF acts as a dominant negative, attenuating the signalling triggered by full-length HER receptors (Morancho et al., 2013).

In addition to the truncated isoforms of HER2, a splice variant lacking exon Delta16 was identified in 1998 by Kwong and Hung in human cancer cell lines. In Delta16 isoform, the in-frame deletion of exon 16 (48 bp) determines the lack of 16 aminoacids, including two cysteines, in the juxtamembrane region (Kwong and Hung, 1998). Due to the loss of these cysteine residues, intermolecular disulfide bonds with other monomers are promoted, triggering a stronger signal transduction in respect to HER2 (Castiglioni et al., 2006). Delta16 isoform is present as 8-10% of HER2 transcript amount in half HER2-positive breast cancer patients and in 90% of women with locally disseminated disease (Castiglioni et al., 2006; Mitra et al., 2009).

In vitro studies in MCF-7 and MCF-10A cells transfected with Delta16 showed an increased activation of PI3K-AKT and MAPK pathways, compared to cells transfected with HER2 full-lenght (Mitra et al., 2009; Alajati et al., 2013). Delta16 oncogenic properties are correlated to Src kinase activation. It can interact with Src on cell membrane, activating both PI3K-AKT and MAPK cascades (Mitra et al., 2009). These results obtained *in vitro* were confirmed as well *in vivo*; on Delta16 transgenic mouse models Marchini and colleagues showed that Delta16 constitutively active homodimers are able to trigger a Src-mediated signal transduction (Marchini et al., 2011). Castagnoli and colleagues either on a cell line derived from a tumor of a Delta16 transgenic mouse, or on human HER2-positive breast tumors highlighted the strong correlation between activated Delta16 dimers/monomers and phospho-Src. However, they did not observe Src-dependent activation of PI3K-AKT and MAPK pathways (Castagnoli et

al., 2014). Furthermore, unlike HER2 full-lenght, overexpression of Delta16 in human breast cells evoked mammary tumors and lung metastases when injected into the mammary gland of immunodeficient mice (Alajati et al., 2013).

The expression of the Delta16 isoform was initially thought to be involved in resistance to HER2 targeted therapies. *In vitro* resistance to trastuzumab was observed in Delta16-expressing cells (Castiglioni et al., 2006; Mitra et al., 2009). On the contrary, other authors, demonstrated *in vivo* trastuzumab susceptibility of Delta16-expressing tumors (Alajati et al., 2013; Castagnoli et al., 2014). Moreover in the study conducted by Castagnoli and colleagues is shown that the coexpression of high levels of both Delta16 and phospho-Src decrease the risk of relapse after trastuzumab treatment in breast cancer patients (Castagnoli et al., 2014).

2.2.2 HER2 Loss

HER2-amplification in breast cancer is an excellent illustration of the oncogene addiction hypothesis, which argues that some cancers are driven by a single oncogene that harbors an activating mutation or is overexpressed through gene amplification (Weinstein & Joe, 2008). As a consequence of this single dominant driver, the activity of other survival pathways in the cell is down-regulated because they are not necessary for the cell to grow, and potent inhibition of the dominant driver should then kill the cell. If other survival pathways remain or become active, then resistance to the therapy evolves and the cell survives (Rimawi et al., 2015).

The HER2 oncogene commonly develops resistance to the humanized HER2 antibody trastuzumab in a slightly different fashion; in this case, the trastuzumab-binding epitope is lost while oncogene function is retained (Scaltriti et al., 2007). *In vitro* and *in vivo* studies have demonstrated that cancer can “escape” from a given state of oncogene addiction, through mutation in the oncogene itself or other genes and pathways, presumably because of the frequent genomic instability of cancers. As such, acquired resistance to HER2-, EGFR-, and ALK-targeted therapies includes selection for activating mutations in the APK or PI3K pathways. As with second-side mutation of the oncogene itself, resistance mutations in key members of an oncogenic signalling pathway highlights that many cancers retain dependence upon specific oncogenic pathways, if not always the oncogene itself.

Cancers are inherently genetically unstable; thus alteration of HER2, ER and PgR expression between primary and metastatic breast cancer is theoretically sound. Numerous, predominantly retrospective studies report discordance rates of around 10–30% for ER and 20–

50% for PgR, while reported HER2 discordance rates are generally lower. A study-level meta-analysis, including 26 trials and around 2.500 patients, found a discordance rate for either HER2 loss or gain of 5.5%. 2 Studies published subsequently have reported discordance rates of a similar magnitude ranging from 1% to 24%. This biological phenomenon may be due either to the heterogeneity inherent in cancer cells or to clonal selection promoted by targeted therapies against HER2 (Turner & Di Leo, 2013). However, it remains unclear what could be the clinical and prognostic effect of the expression of HER2 discordance between primary tumors and metastasis. The available evidence suggests that loss of HER2 may result in worse post relapse survival (PRS) and overall survival (OS), although data were not consistent across trials and were often confounded by lack of treatment in the setting of receptor loss. Conversely, HER2 discordance was not associated with shorter disease free survival (DFS). Furthermore, there was no evidence that indicated specific clinical factors, such as previous treatment, might predict likelihood of HER2 discordance at breast cancer relapse (Turner and Di Leo, 2013).

2.2.3 Activation of compensatory and alternative signalling and survival pathways

It has come to light that cancer cells are able to become resistant to therapies by recruiting the use of a similar, compensatory pathway that continue downstream activation of protein synthesis. This mechanism is referred to as crosstalk between two pathways to allow continued cancer cell growth and survival.

An important trait of the Erbb family is the activation of the PI3K and the MAPK pathways. HER2-mediated activation of PI3K causes the phosphorylation of the serine/threonine-specific protein kinase, AKT, which in turn activates mTOR, able to induce protein synthesis that stimulates cell proliferation, migration, and metabolism (Altomare and Testa, 2005). Alterations in breast cancer resulting in hyperactivity of the PI3K pathway include gain-of-function mutations in PIK3CA (the gene encoding the PI3K catalytic subunit p110α), (Campbell et al., 2004; Bachman et al., 2004), mutations in AKT1 (Carpten et al., 2007), amplifications of AKT2 (Bellacosa et al., 1995), loss of the PTEN lipid phosphatase (Li et al., 1997; Saal et al., 2007) and loss of the tumor suppressor INPP4B (inositol polyphosphate 4-phosphatase type II) (Gewinneret al., 2009). Due to role of AKT in a variety of human solid tumors and hematological malignancies, several therapies have been developed to target components of the AKT pathway

to reduce tumor survival, e.g. Wortmannin and LY294002, which are reversible and non-reversible inhibitors of PI3K respectively.

HER2 mediated activation of the MAPK pathway induces a Ras-mediated phosphorylation cascade resulting in the transcription of a number of genes that promote cell proliferation, survival, and cell migration (Hynes and Lane, 2005). Similar to the AKT pathway, several components of the MAPK pathway are involved in promoting tumorigenesis making these two pathways central nodes where activating mutations are known to trigger tumorigenesis and metastasis. Several inhibitors were designed to target components of the MAPK and mTOR pathways, e.g. U0126 and rapamycin, which inhibit MEK/MAPKK and mTOR respectively.

Resistance to therapies can also involve the upregulation of ligands and HER2 heterodimerization with EGFR, HER3 and interactions with others membrane receptors such as IGF1R or MET. Extensive research has been done in G-Protein Coupled Receptor (GPCR) crosstalk with EGFR/HER2 since some GPCR agonists such as Lysophosphatidic acid (LPA), carbachol (muscarinic acetylcholine inhibitor), and thrombin are known to be able to increase HER activation (Bray, 2006). Emerging preclinical and clinical evidences indicate a complex molecular bidirectional crosstalk between ER and HER2 pathways (Arpino et al., 2008; Lousberg et al., 2016). An inverse relationship has been observed between the expression of growth factor receptor and ER (Massarweh and Schiff, 2007). Preclinical data support the hypothesis that increased growth factor signalling down-regulates ER expression and, vice versa, HER2-overexpressing tumors, that are apparently ER negative, may actually revert to ER positivity after treatment with anti-HER2 therapies (Munzone et al., 2006; Xia et al., 2006).

Mechanisms of crosstalk between the HER family and several other pathways, including the Wnt/β-catenin (Ayyanan et al, 2006), TNFα/IKK/NK-κB (Oswald et al., 1998; Osipo et al., 2008), and Notch pathway (Yamaguchi et al., 2008; Osipo et al., 2008) have been under investigation for several years.

Interesting findings have been made characterizing the novel mechanisms of HER2–Notch bidirectional crosstalk via PTEN, a negative regulator of the PI3K pathway.

Inactivation of PTEN has been shown to occur within 40% of HER2+ breast cancer patients and has been correlated with poor prognosis, treatment resistance, Epithelial to Mesenchymal Transition (EMT), as well as with the propagation and survival of Breast Cancer Stem Cells (BCSCs) (Bailey et al., 2011; Nagata et al., 2004; Mulholland et al., 2012; Sun et al., 2016). Sun and colleagues demonstrated that continued use of trastuzumab in HER2-positive cells with loss

of PTEN induces EMT and transform HER2-positive to a triple negative breast cancer. Moreover, the transformed cells exhibited loss of dependence on ERBB family signalling (such as HER2, HER3, HER4, BTC, HRG, EGF), reduced estrogen and progesterone receptors, increased frequency of cancer stem cells (CSCs) and metastasis potential (Sun et al., 2016).

EMT is a process in which epithelial cells lose cell-cell contacts and acquire a migratory mesenchymal phenotype accompanied by distinct changes in gene expression (Thiery et al., 2009). Recent evidence suggests that cells that undergo EMT acquire stem cell-like properties (Mani et al., 2008; Morel et al., 2008). Normal stem cells and cancer stem cells may share a mesenchymal phenotype that enhances their ability to preserve stemness, to retain migratory properties, and to respond to different stimuli during expansion and differentiation.

EMT has been linked to both chemio- and radio-resistance and resistance to targeted agents (Mallini et al., 2014; Singh and Settleman, 2010). Several *in vitro* and *in vivo* studies have shown that resistance to lapatinib and trastuzumab is associated with induction of EMT (Creedon et al., 2014; Kim et al., 2013; Korkaya et al., 2012; Creedon et al., 2016).

2.3 Experimental approaches targeting HER2

Treatment of HER2-positive breast cancer with a single anti-HER2 agent does not potently suppress HER2 signalling. Due to the complexity of ErbB network and the high incidence of resistance to current anti-HER2 agents, new therapeutic strategies targeting HER2 are required, one it's to overcome "bypass track resistance" by combining multiple anti-HER2 drugs at the same time and targeting its signalling network.

2.3.1 Targeting HER2 signalling network

Besides combinatorial regimens, the efficacy of new drugs targeting HER2 is currently investigated in clinical trials. The efficacy of anti-HER2 tyrosine kinase inhibitors (TKIs) in an attempt to circumvent resistance to trastuzumab has already been proved with lapatinib (Geyer et al., 2006). Clinical trials have shown that the addition of trastuzumab and lapatinib to chemotherapy achieved a higher pathological complete response than either trastuzumab or lapatinib alone (Baselga et a., 2012; Untch et al., 2012). To further enhance HER2 inhibition, irreversible TKIs, such as neratinib (Puma biotechnology), have been developed. Neratinib is a multitargeted, irreversible tyrosine kinase inhibitor that targets the EGFR, HER2, and HER4

kinases (Wissner and Mansour, 2008) shown to have promising preclinical activity against HER2-overexpressing cell lines (Rabindran et al., 2004). Canonici and colleagues as well demonstrated that neratinib improve response and overcome resistance to trastuzumab in sensitive and resistant HER2 amplified breast cancer cells (Canonici et al., 2013). Indeed, it is currently undergoing several phase III clinical trials (Bottle et al., 2012; Bose et al., 2009).

Instead of targeting HER2 receptor, new experimental molecules focus on the inhibition of its signalling network. Activation of signalling pathways involving the PI3K/Akt/mTOR pathway contribute to the development of resistance to HER2-targeted therapies, so several inhibitors of this pathway are under investigation in this disease setting; phase III data for everolimus in combination with trastuzumab and chemotherapy in trastuzumab-refractory, advanced disease are promising (Hurvitz et al., 2013).

Many other PI3K-AKT inhibitors are being developed and investigated, including Buparlisib (Novartis) and GNE317 (Genetech).

Buparlisib is a potent and highly specific oral pan-class I PI3K inhibitor, able to bind the ATP-binding site of PI3K, preventing the phosphorylation of phosphorylates phosphatidylinositol 4,5-bisphosphate (PIP2) to phosphatidylinositol 3,4,5-trisphosphate (PIP3), which decreases the levels of phosphorylated AKT (Estevez et al., 2015). It does not significantly inhibit the related class III (Vps34) and class IV (mTOR) PI3K but results to be active against the most common somatic PI3Kα mutations (Maira et al., 2012; Saini et al., 2013). *In vitro* and *in vivo* preclinical studies demonstrated buparlisib ability to inhibit HER2-positive cell-derived tumor growth. Buparlisib, in addition, has shown *in vivo* antiangiogenic activity through the inhibition of PI3K (Maira et al., 2012). Moreover due to its ability to penetrate the blood-brain barrier it can target as well HER2-positive brain metastasis, as demonstrated by Nanni and colleagues (Nanni et al., 2012).

GNE-317 is a dual PI3K/mTOR inhibitor with excellent blood-brain barrier penetration. Physicochemical properties of PI3K inhibitors were optimized using in silico tools, leading to the identification of GNE-317; Salphati and colleagues (2012) demonstrated its effectiveness in inhibiting tumor growth in orthotopic xenograft models of Glioblastoma.

Continuing on anti-signalling effector, combined anti-MEK/anti-PI3K regimens are under evaluation since the discovery of an association between PI3K inhibition-HER signalling enhancement and acquired dependency on ERK (downstream to MEK) in HER2-positive breast tumors (Serra et al., 2011; Saini et al., 2013, Arteaga and Engelman, 2014).

In addition, Mitra and co-workers showed that dasatinib, a small molecule that inhibits Src kinase family but also receptor tyrosine kinases, is able to suppress the growth, proliferation and invasion ability of HER-2 and Delta16-expressing cell lines (Mitra et al., 2009).

Table 2. Experimental drugs targeting HER2 in HER2-positive breast cancer (modified from Yan et al., 2014; Arteaga and Engelman, 2014).

Therapy	Regimen
anti-HER2	neratinib margetuzimab IJM716 212Pb-TCMC-trastuzumab trastuzumab+neratinib trastuzumab+IJM716
anti-signalling effectors	MEK inhibitors (UO126) PI3K inhibitors (buparlisib) PI3K/mTOR inhibitors (GNE-317) Src inhibitors (dasatinib)
other targets	Hsp90, VEGF, matrix metalloproteinases inhibitors
anti-HER2 + other biological therapies	trastuzumab+erlotinib (EGFR tyrosine kinase inhibitor) trastuzumab+everolimus (mTOR inhibitor) lapatinib+bevacizumab (anti-VEGF-A monoclonal antibody) T-DM1+PI3K inhibitor trastuzumab+pertuzumab+PI3K inhibitors
anti-HER2 + chemotherapy	Anti-HER2agents +capecitabine/docetaxel/gemeitabine/paclitaxel

Among other experimental drugs targeting HER2, agents inhibiting VEGF, Hsp90 and matrix metalloproteinases are currently investigated, as well the combination of anti-HER2 therapies and other biological compounds or chemotherapy (Table 2) (Emde et al., 2012; Hurvitz et al., 2013; Yan et al., 2014; Arteaga and Engelman, 2014).

2.3.2 Targeting Myc

As discussed previously, therapeutic efficacy depends on not only how effectively a drug inhibits its target, but also on the innate or adaptive functional redundancy of that target and its attendant pathway. In this regard, central transducers such as Ras, Myc, and E2F are intriguing therapeutic targets because they serve the unique and irreplaceable role of coordinating expression of the many diverse genes that, together, are required for somatic cell proliferation.

To this end, we focused our attention on Myc, three broadly isofunctional transcription factors that integrate diverse upstream growth signals and coordinate them to the thousands of disparate target genes that, together, support somatic cell proliferation (Larsson and Henriksson 2010). Aberrantly high and/or deregulated Myc activity is causally implicated in most cancers and is often associated with aggressive, poorly differentiated, and angiogenic tumors (http://www.myccancergene.org; Dang et al. 2010) (Figure 3). Interestingly, however, direct mutational activation of Myc genes is relatively uncommon in tumors, at least in their early stages; rather, the aberrantly high levels of expression of Myc are frequently a consequence of its relentless induction by upstream oncogenic signals (Larsson and Henriksson 2010).

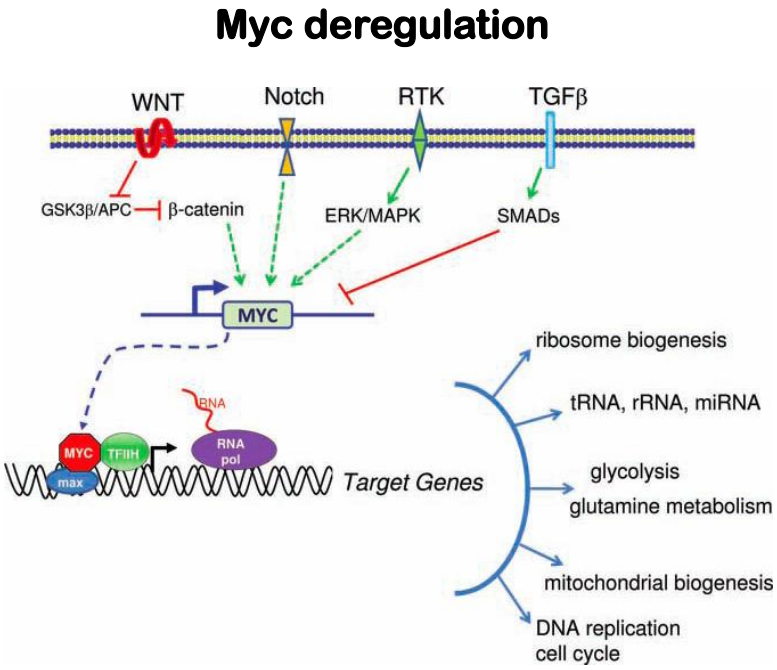

(Dang et al. 2010)

Figure 3: Myc deregulation. Figure adapted from Dang et al., 2010

The Myc proteins comprise three broadly isofunctional transcription factors: c-Myc, N-Myc, and L-Myc. All share a similar HLHZip domain that mediates dimerization with their common obligate partner protein, Max. Such dimerization, which is essential for Myc proliferative and oncogenic activities, is blocked by the dominant-negative omomyc mutant.

Omomyc is a dominant-negative Myc dimerization domain mutant comprising the basic helix–loop–helix zipper (HLHZip) domain of Myc with four amino acid substitutions in the Myc leucine zipper that confer altered dimerization specificity (Soucek et al. 1998, 2002) (Figure 4). Omomyc retains the ability to bind its physiological partner, Max, but also heterodimerizes with wild-type c-Myc, N-Myc, and L-Myc proteins. Since Myc:omomyc heterodimers can no longer bind to the canonical Myc E-box CACGTG DNA recognition element, omomyc overexpression inhibits Myc-dependent target gene transactivation (Soucek et al. 2002; 2004; Savino et al. 2011). Switchable genetic studies have been showed that transient systemic inhibition of Myc by the dominant-negative omomyc, which expression can be systemically but reversibly induced by administration of doxycycline to TRE-omomyc;CMVrtTA mice (Soucek et al. 2008), has a profound therapeutic effect on diverse tumor types yet elicits surprisingly mild and rapidly reversible side effects on normal tissues (Soucek et al. 2008; Sodir et al. 2011).

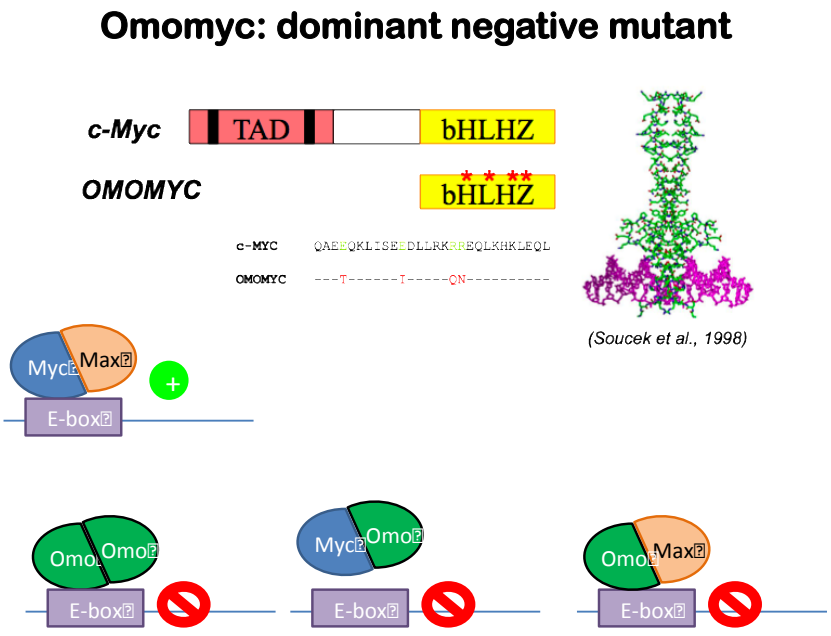

Figure 4: Omomyc as dominant negative mutant of Myc. Figure adpted from Soucek et al., 1998.

The elevated and/or deregulated activity of Myc gene is associated with the majority of human cancers, as well to HER2-positive breast cancer.

Nair and colleagues demonstrated that HER2 and c-Myc interaction drives mammary oncogenesis. They showed, in a chimeric transgenic mouse model double positive for the two oncogenes, that the co-expression of HER2 and c-Myc was sufficient to significantly decrease survival time of mice, increase self-renewal in sphere-forming assays and was associated with an average 20-fold increase of *in vivo* tumour-propagating capacity (Nair et al., 2014).

Myc is implicated as well in HER2-targeted therapy mechanisms of resistance.

Amplifications of MYC, EGFR, HER2, CCND1, and TOP2-A have been identified from a trastuzumab-resistant breast cancer cell line (B585) by comparative genomic hybridization and FISH analysis (Barok et al., 2010).

Furthermore, a recent study proved that the treatment of BT474 HER2-positive cells with an epigenetic inhibitor suppressing c-Myc and lapatinib, synergically suppressed HER2-positive cancer cells *in vitro* and *in vivo*, by targeting the MLL2/FOX/c-Myc axis (Matkar et al., 2015). Thus this result suggests an epigenetically regulated FOXO/c-Myc axis as a potential target to improve HER2-positive breast cancer therapy.

3. Preclinical models for the study of mammary carcinoma

Experimental oncology research and drug development both require highly specific and clinically relevant *in vitro* and *in vivo* tumor models. Investigating the progression of human breast cancer in patients is very problematic for several reasons, including the numerous genetic and phenotypic alterations involved in the human disease and the intrinsic heterogeneity associated with breast tumors. Therefore, breast cancer disease is hard to mimic in all its characteristics in a single model, however existing models continue to provide priceless knowledge about the induction and the progression of the disease that would be impossible to obtain using *in vitro* models alone (Ottewell et al., 2005).

3.1 Relevance and evolution of preclinical models in oncology

The ideal preclinical model of breast cancer should recapitulate all the genetic and phenotypic alterations that occur in patients. Furthermore it should be easy to manipulate and genetically similar to human. Amongst the large repertoire of *in vivo* systems used to study

cancer, mouse models represent the most widely used system. Mice are a useful model for genetic manipulation and research, as their tissues and organs are similar to that of a human and they carry virtually all the same genes that operate in humans. Currently several mouse models are available, each of which is able to partially reproduce several human diseases.

Genetically engineered mouse models (GEMMs) and transplantation models are extensively used in research as models of breast cancer (Ottewell et al., 2006). GEMMs are modified in order to express (transgenic mice) or to lack (knockout mice) a gene of interest. They have been widely employed to study the early stages of many cancers but, due to the low incidence of metastases, they seem inappropriate for advanced disease studies (Ottewell et al., 2006; Saxena and Christofori, 2013). These models have the big advantage that the specific alteration that determines the tumor phenotype is known, resulting useful to investigate the molecular changes related to it. On the other hand the expression of the transgene in mice is usually induced at higher levels than those expressed physiologically in human tumors (Williams et al., 2013). The use of conditional and inducible systems usually are the solution to overcome these limitations.

Transplantation models consist of the injection of murine (syngeneic model) or human (xenogeneic model) cancer cells in mice. They are useful for studies on the various cancer stages as well as for the evaluation of new therapeutic approaches (Saxena and Christofori, 2013).

Patient Derived Xenograft (PDX) and co-clinical trials represent emerging applications of mouse modeling to the study of cancer (Prerna et al., 2014). PDX models are created when cancerous tissue from a patient's primary tumor is implanted directly into an immunodeficient mouse. This model offers a reliable first stride towards the goal of developing an efficient personalized therapy against cancer. A co-clinical trial refers to trials that are conducted simultaneously in GEMMs and human patients as part of the phase I/II trials for drug development. This project aims at real-time integration of murine and human trial data in an attempt to improve clinical decisions and outcomes. Although conceptually different, both these applications emphasize the need for tailoring therapeutic regimens based on individual molecular profiles of tumors, to develop a bench-to-bedside transition (Malaney et al., 2014).

3.1.1 HER2 transgenic mice

The first genetically modified models developed for the study of HER-2-positive breast cancer were transgenic for the rat homologue Neu, either the normal or the mutated form (NeuT) (Muller et al., 1988; Guy et al., 1992). Despite their usefulness in shedding light on HER-2/Neu driven transformation in breast cancer, they could not be used for the investigation of human HER-2-targeted therapies. Finkle and colleagues in 2004 developed the first model that successfully reproduces HER2 positive breast cancer (Finkle et al., 2004). In a FVB background 20-50 copies of the transgene were integrated on murine chromosome 6, under the promotion of the Murine Mammary Tumor Virus (MMTV). They demonstrated in a tumor-free survival study conducted on transgenic female mice that, at 52 weeks, 73% of mice developed spontaneous mammary tumors, with a mean latency of 36 weeks of age, and in the 40% of mice were detected as well lung metastases (Finkle et al., 2004).

After the identification of Delta16 deletion Marchini and colleagues generated a model expressing this isoform. FVBhuDelta16 mice are characterized by the expression of human Delta16 oncogene under the promotion of MMTV. Firefly luciferase was included as reporter transgene to allow the bioluminescent visualization of Delta16 expression in murine tissues. In this model mammary carcinogenesis was faster in respect to HER2 full-length transgenic model, (mean latency of 15 weeks of age), and multiple tumors developed (4-5 tumors/mouse were detected in animals between 12 and 19 weeks of age). Furthermore, at 25 weeks of age lung metastases were already present. All these findings highlighted the high transforming and invasive ability of Delta16 (Marchini et al., 2011).

Nowadays these two models best recapitulate HER2 full-length and Delta16 breast cancers in GEMMs, and are employed in the study described in this thesis (referred to as HER2 model and Delta16 model).

HER2 expression can be downregulated in order to mimic HER2 loss mechanism, using gene-silencing methods (ribozymes, antisense oligonucleotides, small interfering RNA). However, these knockdown studies do not reflect what happens in clinic, since tumors maintain their dependence on HER2 pathway (Sergina & Moasser, 2007).

The same regards inducible tetracycline/doxicycline systems, where in absence of HER2 expression it is observed a regression of tumor growth, e.g. in MMTV-neuT mice (Moasser, 2007), but not the loss of the oncogene addiction. Therefore, none HER2 loss model is currently

available.

In the Laboratory of Immunology and Biology of Metastasis of Bologna it has been established a panel of three cell lines that exhibit one of three phenotypes: a) high and stable HER2 expression *in vitro* and *in vivo*, b) high but labile HER2 expression which is lost either during *in vitro* culture or after tumor growth in mice, and c) complete loss of HER2 expression (Nanni et al., AACR 2014, Abstract number 1820). This panel of cell lines is a useful model to study the dynamics of HER2 loss in advanced HER2-positive mammary carcinoma, and to analyze alternative therapeutic strategies.

3.1.2 Transplantation models

The most commonly used *in vivo* models for studying the biology of tumors are transplantation models. Depending on the purpose of the research syngenic or xenograft model is preferable. In syngeneic mice cell lines derived from spontaneous murine tumors or from carcinogen-, transgene- or gene knockout- induced tumors can be injected in immunocompetent mice (Saxena and Christofori, 2013). In the xenograft model the implanted cells or tissues are of human origin, and the animal host has to be immunodeficient, in order to prevent an immune rejection by the host (Jonkers and Derksen, 2007; Saxena and Christofori, 2013). Many mouse strains carrying different gene mutations and therefore exhibiting various levels of immunodeficiency have been developed over the years, e.g. nude and Rag-/-;Il2rg-/- mice (Thomsen et al., 2008).

The syngenic model is particularly useful to study the interactions between cancer therapies and a functional immune system, e.g. in immunotherapy approach (Ottewell et al., 2006). Cancer immunotherapies are designed to work in conjunction with a patient's immune system in order to increase native anti-tumor responses. In this field of study, conventional xenograft models lack relevance due to the animals' immunocompromised status.

Among xenograft models there are different features and, as well, advantages and disadvantages. Tumor cell line-based ectopic xenograft models are useful to study anti-tumor efficacy and overall tolerability *in vivo* and to screen new therapies, due to their reproducibility, modest cost, time-effectiveness and availability of a wide range of tumor cell types. However, despite these utilities, this model possesses limited pathophysiological relevance and clinical predictability. Most tumor cell lines have been maintained for decades in enriched grow media

before being injected, resulting in the artificial selection of tumor cell clones with high proliferative potential. Consequently, they do not represent the genetic and epigenetic heterogeneity of the original primary tumor (Williams et al., 2013). Patient derived xenograft models can be chosen in order to overcome this issue (Cassidy et al., 2015; Aparicio et al., 2015).

Depending on the route of cancer cells delivery, either in syngeneic or xenogeneic mice, different aspects of tumor and metastatic processes of breast cancer can be evaluated.

The subcutaneous injection (s.c.) is a common route of delivery choose to study and monitor tumor growth, due to the high vascularization and convenient anatomical location of skin. Moreover it is convenient in order to evaluate the response to new localized strategies (Ottewell et al., 2006). However, this ectopic transplantation model fails to mimic advanced breast cancer and the development of metastases (Saxena and Christofori, 2013).

Orthotopic injection involves the implantation of tumor cells or tissues into the originating tissue site of the cancer. Compared to ectotopic s.c. tumor-implantation model, orthotopic implantation more closely simulates the natural environment of the original tumor (Ruggieri et al., 2014). However, the metastatic spread has a relative high latency, and primary tumor resection could be required to observe advanced disease in mice (Ottewell et al., 2006; Saxena and Christofori, 2013).

Injection of tumors cells directly into the vascular blood system is useful for studies focused on the late phases of the metastatic process. The administration of cells in the lateral tail vein (intravenous injection) is the most common way to obtain induced metastases. The first colonized organs are the lungs, with further metastases to other organs, including the brain. Intracarotid and intracardiac injections allow the development of metastases in the brain bypassing the pulmonary circulation. Another systemic delivery that causes local invasion consists of the intraperitoneal injection of tumor cells (Khanna and Hunter, 2005; Ottewell et al., 2006; Saxena and Christofori, 2013; Daphu et al., 2013).

3.1.3 Patient-Derived Xenografts

Direct transfer of human tumor fragments or cells isolated from patient tumors to immunodeficient mice generates PDX tumors. Even if no animal model can insure identical results in humans, considering that the tumor engrafted is of human origin, PDX model represents a very powerful tool for investigating tumor biology.

One of the key premises of developing PDX models for cancer research is the assumption that these models faithfully represent the original tumor from which they were developed and that this similarity is maintained across passages (Aparicio et al., 2015). Indeed, a number of studies have demonstrated that PDX tumors maintain the original tumor heterogeneity (Cassidy et al., 2015). Serial passages of tumors in mice allow studying tumor biology and pharmacology without subjecting tumor cells to artificial *in vitro* cell culture conditions (Rosfjord et al., 2014). Furthermore subsequent passages permit to amplify the biologic material on which perform studies in the long term. Detailed cytogenetic analysis of PDX tumors revealed strong preservation of the chromosomal architecture found in patients, as well as high fidelity in histology, trascriptome and polymorphisms (Rosfjord et al., 2014).

The level of concordance between the profiles of the tumor of origin and the tumor from different serial passages in mice is important in order to establish the degree of reliability of PDX. Another key observation is that PDX model maintains stromal and stem cell components of primary tumor in the early phases of the transplant, useful to study how the interaction between tumor cells and microenvironment can change (Rosfjord et al., 2014).

Thanks to correlation with the tumor of origin and to the stability of the model, PDX is a viable tool for preclinical assessment of both drug response and mechanisms of resistance.

One of the main challenges faced when developing a panel of PDX is the variable engraftment rate (Siolas and Hannon, 2013). Engraftment rates typically vary between 23% and 75% depending on tumor type. Higher engraftment rates are associated with more clinically aggressive tumors (Zhang et al., 2012), as well as with the site of the injection (DeRose et al., 2013) and the maintenance of appropriate steroid hormone receptor expression between patient tumors and PDX (Zhang et al. 2013). Moreover the origin of the tumor (primary tumor or metastasis) (Marangoni et al., 2007) and the treatment received by the patient before the surgery are involved (Moon et al., 2015). Furthermore, PDXs are often characterized by a long latency period after the engraftment, limiting their feasible employment (e.g. the evaluation of the sensitivity to a selected therapy) (Siolas & Hannon, 2013; Ledford, 2016).

With the aim to improve the take rates of tumors, immunodeficient mice with different levels of immunodeficiency can be employed. Since the discovery of the nude mouse strain over 40 years ago, investigators have attempted to model human tumor growth in immunodeficient mice. Nude mice carry a single homozygous base deletion on $Foxn1^{nu}$ gene in chromosome 11 that determines a phenotype of hairlessness, athymia and T-cell deficiency (Hirasawa *et al.*,

1998). The field has advanced significantly over the years due to improvements in the murine recipient of human tumors. These improvements include the discovery of the "Severe Combined Immunodeficiency" (Scid) mutation and the development of targeted mutations in the Recombination Activating Genes 1 and 2 (Rag1null; Rag2null), which severely cripple the adaptive immune response of the murine host. The homozygous mutation of Rag2, that usually participates in V(D)J recombination reaction for the formation of T cells receptors and B cells immunoglobulins, determines the absence of mature T and B cells in mice (Oettinger *et al*., 1990; Shinkai *et al*., 1992). More recently, mice deficient in adaptive immunity have been crossed with mice bearing targeted mutations designed to weaken the innate immune system, ultimately leading to the development of immunodeficient mice bearing a targeted mutation in the Interleukin 2 Receptor Common Gamma chain gene (IL2rγnull). The IL2 gene encodes for the common gamma chain of IL-2, IL-4, IL-7, IL-9, IL-15 and IL-21 receptors, when mutated mice are defective in mature T and B cells and totally deficient in NK cells (Cao *et al*., 1995; Kovanen and Leonard, 2004). The IL2rγnull mutation has been used to develop several immunodeficient strains of mice, including the NOD-scid IL2rγnull (NSG) strain. Using NSG mice as human xenograft recipients, it is now possible to grow almost all types of primary human tumors *in vivo*, including most solid tumors and hematological malignancies.

However, these models fail to reproduce microenviroment and tumor cell interactions with the innate immune system, both of which are integral to tumor development, proliferation, methastasis and expecially have limited utility to study therapeutic compounds whose pharmacological activities depend mostly on the presence of an intact immune system (Siolas and hannon, 2013; Rosfjord et al., 2014). Additional model refinement will be required to make PDX feasible for the valuation of immunomodulatory compounds (Rosfjord et al., 2014). Reconstituing a patient-matched immune system in PDX models is a significant challenge. Standard methods consist in the transplantation of hematopoietic stem cells (HSC) or mature circulating cells (PBMCs), but as a conquence an inappropiate immune response against murine or human tissues respectively, can occur. Therefore, a solution to study the interaction between tumor and immune system could be a humanized mouse model (HM), which allow researchers to examine xenograft growth in the context of a human immune system and resultant tumor microenvironment (Cassidy et al., 2015; Morton et al., 2016).

Finally another restriction factor of the use of PDX mice is the cost: tumor grafts can only be mantained in expensive immunocompromised mice and their passages require a very

specialized skills set (Siolas & Hannon, 2013).

PDX are currently used in several oncologic fields and numerous tumor-specific PDX models have been established. Table 3 reports the results of some representative works for each type of tumor.

Table3. Comparison of the engraftments rate reported in the literature for PDX derived from tumors of different organs

Tumor	Engraftment		Location of implant	Mouse strain	Reference
Non small lung cancer	35/100	35%	subcutaneus	Nude, SCID	Illie et al., 2015
	23/88	26%	subcutaneus, flank	NOD-SCID	Hao et al., 2015
	21/63	33%	subcutaneus, retronuchal	NSG	Guerrera et al., 2016
Colorectal cancer	54/85	64%	subcutaneus, interscapular or flank	Nude, SCID	Julien et al., 2012
	150/241	62%	subcutaneus, lower back	Balb C Nude	Oh et al., 2015
	10/10	100%	subcutaneus	Nude, NOD-SCID	Lee et al., 2014
	33/57	58%	subcutaneus	NSG	Chou et al., 2013
	97/143	68%	subcutaneus, lower back	Balb C Nude	Cho et al., 2013
Breast Cancer	25/200	13%	subcutaneus,interscapolar	Swiss Nude	Marangoni et al., 2007
	6/30	20%	Subcutaneus, back, pellet estradiol	SCID	Bergamaschi et al., 2009
	10/24	42%	orthotopic (mammary fat-pad)	NOD-SCID, NSG	Kabos et al., 2012
	18/49	37%	orthotopic (mammary fat-pad)	NOD-SCID	DeRose et al., 2013
	19/81	23%	orthotopic (mammary fat-pad)	NSG	Moon et al., 2015
Ovarian cancer	29/34	85%	subcutaneus	SCID	Dobbin et al., 2014
	14/22	64%	fat pad	SCID	Dobbin et al., 2014
	4/18	22%	intraperitoneal	SCID	Dobbin et al., 2014
	1/12	8%	adrenal capsule	SCID	Dobbin et al., 2014
	10/12	83%	subcutaneus, pellet of estradiol	NSG	Topp et al., 2014
	168/214	79%	intraperitoneal	SCID	Weroha et al., 2014
	47/66	71%	Fat pad, interscapular interscapular	Nude	Colombo et al., 2015
Sarcoma (advanced stadium)	22/29	76%	subcutaneus, flank	Nude	Stebbing et al., 2014
Metastasis from melanoma	23/26	88%	subcutaneus, flank	NOD-SCID IL-2Rγnull	Einarsdottir et al., 2014

Breast cancer PDX models in respect to other tumors have a lesser rate of engraftment, between 10 and 40% (Table 4) (Marangoni and Poupon, 2014; Kabos et al., 2012). Among all subtypes HER2-positive PDX results one of the most difficult to obtain (Whittle et al., 2015, Marangoni et al., 2007). Some examples of achievement are the two cell lines established from Marangoni and colleagues (2007), resulted to be as well sensitive to trastuzumab. DeRose and colleagues (2013) on a panel of 5 HER2-positive PDX studied the stability of the model analyzing the expression of HER2 in subsequent passages *in vivo*, demonstrating the stability of their model. Moreover, Zhang and colleagues (2013) obtained a panel of 6 HER2-positive PDX with metastatic ability.

Nowadays exist several initiatives of shared PDX models for collaborative research projects and multicentre preclinical trials, like the EurOPDX Consortium, an initiative of translational and clinical researchers across 10 European countries, with the common goal of creating a network of clinically relevant models of human cancer, and in particular PDX models.

The aim of this project is focused on dissecting the mechanism of action by which HER2-loss variants and Delta16 isoform mediate HER2 oncogenic activity and condition the response to HER2 therapies in breast cancer. To this end, preclinical cancer models representative of cancer heterogeneity and able to mimic all possible scenarios observed in human tumors were developed and studied.

Table 4. Published data on breast cancer PDX models

Paper	Strain	Injection	Estrogen	Engraftment		Metastasis
				First engraftment	**Serial passages**	
Visonneau et al., 1998	SCID + etoposide	subcutaneus	no	8/16 (50%)	2/16 (13%)	lung (75%), limphnode(25%)
Marangoni et al., 2007	*Swiss Nude*	subcutaneus, mammary fat pad, interscapolar	yes	25/200 (13%)	22/200 (11%)	polmonari (33%)
Bergamaschi et al., 2009	SCID	subcutaneus	yes	6/30 (20%)	2/30 (7%)	*nd*
Kabos et al., 2012	NOD-SCID, NSG	orthotopic	only in ER+	10/24 (42%)	10/24 (42%)	*nd*
DeRose et al., 2013	NOD-SCID	orthotopic	yes	18/49 (37%)	13/49 (27%)	90%
Zhang et al., 2013	SCID/Bg o NSG	orthotopic	SCID SCID + pellet SCID + pellet + fibroblasti NSG + pellet	18/38 (47%) 28/70 (40%) 13/29 (45%) 10/32 (31%)	1/38 (3%) 15/70 (21%) 1/29 (3%) 6/32 (19%)	Lung (48%)
Du Manoir et al., 2014	*Swiss Nude*	mammary fat pad, interscapolar	only in ER+	39/130 (30%)	20/130 (15%)	rare lung
Moon et al., 2015	NSG	orthotopic	no	19/81 (23%)	*nd*	*nd*

MATERIAL AND METHODS

1. Mice

For the studies on FVB-huHER2 mice (Finkle *et al.*, 2004), here referred to as HER2 model, were obtained from Genentech Inc. (South San Francisco, CA, USA). This line carries in heterozygosis the human full-length normal HER2 gene under the control of the Murine Mammary Tumor Virus (MMTV) promoter on a FVB background. HER2 gene heterozygosis was maintained by crossing $HER2^{+/-}$ male mice with non-transgenic FVB female mice (purchased from Charles River, Calco, Italy).

Δ16-HER2-LUC mice (Marchini *et al*., 2011), here referred to as Delta16 model, were kindly given by Prof. Augusto Amici (University of Camerino, Italy) and Dr. Serenella Pupa (Istituto Tumori, Milan). This line carries in heterozygosis the human splice variant Delta16 gene under the control of MMTV promoter on a FVB background. Delta16 gene heterozygosis was maintained as described above for HER2 model.

F1 HER2/Delta16 mice, transgenic for both genes, were obtained in the Laboratory of Immunology and Biology of Metastasis by crossing Delta16 male mice with HER2 female mice.

Transgenic mice were screened by routine genotyping with PCR analysis (Finkle *et al*., 2004; Marchini *et al*., 2011).

For the generation of Breast cancer PDX models Balb/c $Rag2^{-/-}$;$Il2rg^{-/-}$ breeders were kindly given by Drs. T. Nomura and M. Ito of the Central Institute for Experimental Animals (Kawasaki, Japan). This line is double knockout for the Recombination Activating gene 2 (Rag2) and for the Interleukin 2 Receptor Gamma chain gene (Il2rg) (Goldman *et al*., 1998).

NOD-SCID $Il2rg^{-/-}$ mice (NOD SCID Gamma, NSG) were purchased from The Jackson Laboratories (California). Both immunodeficient strains lacking mature T cells, B cells and natural killer (NK) cells were kept under sterile conditions and used for the generation of PDX models.

All animals were bred in the animal facility of the Laboratory of Immunology and Biology of Metastasis (Department of Specialistic, Diagnostic and Experimental Medicine, University of Bologna, Italy). Virgin female mice were used in the experiments. Experiments were authorized by the institutional review board of the University of Bologna and done according to Italian and European guidelines.

2. Cells

Five mouse mammary tumor cell lines were employed in this project: MAMBO 89^{HER2stable}, MAMBO38^{HER2loss}, MAMBO43^{HER2lable}, 302-IVD and 156-IS. Mambo89^{HER2stable} cell line was established from a spontaneous mammary carcinoma of a huHER2 female mouse; Mambo43^{HER2labile} cell line was derived from a mammary carcinoma grown after the subcutaneous injection in a huHER2 female mouse of a HER2 cell line established from a spontaneous huHER2 mammary carcinoma; Mambo38^{HER2loss} line was obtained and established *in vitro* from tumors grown after the subcutaneous injection of Mambo43^{HER2labile}. 302-IVD and 156-IS cell line were established from spontaneous primary mammary carcinomas arisen in F1 model.

All cell lines were obtained in the Laboratory of Immunology and Biology of Metastasis. MAMBO 89^{HER2stable} and MAMBO43^{HER2lable} cell lines were stabilized in Dulbecco's Modified Eagle Medium (DMEM; Life Technologies) +20% FCS, supplemented with Bovine Pituitary Extract 30 μg/ml (BPE; BD Biosciences, USA) and MITO Serum Extender 1:200 (BD Biosciences). MAMBO38^{HER2loss} was stabilized in Dulbecco's Modified Eagle Medium (DMEM; Life Technologies) +20% FCS. F1 murine cell lines were stabilized and cultured in MammoCult complete medium (StemCell Technologies, Canada) supplemented with 1% FCS.

For the experiment of Myc inhibition JMT-1 human cell line was used. It is a cell line established from the pleural effusion of a 62-year-old woman with ductal breast cancer (grade 3 invasive, T2N1M0) after postoperative radiation in 2003; it was described to carry an amplified HER2 oncogene and to be insensitive to HER2-inhibiting drugs, e.g. trastuzumab (Herceptin). This cell line transfected with pSlik-omomyc vector was kindly provided by Dr. Laura Soucek (Vall d'Hebron Hospital, Barcelona). JMT-1 cells were routinely cultured in DMEM:F12 medium (Gibco BRL, Grand Island, NY, USA) medium supplemented with 10% heat-inactivated foetal bovine serum (FCS) (Life Technologies, Milan, Italy).

Stable transfected cells were selected adding Hygromycin B (Invitrogen) at a final concentration of 100μg/ml to the medium.

As regards PDX models, a primary cell line established from a FO4 PDX tumor at the VII consecutive passage *in vivo* was employed. FO4 primary cell line was stabilized in HuMEC BPE (Bovine Pituitary Extract) and HuMEC Supplement (Life Technologies, Milano) +20% FCS.

All mediums were supplemented with penicillin 100 U/ml and streptomycin 100 µg/ml (Sigma-Aldrich, Milan, Italy). All cell lines were maintained at 37°C in a humidified 5% CO_2 atmosphere but FO4 derived primary culture cells, maintained at 37°C in a humidified 7% CO_2 atmosphere.

For the maintenance culture, cells were washed with Phosphate Buffer Saline (PBS; Life Technologies) and harvested by trypsin (0.05%)-EDTA (0.002%) treatment (Life Technologies). Cell number and viability was determined through erythrosine dye exclusion (Sigma-Aldrich) and hemocytometer count.

2.1 Mammospheres

In order to obtain mammospheres, cells were cultured in Ultra Low Attachment 6-well plates (Corning, Life Technologies, USA) in Mammocult complete medium (StemCell Technologies) at a dose of 40000 cells per well in 4 ml. After 7 days, spheres were counted, and then they were collected and disaggregated to quantify total cell count.

3. Immunofluorescence and cytofluorimetric analysis

The expression of several cell surface markers was evaluated in tumors and cell lines from HER2, F1 and FO4 PDX models by direct or indirect immunofluorescence (IF) and cytofluorimetric analysis.

Single cell suspensions of cultured cells or tumor masses were analyzed for specific markers expression on the membrane. In the case of tumor masses, after necropsy they were minced with scissors, incubated for 5 minutes with trypsin and passed through a 70 µm cell strainer (Becton Dickinson, Bedford, MA, USA) to obtain a homogeneous cell suspension. Before the incubation with the primary antibody, tumor suspensions were incubated with Rat anti-mouse CD16/CD32 clone 2.4G2 antibody Fc block (1:100 dilution; BD PharMingen, San Diego, CA).

For direct IM the following antibodies were used:

- anti-mCD24-AF (M1/69), diluted 1:10 (Bio-Legend, San Diego, CA, USA);
- anti-mCD44-PE (IM7) diluted 1:10 (Bio-Legend, San Diego, CA, USA);
- anti-mCD29-PE (HMß1-1) diluted 1:100 (Bio-Legend, San Diego, CA, USA);
- anti-mSca-1-PE (E13-161.7) diluted 1:100 (Bio-Legend, San Diego, CA, USA).

For indirect IF the following antibodies were used:

- anti-huHER2 (MGR-2), diluted 1:100 (Alexis, Enzo Life Science),
- anti-huHER1 (528), diluted 1:40 (Calbiochem),
- anti-huHER3 (SGP1), diluted 1:40 (Thermo Fischer Scientific),
- anti-huIGFR (αIR3), diluted 1:20 (Calbiochemtumor).

Then, samples were incubated with the secondary AlexaFluor-conjugated goat anti-mouse IgGs antibody (IgG AlexaFluor 488, 1:100 dilution; Thermo Fisher Scientific). Fluorescence intensity was determined through flow cytometry (FACScan, Becton Dickinson); analysis was performed with FCS EXPRESS 4 (De Novo Software, Gledale, California, USA).

4. Sensitivity to drugs *in vitro*

4.1 Continuous culture

Mambo89^{HER2stable} and Mambo43^{HER2labile} continuous culture with trastuzumab (Roche, Switzerland) was performed adding the drug at a final concentration of 30 μg/ml to DMEM + 20% FCS + BPE + MITO^{TM} Serum Extender.
FVBhuHER2 cell lines were cultured in 25 cm^2 flasks (Falcon, BD BioSciences, USA) Cells were splitted once a week and cultured with Trastuzumab, kindly given by Dr. Serenella Pupa, for 30 days. At the end of this period, part of the cells were cultured without the drug for other 30 days; the other part was analyzed for HER2 expression by immunofluorescence (paragraph 3.). The same analysis was repeated at the end of the recovery period without the treatment. Cell number and viability was determined through erythrosine dye exclusion (Sigma-Aldrich) and hemocytometer count.

4.2 Soft agar 3-D culture

The sensitivity *in vitro* to anti HER2 drugs was evaluated in cell lines derived from HER2 and F1 models in 3-D culture (0.33% soft-agar containing the drug in MammoCult complete medium + 1% FCS). Trastuzumab, lapatinib and dasatinib were kindly given by Dr. Serenella Pupa, buparlisib was obtained from Novartis Institutes for BioMedical Research, Oncology (Basel, Switzerland). Cells were suspended in MammoCult + 1% FCS containing 0.33% agar (overlayer) and layered on a base of MammoCult + 1% FCS containing 0.5% agar (underlayer) on a Costar 24-well plate (Corning Life Sciences, USA). Drugs alone or in combination were added both to

underlayer and to overlayer. Plates were maintained at 37°C in a humidified 7% CO2 atmosphere. Colony growth was monitored weekly and determined by counting at 31.25X magnification with Diavert microscope (Leitz, Milan, Italy) after 2-3 weeks from seeding. MAMBO38^{HER2loss} was seeded at 1000 cells/well, the other cell lines at 10.000 cells/well. Drug's efficacy was assessed as percentage of colonies grown over control. Cells from grown colonies were then collected and seeded in adherent cultures for subsequent molecular analyses.

5. Real-time PCR

RNA was extracted using TRIzol protocol (Total RNA Isolation Reagent; Life Technologies). Tissue samples were first disrupted using the gentleMACS Octo Dissociator (Miltenyi, Germania) (program RNA_02), wuth 1ml of TriZol reagent. Then the protocol provided with the reagent was followed. The concentration and purity of RNA was determined by measuring the absorbance at 260 and 280 nm in a spectrophotometer (Ultrospec 1100 pro, Biochron, England) or by Qubit RNA Assay Kit (Life Technologies, Milano).

1 µg of total RNA was reverse transcribed using iScript cDNA Synthesis Kit (Bio-Rad, CA, USA). Gene expression was analyzed by Real-Time PCR using Thermal Cycler CFX96 (Bio-Rad Laboratories, USA). Initially cDNA were diluted 1:20 with DNasi/RNasi free H_2O, then 4 µl of cDNA was amplified. Real-Time PCR was performed using Sso Advanced SyBR Green Supermix (Bio-Rad Laboratories, USA) reagents. Evaluated target genes were: human HER2 and Delta16. The steps of amplification were: 95°C for 30 seconds and then 40 cycles including 5 seconds at 95°C and 15 seconds at 60°C. A default melting curve program was used to obtain the dissociation curve for each gene. mRNA expression levels were normalized to GAPDH (gliceraldeide-3-fosfato deidrogenasi) (human or mouse) or TBP (TATA binding protein) (human, mouse and total), as endogenous reference gene. All primers were used at a final concentration of 200 nM. The analysis was performed using Bio-Rad CFX Manager 3.1 software. For relative quantification, ΔCt method was used:

$$\mathbf{\Delta Ct_{HER2/Delta16} = Ct_{HER2/Delta16} - Ct_{housekeeping.}}$$

$$\mathbf{2^{-\Delta CT} = 2^{-(CT\ gene - CT\ housekeeping)}}$$

Gene	Sequence (5'- 3')
h-HER2 *full length* (Mitra et al., 2009)	Dir: GTGTGGACCTGGATGACAAGGG Rev: GCTCCACCAGCTCCGTTTCCTG
h-HER2Δ16 (Mitra et al., 2009)	Dir: CACCCACTCCCCTCTGAC Rev: GCTCCACCAGCTCCGTTTCCTG
*Human*GAPDH	Dir: ATCAGCAATGCCTCCTGCAC Rev: TGGTCATGAGTCCTTCCACG
MouseGAPDH	Dir:GCTCACTGGCATGGCCTTC Rev: CCTTCTTGATGTCATCATACTTGGC
*Human*TBP (Bieche et al., 2014)	Dir: AGAACAACAGCCTGCCACCTTAC Rev: GGGAGTCATGGCACCCTGAG
*Mouse*TBP (Bieche et al., 2014)	Dir: CCCTTGTACCCTTCACCAATGAC Rev: TCACGGTAGATACAATATTTTGAAGCTG
*Total*TBP (Bieche et al., 2014)	Dir: TGCACAGGAGCCAAGAGTGAA Rev: CACATCACAGCTCCCCACCA

All primers purchased by Life Techologies

5.1 PCR-Array

RT^2 Profiler PCR Array (Qiagen) takes advantage of Real-Time PCR performance and combines it with the ability of microarrays to detect the expression of many genes simultaneously. The Mouse Epithelial to Mesenchymal Transition pathway (PAMM-090ZA) in $Mambo89^{HER2stable}$ and $Mambo38^{HER2loss}$ cell lines was investigated. This PCR array contains a panel of 84 pathway-focused genes that either change their expression during EMT or regulate those gene expression changes, plus five housekeeping genes and three RNA and PCR quality controls.

The RNA samples extracted by TRIzol, purified by the Rneasy Plus Micro kit (Qiagen, Milano) and quantified by spectrophotometer were converted into first strand cDNA by using the RT2 First Strand Kit (Qiagen). 1μg of total RNA was first treated with GE 5× buffer in order to eliminate any residual genomic DNA contamination, than RNAasi-free H_2O was added to reach a final volume of 10 μl. RNA samples were incubated 5 minutes at 42° C. Then was reverse transcribed in 10ul of RT Cocktail,

containing: 4 µl of Buffer RT 5X (BC3), 1 µl of Primer (P2), 2 µl of Retrotranscriptase (RE3), 3 µl of RNAasi-free H_2O. RNA was incubated at 42°C for 15 minutes and then the reaction was stopped by heating at 95°C for 5 minutes. 91 µl of ddH_2O to each cDNA sample were added.

Real-Time PCR was performed using the SyBR Green method, following the protocol provided with the reagents. A solution containing the RT^2 qPCR Master Mix 2× (Quiagene) and 102 µl of cDNA diluted in 1173 µl of ddH2O was prepared. Then 25 µl were dispensed in each well of the PCR array. The amplification was carried out by using Thermal Cycler Gene Amp 5700 Detection System, Applera, as follows: 95°C for 10 minutes to activate the HOSTstart DNA polymerase, then 40 cycles composed by 95°C for 15 seconds and 60°C for 1 minute. A default melting curve program was used to obtain the dissociation curve for each well in the entire plate.

For each well the threshold cycle (Ct) was calculated. When Ct values were greater than 35 or genes were N/A (not detected), a value of 35 was assigned and genes were considered as not expressed. Data were analyzed and interpreted calculating the ΔΔCt value, in order to do normalization over the mean of housekeeping genes and to obtain the relative expression value in respect to $Mambo89^{HER2stable}$, the internal calibrator.

$$\Delta Ct = Ct\ gene - Ct\ mean\ of\ housekeeping\ genes$$

$$\Delta\Delta Ct = \Delta Ct\ Mambo38 - \Delta Ct\ Mambo89$$

The relative quantity fold change (Qr) of mRNA expression levels for each sample was calculated from the following formula

$$Qr = 2^{(-\Delta\Delta Ct)}$$

A relative expression corresponding to +4/-4 was considered associated to up-regulated or to down-regulated genes respectively.

6. Western Blot analysis

Frozen tumor tissue was completely immersed in lysis buffer consisting of Novagen PhosphoSafe Extraction Reagent (EMD Millipore) plus phosphatase and protease inhibitors (Sigma-Aldrich). Tissue was dissociated and homogenized by gentleMACS Octo Dissociator (Miltenyi) and then incubated for 10 minutes at room temperature. Nuclei were removed by centrifugation at 12.000 RCF at 4°C for 15 minutes, and the protein concentration in the supernatants was determined by DC Protein Assay (Bio-Rad Laboratories) using bovine serum albumin as the standard.

Proteins were separated on an 8% polyacrylamide gel (20 μg of total lysate) and then transferred to polyvinylidene difluoride membranes (Bio-Rad Laboratories). After blocking with PBS containing 0.1% Tween 20 plus 5% nonfat dry milk for 2 hours at room temperature, membranes were incubated overnight at 4°C with primary antibodies diluted in blocking buffer. After incubation with the respective horseradish peroxidase–labeled secondary antibodies (Santa Cruz Biotechnology), protein presence was revealed by chemiluminescence reaction (LiteAblotplus chemiluminescence substrate; EuroClone). Densitometric analysis was performed on the scanned images using gel analysis software (TotalLab). Actin was employed for western blot normalization as internal loading control.

Table 6. Antibodies used in Western blot

Primary antibody	Clone	Company	Dilution	Secondary antibody	Dilution	PM (kDa)
α-HER2	3B5	Calbiochem, USA	1:1000	Goat-α-mouse IgG-HRP	1:10000	185
α-pHER2 (Tyr1248)	policlonal	Santa Cruz Biotechnology, Inc.	1:1000	Goat-α-rabbit IgG-HRP	1:1000	185
α-Akt	policlonal	Cell Signaling Techology	1:1000	Goat-α-rabbit IgG-HRP	1:1000	60
α-pAkt (Ser473)	D9E	Cell Signaling Techology	1:1000	Goat-α-rabbit IgG-HRP	1:1000	60
α-MAPK	137F5	Cell Signaling Techology	1:1000	Goat-α-rabbit IgG-HRP	1:1000	42-44
α-pMAPK Erk1/2 (Thr202/Tyr204)	policlonal	Cell Signaling Techology	1:500	Goat-α-rabbit IgG-HRP	1:1000	42-44
α-actin	policlonal	Sigma-Aldrich	1:800	Goat-α-rabbit IgG-HRP	1:1000	42-43

PM = molecular weight

7. MYC inhibition and signaling

The experiments on Myc inhibition were performed in the Laboratory of Dr. Laura Soucek (Mouse Models of Cancer Therapies Laboratory, Vall d'Hebron Hospital, Barcelona). Three mouse mammary tumor cell lines were employed in this project: MAMBO 89^{HER2stable}, MAMBO38^{HER2loss}, MAMBO43^{HER2lable}.

7.1 Viral vectors and infection

Complete lentiviral vectors (pTRIPz and/or pSLIK) harbouring both the rtTA and TRE elements were beforehand constructed to provide doxycycline (dox) regulated expression of omomyc. The Red Fluorescent Protein (RFP) gene was cloned in pTRIPz vector under the same promoter as a reporter gene.

For infections, 293T cells were seeded at 70% confluence and the following morning 25 μM chloroquinone added. Two hours later, 293 cells were transfected with pTRIPZ-omomyc plus the lentiviral vectors pMD2G and psPAX2 by the CaPO4 method. The medium was changed the following day and sodium butyrate added at 5 mM. Viral supernatants were harvested on the subsequent 2 days, filtered and added to target cells with polybrene (0.8 μg ml−1). The infected cells were selected using Puromicyn dose antibiotic (Gibco).

7.2 Omomyc detection

The expression of omomyc was detected by checking RFP expression after 4 days of doxycycline dose subministration measured by Invitrogen™ Tali™ Image-based Cytometer.

Omomyc expression was analyzed as well by direct immunofluorescence on cell culture. Cells were seeded on coverslips in six-well plates and treated with dox (1ug/ml). MAMBO43^{HER2labile} was seeded at 10.000 cells/well and MAMBO38^{HER2loss} was seeded at 1000 cells/well. At 96 h from the treatment, after removing the medium cells were washed with PBS, then fixed with 4% Paraformaldehyde (Sigma Aldrich). Cells were then permeabilized in PBS containing 0.5% Triton X-100 and blocked in Blocking buffer containing: 0.2 % Triton X-100, 2% BSA and 1 % goat serum.
Omomyc was detected by using a primary rabbit polyclonal antibody affinity purified and selected against the MYC b-HLH-LZ epitope (omomyc IG-1325 dil 1:50 in blocking buffer) and a secondary anti-rabbit polyclonal antibody conjugated to Alexafluor (488 Invirogen, 1:500). After immunostaining, cells were mounted on microscope slides with DAPI-containing Vectashield mounting solution (Vector Laboratories). For both omomyc-expressing and control cells. Images were collected with an Axiovert S100 TV inverted fluorescence microscope (Zeiss) and Open Lab 3.5.1 software.

7.3 Omomyc antiproliferative assays *in vitro*

The efficacy of omomyc expression upon dox (1μg/ml) subministration was evaluated in MAMBO38^{HER2loss} and MAMBO43^{HER2labile} pTRIPz-omomyc infected cell lines *in vitro* by Colony Formation Assay in 1-3 independent experiments.

Cells were seeded at 500 cells/well in a 6 well plate, in triplicate with dox (1ug/ml) or without as control. After 2 weeks of treatment cells were fixed and stained with crystal violet. The sensivity to the treatment was measured as percentage of grown colonies compared to the control and quantified by ImageJ program.

7.4 BrdU incorporation assay

A total of 106 cells were seeded in triplicate in 12-well plates with or without dox (1ug/ml). On the third day, cells were incubated for 2 h with the BrdU substrate (Roche), collected and fixed overnight in 70% ethanol. Staining with the BrdU antibody (BD Biosciences) was performed following the manufacturer's instructions. Cells were then stained with propidium iodide and analysed with a FACSCalibur flow cytometer (BD Biosciences) for cell cycle analysis.

7.5 Drug sensivity *in vitro*

The therapeutic effect of omomyc alone or in combination with lapatinib was tested *in vitro* on MAMBO43^{HER2labile} and MAMBO^{38HER2loss} inducible cells lines. The inducible cell line JIMT-1 pSLIK-omomyc already developed in the host laboratory, was included as control. Cells were seeded in triplicate in 24 well plates. MAMBO38^{HER2loss} was seeded at 4000 cells/well, the other cell lines at 9,000 cells/well. Cells were treated after 24 hours from seeding. The following drugs, alone or in combination, were added to the medium: lapatinib (1uM) and dox (1ug/ml). As control, cells were grown without any treatment or with DMSO (0,01%). Plates were maintained at 37°C in a humidified 5% CO2 atmosphere. At 72 hours and 96 hours from treatment cells were trypsinized and counted by cell counter (Vi-CELL XR Cell Viability Analyzer Beckman Coulter). Drugs' efficacy was assessed in 1-4 independent experiments.

Cell lysates were obtained and Western blot was performed in the Laboratory of Biology and Immunology of Metastases as described in paraghraph 6 of this section.

8. Preclinical models

8.1 Spontaneous carcinogenesis in transgenic models and preventive therapy

HER2, Delta16 and F1 female mice were inspected weekly by palpation to investigate tumor incidence, latency and number of tumors per mouse (multiplicity). During inspection, diameters of the first tumors arisen in animals were measured with caliper to evaluate tumor dimensions (progressively growing masses ≥50 mm^3 were scored as tumors). Tumor size was calculated as follows:

$$\frac{\pi}{6}(\sqrt{a \times b})^3$$

where a = maximal tumor diameter, b = maximal tumor diameter perpendicular to a.

At necropsy, samples of tumor masses were collected for further analyses (Immunofluorescence or Real-time PCR, see paragraph 3 and 5). Samples for molecular analyses were frozen in liquid nitrogen and stored at -80°C. Non-neoplastic mammary glands were collected from 5-week-old F1 HER2/Delta16 mice.

Lungs were perfused with black India ink (15% in water, Rotring) to outline metastases and fixed in a modified-Fekete's solution (95.7% ethanol 96%, 4.3% glacial acetic acid). Autochthonous lung metastases were counted using a dissection microscope.

To study the prevention of primary tumor growth, HER2 mice, Delta16 mice and F1 HER2/Delta16 mice were treated twice weekly intraperitoneally with trastuzumab (4 mg/kg) starting from 17 weeks of age for HER2 mice and from 5-8 weeks of age for Delta16 and F1 HER2/Delta16 mice. Control mice were treated with physiological solution.

8.2 Syngeneic transplantation models and therapy

In HER2 model, $MAMBO38^{HER2loss}$ (10^5 cells) or $MAMBO43^{HER2labile}$ (10^6 cells) were injected subcutaneously in 10 HER2 mice per group (7-23 weeks old) in 0.2 ml of PBS to obtain the development of mammary tumors.

1 day after cell injection, mice were randomized into two groups (5 mice/group) and treatments started. Treated mice (two groups) received daily per os 40 mg/kg of GNE-317. Control mice received Metocell 0.5% Tween80 + 0.4% per os (vehicle of GNE-

317 therapy). Mice were sacrificed 3 weeks (MAMBO38^{HER2loss}) or 7-9 weeks (MAMBO43^{HER2labile}) after cell injection.

To study the inhibition of tumor growth, fragments of a pool of 4 F1 tumors, expressing different levels of HER2 and Delta16, were implanted in the fourth left mammary fatpad of 10-16-week-old FVB (non-transgenic) female mice (n=10 for each group). Starting 7 days after fragment implantation, mice received twice weekly the intraperitoneal injection of trastuzumab (4 mg/kg) for four weeks, or five times a week orally buparlisib (50 mg/kg) for 4 weeks; control group received the administration of NaCl solution 0.9%.

For mouse-derived isograft, fragments of F1 mammary tumors were serially implanted in the fourth left mammary fatpad of 5-17–week–old HER2 transgenic female mice. Tumors grown from serial grafts of fragments from two F1 tumors (here referred to as HER^{high}Delta16^{high} and HER^{low}Delta16^{high}) were harvested for molecular investigation and also immediately implanted into other mice.

8.3 Patient Derived Xenograft

For the PDX model generation fresh fragments of human breast tumors were sterilely collected during surgical procedures by S.Orsola-Malpighi Hospital, Bologna and Bellaria Hospital, Bologna, put in cold complete medium, stored on ice and immediately delivered by the animal facility. Specimens were serially implanted in the fourth left mammary fat pad in 5-10 week-old NOD-SCID-Il2rg−/− female mice (Jackson Laboratories) or BALB/cRag2−/−Il2rg−/− female mice (CIEA, Japan). Written informed consent was obtained from patients and all experiments were authorized by the institutional review board of the University of Bologna and done according to Italian and European laws and guidelines.

Mice were inspected weekly by palpation to investigate tumor growth. During inspection, the diameter of the tumor arisen was measured with caliper to evaluate tumor dimensions as described in paragraph 8.1.

Mice were sacrificed when tumoral burden was equivalent to 10% of body mass. At necropsy, tumor fragments were harvested for cellular and molecular investigation and also immediately implanted into other mice. Tumor masses collected for immunofluorescence were handled as described in paragraph 3.

Samples collected for Western Blot or Real-time PCR (see paragraph 5 and 6) were frozen in liquid nitrogen and stored at -80°C. Samples for immunohistochemistry were fixed in 10% neutral buffered formalin and then analyzed by the Pathology Unit of Bellaria Hospital of Bologna or by the Patology Unit of Sant'Orsola Hospital of Bologna.

To study the sensitivity to HER2 targeted drugs *in vivo*, FO4 HER2-positive breast PDX bearing mice were treated, when tumors were palpable, with trastuzumab (Herceptin, Roche) 4mg/kg, 2 times a week through intraperitoneal injection (ip) or with neratinib (Puma Biotechnology) 40mg/kg, 5 times a week per os. Control groups did not receive any treatment.

9. Statistical analysis

Mantel-Haenszel's test, Student's t test and X^2 Fisher's exact test were used to analyze and compare the data presented in this thesis.

RESULTS

1.HER2 loss

Progression of HER2 positive breast cancer can result in the emergence of HER2-negative tumor variants that activate alternative mitogenic pathways, either spontaneously or after therapy. We found that HER2 loss occurs even in transgenic mouse models in which the oncogene is driven by viral promoters (MMTV), thus mammary carcinoma of human HER2 transgenic mice (huHER2 mice) can be used to study not only the early phases of HER2-driven mammary carcinogenesis, but also tumor progression beyond HER2 addiction.

1.1 Loss of HER2 expression in FVBhuHER2 cell lines

Cell lines grown from HER2 positive mammary carcinomas can present progressive loss of HER2 expression; In the Laboratory of Immunology and Biology of Metastasis of Bologna, it has been established a model system consisting of cell lines, clones and variants that exhibit one of three phenotypes: a) high and stable HER2 expression *in vitro* and *in vivo*, b) high but labile HER2 expression which is lost either during *in vitro* culture or after tumor growth in mice, and c) complete loss of HER2 expression (Nanni et al., AACR 2014, Abstract number 1820). This panel of cell lines is a useful model to study the dynamics of HER2 loss in advanced HER2-positive mammary carcinoma, and to analyze alternative therapeutic strategies.

Mambo89^{HER2stable} cell line was established from a spontaneous mammary carcinoma of a huHER2 female mouse, it presents a high and stable expression of huHER2, both *in vitro* and *in vivo*. Mambo43^{HER2labile} cell line was derived from a mammary carcinoma grown after the subcutaneous injection in a huHER2 female mouse of a HER2 cell line established from a spontaneous huHER2 mammary carcinoma; it presents a high but unstable expression of HER2, which it is lost either after *in vitro* cloning or after *in vivo* growth. From tumors grown after the subcutaneous injection of Mambo43^{HER2labile}, Mambo38^{HER2loss} line was obtained and established *in vitro*. Mambo38^{HER2loss} has completely lost the expression of HER2 and showed both an increased tumorigenic capacity and a higher metastatic capacity, in particular for what concerns the metastatic load in the lungs, as compared to Mambo89^{HER2stable}.
While Mambo89^{HER2stable} and Mambo43^{HER2labile} lines have epithelial morphologies and grow in monolayer, Mambo38^{HER2loss} has a fusiform morphology that resembles

mesenchymal cells. Therefore the correlation between HER2 expression, stem cell phenotype and ability to undergo the epithelial-mesenchymal transition were studied.

1.1.1 Stemness of FVBhuHER2 cell lines

The stemness of FVBhuHER2 cell lines was analyzed by studying their ability to growth in non-differentiating conditions forming mammospheres and characterizing cells by their surface phenotype in order to identify specific surface markers.

Single-cell suspensions of FVBhuHER2 cell lines were grown under conditions that do not allow adherence to the substratum, as described in the Materials and Methods. Figure 1 shows mammospheres cultured from the three breast cancer cell lines.

Mambo38^{HER2loss} produced a significantly higher number of mammospheres as compared to Mambo89^{HER2stable} and Mambo43^{HER2labile}. Furthermore, Mambo38^{HER2loss} mammospheres were larger in respect to the other cell lines.

(A)

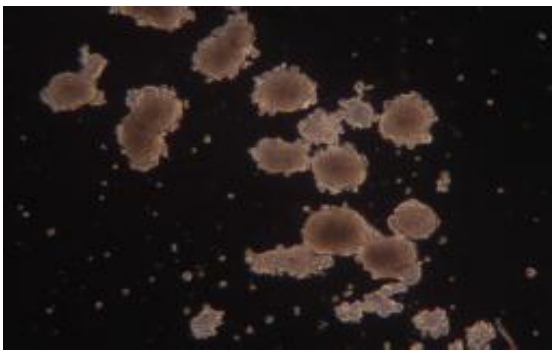

Mambo89^{HER2stable}	
N° mammospheres	23±1$^{\#\#}$
N° Cells/mammosphere	806

(B)

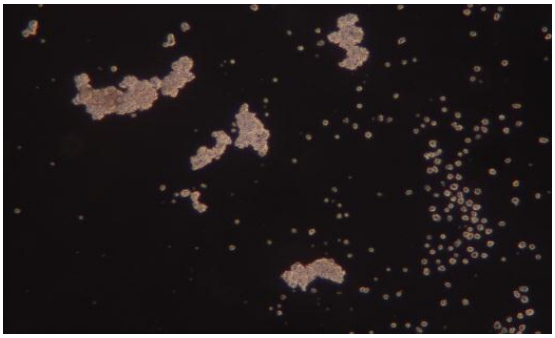

Mambo43^{HER2labile}	
N° mammospheres	17±1
N° Cells/mammosphere	Non detectable

(C)

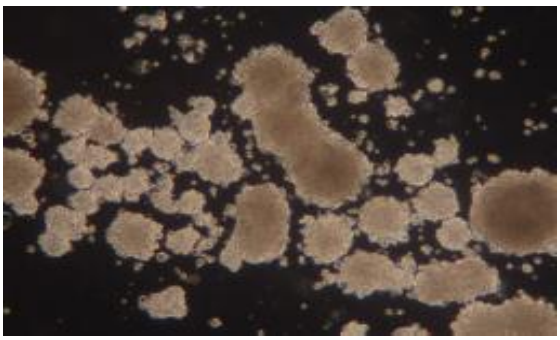

Mambo38^{HER2loss}	
N° mammospheres	69±9**
N°Cells/mammospheres	5100

Figure 5: Capability of FVBhuHER2 cell lines to form mammospheres. The figure represents the images of mammospheres obtained from FVBhuHER2 cell lines, obtained through Diavert (2.5 × objective) inverted microscope and shot with Canon EOS600D Camera: (A) Mambo89^{HER2stable}, (B) Mambo43^{HER2labile}, (C) Mambo38HER2loss e (D) Mambo34 L2. The table at the right side of each image indicates the average number of mammospheres, in 4 independent experiments; Statistical analysis: (Test t Student): Mambo38HER2loss vs all cell lines p<0,01 (**); Mambo34 L2 vs Mambo43^{HER2labile} p<0,05(*); Mambo89^{HER2stable} vs Mambo43^{HER2labile} p<0,01 (##); and the number of cells contained in each mammosphere, counted in one single well.

Cancer stem cells have been identified by immunofluorescence using different surface markers: $CD44^{+}/CD24^{-,}$ associated to a subpopulation of breast cells reported to have stem properties (Sheridan et al., 2006); CD29 surface antigen, expressed in isolated fibroblastic mesenchymal stem-cell like cells (Lorenz et al., 2008); Sca-1, present in murine mammary stem cells (Grange et al., 2008) (Figure 5).

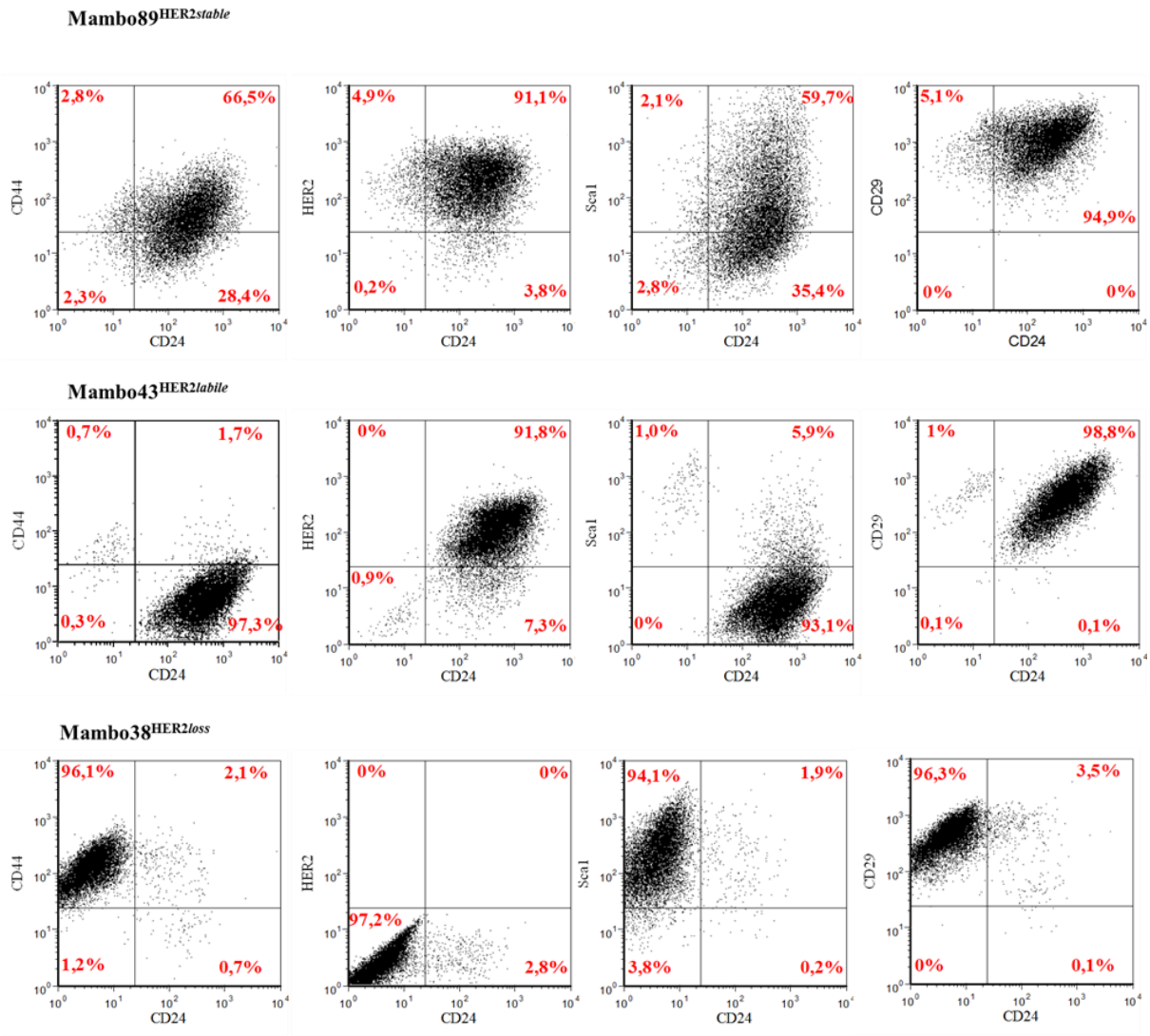

Figure 6: Expression of stem cell markers in FVBhuHER2 lines. For each FVBhuHER2 cell line grown in continuos culture, is reported the basal expression of huHER2 and stem cell markers CD24, CD44, Sca-1 and CD29. The percentage of cells contained in each quadrant is shown in red.

Mambo38^{HER2loss} showed the most expressed stem-like profile, with 96% of CD44+CD24− cells, 94% of Sca-1+CD24- cells and the 96% of CD29+CD24- cells. Mambo89^{HER2stable} was positive for Sca-1 (60% of cells), but only 5% of analyzed cells were CD29+CD24-. Mambo43^{HER2labile} cell line expressed the lowest amount of stem markers (0.7% CD44+CD24-, 1% Sca-1+CD24-, 1% CD29+CD24-) (Figure 6).

1.1.2 Epithelial to Mesenchymal transition (EMT) and HER2 loss

To determine whether EMT occurs, the genes most specifically expressed in each state were studied. Among 84 key genes analyzed, that either change their expression during this process or regulate those gene expression changes, we have found that 16 were overexpressed (19%) and 19 down-expressed (23%) in Mambo38^{HER2loss} in comparison to Mambo89^{HER2stable} (Table 5).

The up-regulated genes included genes mediating cell adhesion, migration, motility, and morphogenesis: collagen genes Col3a1 and Col5a2, known to be up-regulated by TGF-1β induction of EMT (Hosper et al, 2013); Secreted Protein Acidic and Rich in Cysteine (SPARC), a matricellular protein that is important for the regulation of cell growth and adhesion; Versican, a large extracellular matrix proteoglycan supposed to promote cancer metastasis by facilitating cell proliferation, adhesion, migration and angiogenesis; Insulin-like growth factor binding protein 4 (Igfb4), a protein able to control the up-regulation of several factors involved in tumor growth, EMT and invasion such as pAkt, pErk, Vimentin, and N-cadherin and down-regulation of E-cadherin (Praveen et al, 2014). Moreover was detected an increased gene-expression of proteases, such as the matrix metalloproteinases MMP2 and MMP9, these proteins enhance ECM protein degradation and enable invasion (Nistico P. et al, 2012).

Among the 19 underexpressed genes, we identified some hallmarks of EMT, e.g. E-cadherin, whose downregulation is important in order to reinforce the destabilization of adherens junctions; In addition, it was observed the repression of genes encoding claudins and occluding, desmoplakin and plakophilin, that respectively stabilizes the dissolution of apical tight junctions and desmosomes (Huang RY et al, 2012). Summarising HER2 loss seems associated to EMT mechanism.

Genes up and down expressed in Mambo38^{HER2loss} compared to Mambo89^{HER2stable}

Over expressed	**Relative expression**	**Under expressed**	**Relative expression**
Col3a1	513	Cadherin	-438
Col5a2	34733	Occludin	-49
Col 12	45	Keratin 7	-270
Pdgfrb	134	Keratin 14	-19
Igfbp4	275	Fgfbp1	-252
Sparc	8	Il1rec. antag.	-112
Versican	130	Desmoplakin	-1021
Mmp2	15	Desmocollin2	-26
Wnt5a	113	F11r	-18
Itg5a	21	Sox10	-309
Nudt13	6	Wnt5b	-37
Mtap1	5	Serpine1	-19
TCF4	11	Snai3	-11
ZEB-1	7	Notch1	-9
ZEB-2	5	Mmp9	-5
TGF-β1	5	ErbB3	-16
		EGFR	-4
		Tmeff	-9
		Bmp7	-4

Table 5: Gene expression associated with HER2 loss. The left side of the table shows over-expressed genes in Mambo38^{HER2loss} compared to Mambo89^{HER2stable} line, while the right column shows those under-expressed. The analysis was performed by RT2 Profiler PCR Array, using the mouse Epithelial to Mesenchimal Transition Pathway. Genes are reported with relative expression value higher than +4 and lesser than -4.

1.2 Sensivity to anti-cancer therapies

The therapeutic efficacy of clinically approved or under experimentation drugs targeting HER2 or its signaling was studied in vitro and *in vivo*. Susceptibility to the following drugs was analysed:

- Trastuzumab (recombinant humanized monoclonal antibody that targets the extracellular domain of HER2), (Herceptin, Roche);
- Lapatinib (reversible kinase inhibitor that blocks the catalytic domain of HER2 and EGFR), (Tykerb and Tyverb, GlaxoSmithKline);
- Dasatinib (kinase inhibitor directed against Src kinase), (Sprycel, Bristol-Myers Squibb);
- Buparlisib (pan-class I PI3K inhibitor that penetrates the blood-brain barrier (BBB)); (Novartis);
- GNE-317 (dual PI3K/ mTOR inhibitor), (Genetech);
- Omomyc (dominant negative inhibitor of Myc), (proprietary of Dr. Soucek's laboratory).

1.2.1 HER2 loss as mechanism of resistance to Trastuzumab *in vitro*

MAMBO89^{HER2stable} and MAMBO43^{HER2labile} cell lines were grown in continuous culture (30 days) with trastuzumab (30μg/ml). After the treatment, cells were cultured without the drug for other 30 days. After 30 days of treatment and 30 days of recovery, the expression of HER2 was analyzed by immunofluorescence (Figure 6).

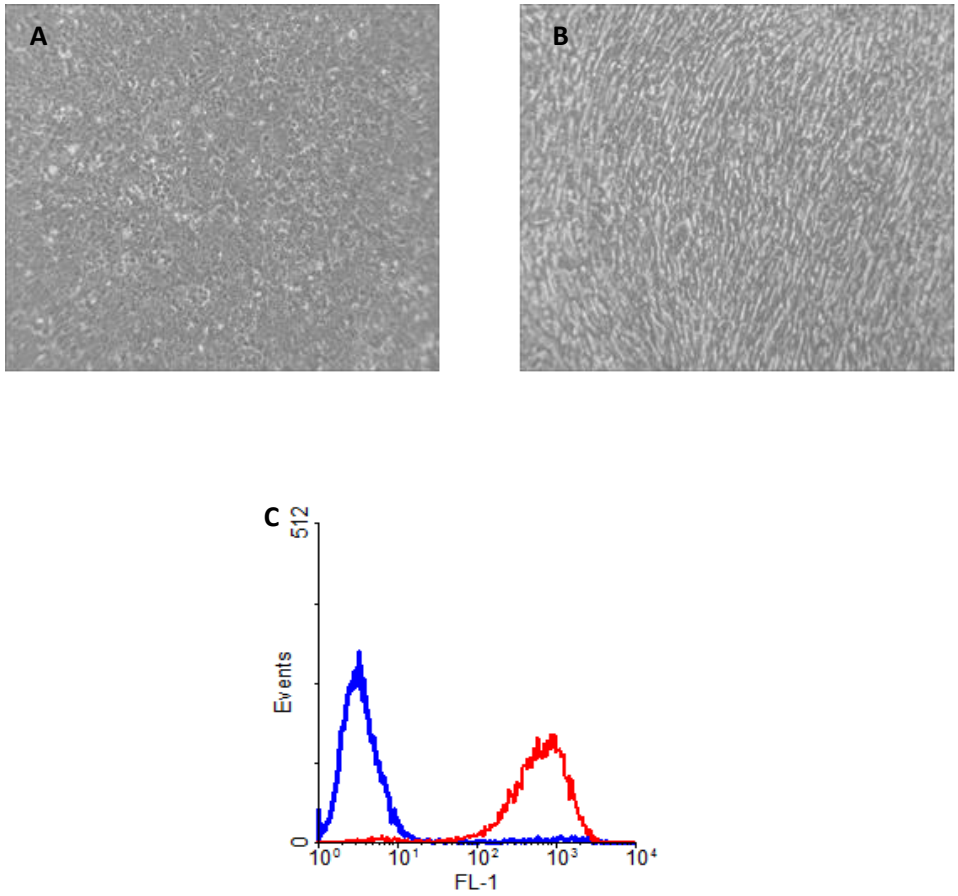

Figure 7: Sensivity to Trastuzumab of Mambo43HER2labile cell line. Images obtained by the observation of Mambo43^{HER2labile} cells cultured *in vitro* in absence (A) or in presence (B) of Trastuzumab (30 g/mL). (C) Mambo43^{HER2labile} cell line grown for 30 days in presence of Trastuzumab 30 mg / mL (blue profile) analyzed by flow cytometry to assess the expression of HER2, in comparison to Mambo43^{HER2labile} grown in medium alone (red outline). On the x-axis it is indicated the fluorescence intensity in arbitrary units is indicated on a logarithmic scale, while the y-axis shows the number of cells.

MAMBO89^{HER2stable} cell line was resistant to trastuzumab *in vitro* and showed a stable and high expression of HER2, either after the treatment or after the recovery period without trastuzumab. On the other hand, MAMBO43^{HER2labile} was sensitive to trastuzumab with approximately 60% of treated cells grown in respect to the control. Moreover, after the treatment this cell line changed from an epithelial shape to a mesencymal/fusiform-shaped phenotype, and did not express anymore HER2 even after the period of recovery (Figure 7).

1.2.2 Targeting HER2 and downstream targets

In vitro sensitivity to lapatinib, dasatinib and buparlisib of MAMBO89^{HER2stable} and MAMBO38^{HER2labile} were evaluated as percentage of grown colonies compared to the control in 3-D culture (0.33% soft agar containing the drug at a final concentration of 1 μM both in the underlayer and in the overlayer) (Figure 8). HER2 loss was accompanied by the loss of sensitivity to HER2 kinase inhibitor and to Src inhibitor, whereas the PI3K inhibitor was highly effective regardless of HER2 expression.

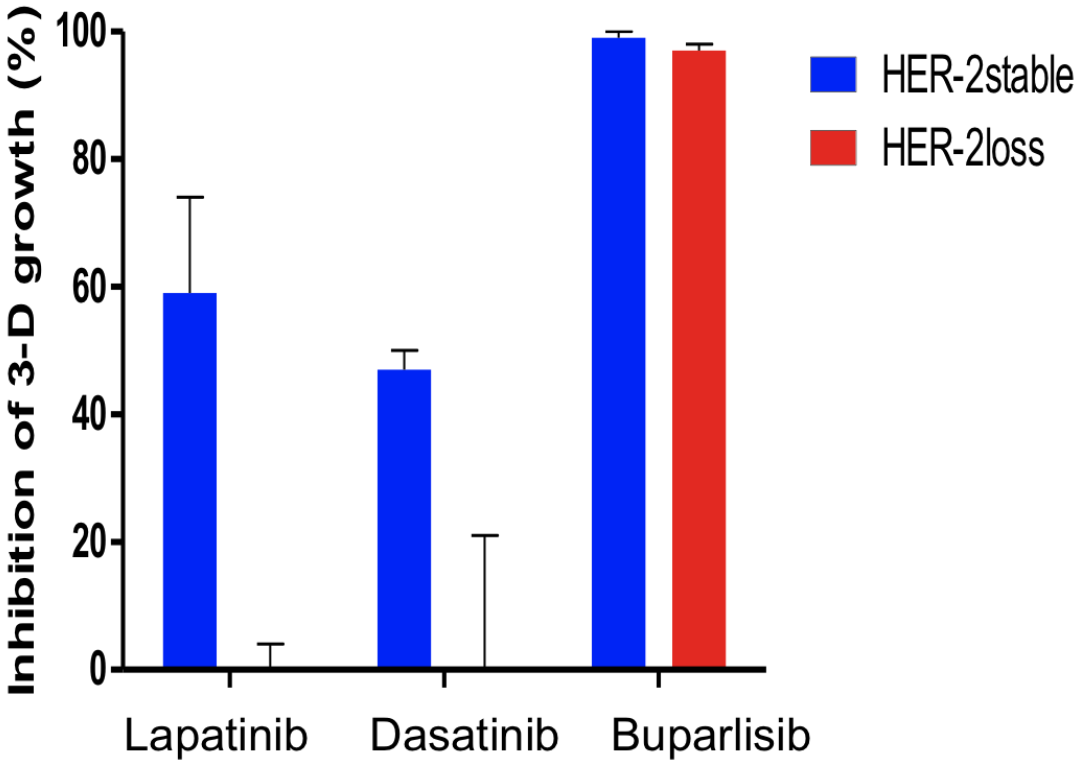

Figure 8: In vitro sensivity to target therapies. In vitro resistance to Lapatinib, Dasatinib (kind gifts from Dr. S Pupa, INT, Milan) and Buparlisib (Novartis) was evaluated by analyzing the growth inhibition of cell lines in a 3-D culture (soft-agar + MammoCult complete medium + 1% FCS). Drugs were added at a final concentration of 1 μM both in the underlayer and in the overlayer. Growth quantification was performed by colony counting and growth inhibition percentage was calculated.

The total and phosphorylated amount of protein factors that mediate the intracellular signaling of huHER2 in FVBhuHER2 lines was tested by western blot, 96h after the treatment with trastuzumab, buparlisib or their combination (Figure 9).

.

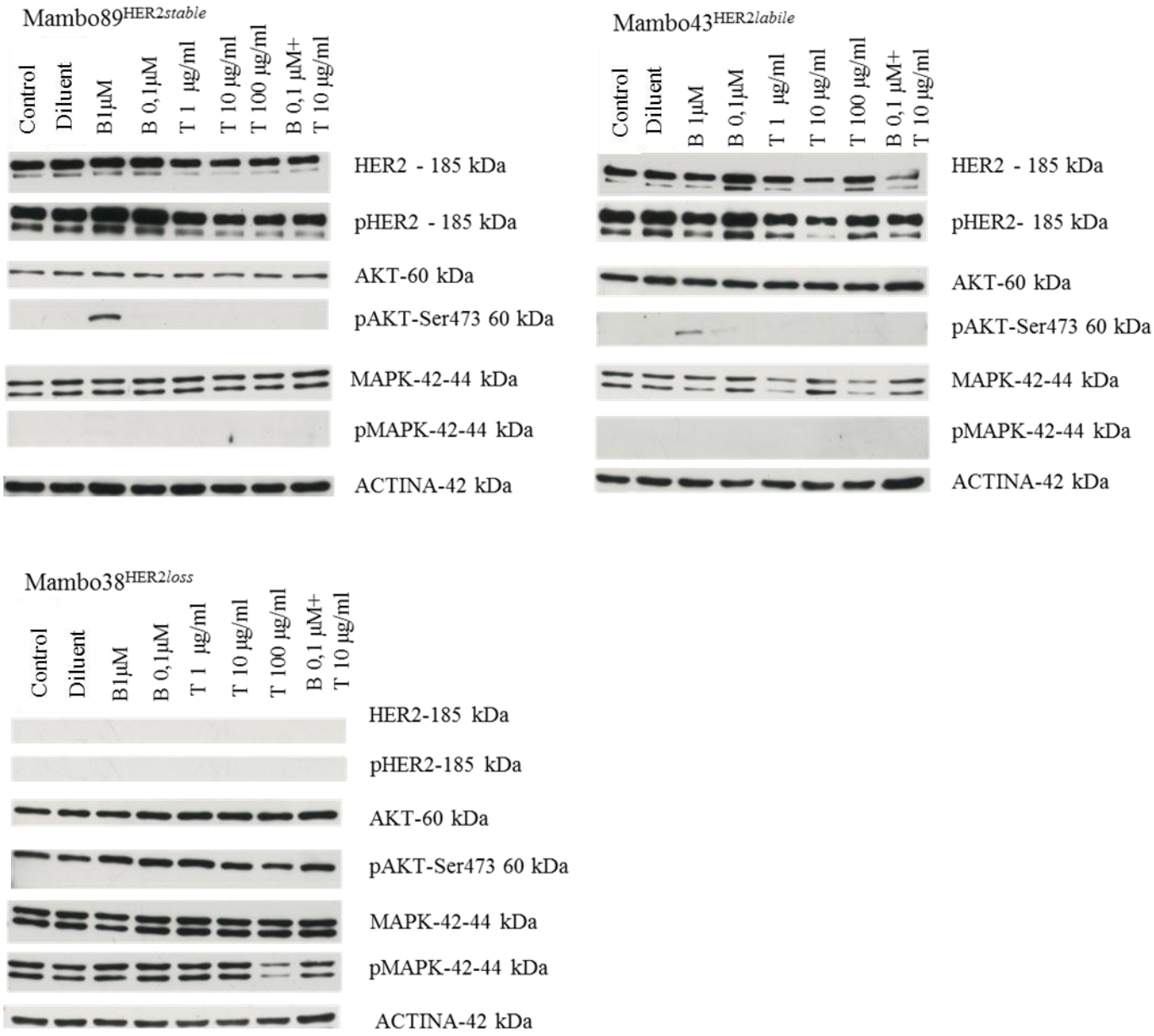

Figure 9: Modulation of the expression of second messengers downstream of HER2 in FVBhuHER2 cell lines after treatment with trastuzumab and buparlisib. The western blot images show, for each cell line, the protein expression of HER2, of the main downstream signal transducers of HER2, and their phosphorylated forms after 96 h of treatment with different concentrations of Trastuzumab (T) and Buparlisib (B) or their combinations,. Next to the name of each protein the molecular weight in kDa is reported.

In Mambo89^{HER2stable} and Mambo43^{HER2labile} cell lines pharmacological treatments did not significantly change the expression of HER2 and phosphoHER2. Notably, phospho-Akt was detectable only in the samples treated with buparlisib 1uM. Mambo38^{HER2loss} did not express neither HER2 nor pHER2 but the expression of Akt, MAPK and their phosphorylated counterparts were already higher in basal conditions compared to Mambo89^{HER2stable} and Mambo43^{HER2labile}. The high expression of pAkt and pMAPK in Mambo38^{HER2loss} could represent an index of their independence from the pathway of the huHER2 signaling, as demonstrated by the *in vitro* sensivity only to buparlisib.

The therapeutic effectiveness of the inhibition of the PI3K pathway was studied also *in vivo* by testing GNE-317, a dual PI3K/ mTOR inhibitor, in the HER2loss model. MAMBO43^{HER2labile} and MAMBO38^{HER2stable} were injected subcutaneously in FVB mice. The intraperitoneal (i.p) treatment with GNE-317 (40 mg/kg) compared to the vehicle (Metocell 0,5%+Tween80 0,4%, i.p.), significantly inhibited the growth of MAMBO38^{HER2loss} and MAMBO43^{HER2labile} (Student's t test, $p<0.005$ or $p<0,001$ respectively) (Figure 10).

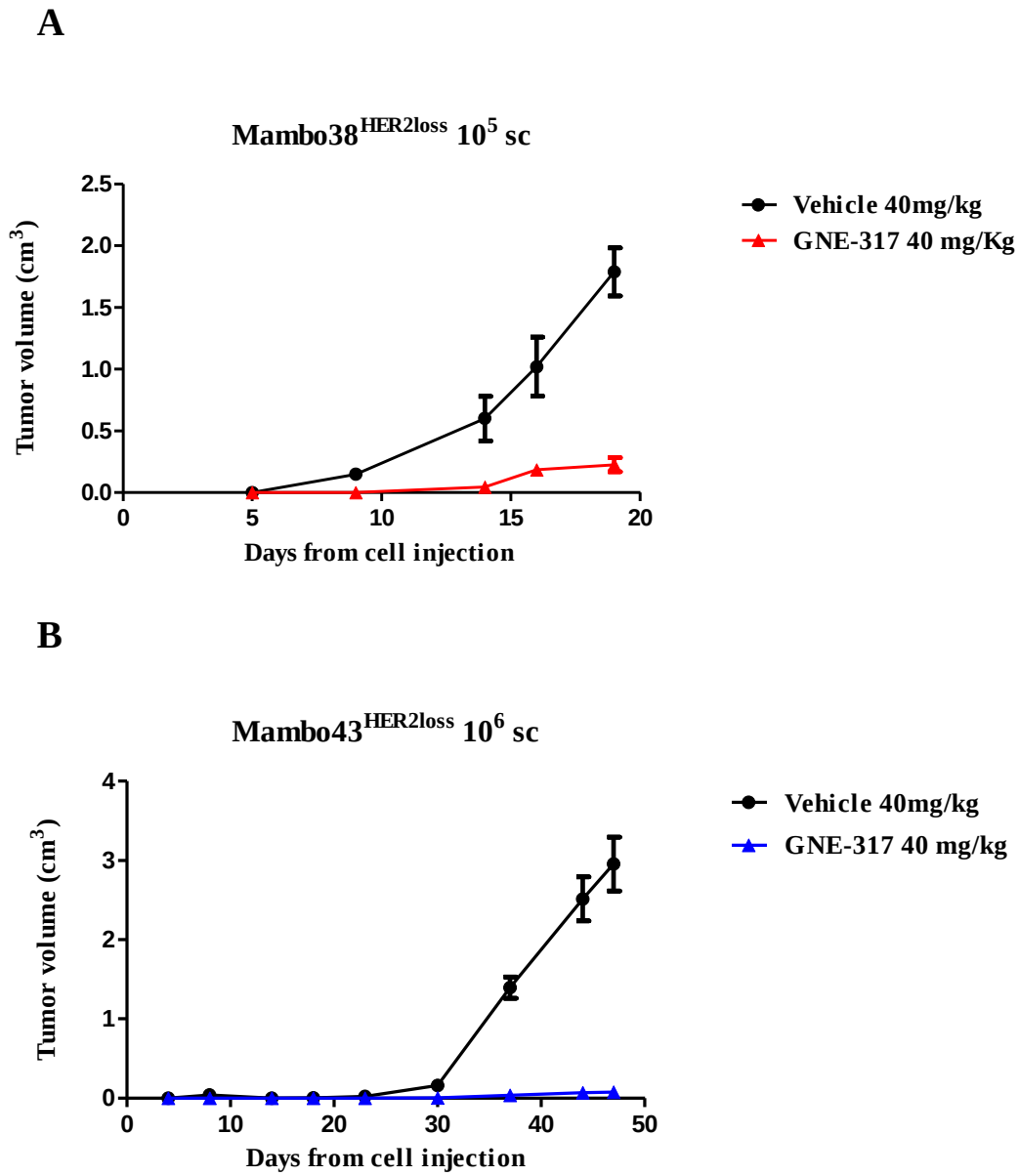

Figure 10: Therapy of localized HER2-positive breast cancer with GNE-317.

Study of the efficacy of GNE-317 (40 mg / kg per os) on the local growth of (A) Mambo38^{HER2loss} cell line (10^5 sc / 0.2 ml PBS) and (B) Mambo43^{HER2labile} cell line (10^6 sc / 0.2 ml PBS) in female FVBhuHER2 mice. For each cell line injected two groups of treatment are present, one receiving the vehicle (Metocell 0.5% Tween80 + 0.4%, n = 5), and the other treated with GNE-317. (A) n = 3, starting from n=5 two animals died for drug toxicity after 10 days of treatment, Statistical significance (Student's t test) : from day 16 $p<0.05$; (B) n = 4, starting from n=5 one animal died after the first treatment; from day 30 $p<0.001$ (Student's t test). Each point represents the mean tumor volume ± standard error until all mice per group are alive.

1.2.3 Myc inhibition

The inhibition of Myc was studied in collaboration with the Laboratory of Dr. Laura Soucek (Vall d'Hebron Institute of Oncology (VHIO), Barcelona, Spain).

Our goal in this project was to validate Myc inhibition as a therapeutic strategy to overcome resistance to therapy in HER2-positive tumors. In order to characterize omomyc's effect *in vitro* on MAMBO89^{HER2stable}, MAMBO43^{HER2labile} and MAMBO38^{HER2loss} cells lines, we have generated an inducible stable system of cell lines using a doxycycline-switchable lentiviral vector to drive the expression of omomyc.

Omomyc was cloned into the pTRIPZ lentiviral vector (Open Biosystems, Thermo Scientific) harbouring both the rtTA and TRE elements to provide doxycycline (dox) regulated expression of omomyc. The RFP gene was cloned under the same promoter as a reporter gene. The infected cells were selected using puromycin antibiotic and the expression of omomyc confirmed by checking RFP expression after 4 days of dox (1µg/ml) administration (Figure 11A-12A).

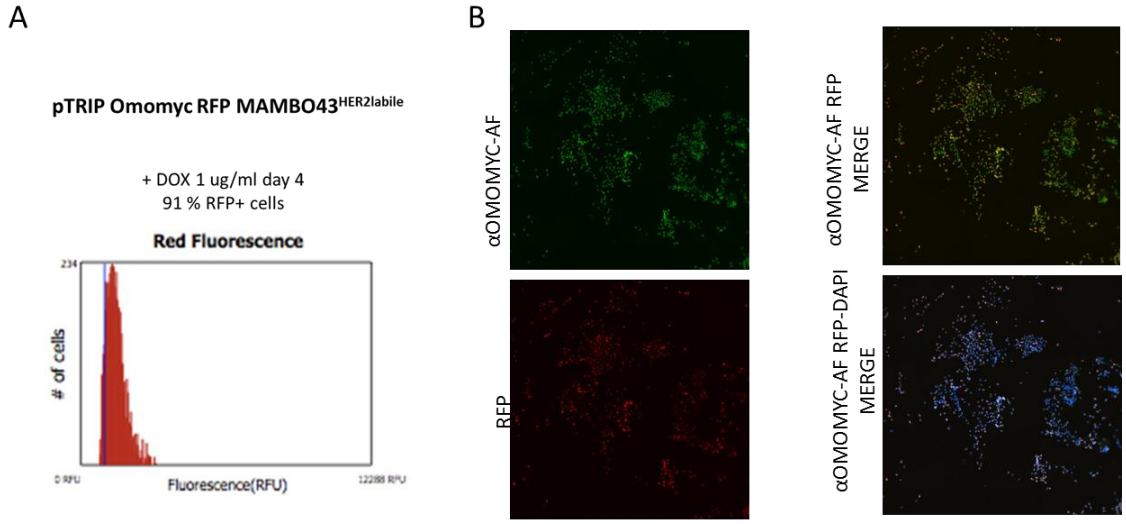

Figure 11: Omomyc induced expression in MAMBO43^{HER2labile} pTripz-omomyc infected cell line. (A) Intensity of RFP fluorescence measured by Invitrogen™ Tali™ Image-based Cytometer after 4 days of treatment with dox (1µg/ml). (B) Immunofluorescence assay showing omomyc expression in green, RFP in red, DAPI in blue; detected by fluorescence microscopy after 4 days of treatment with dox (1µg/ml).

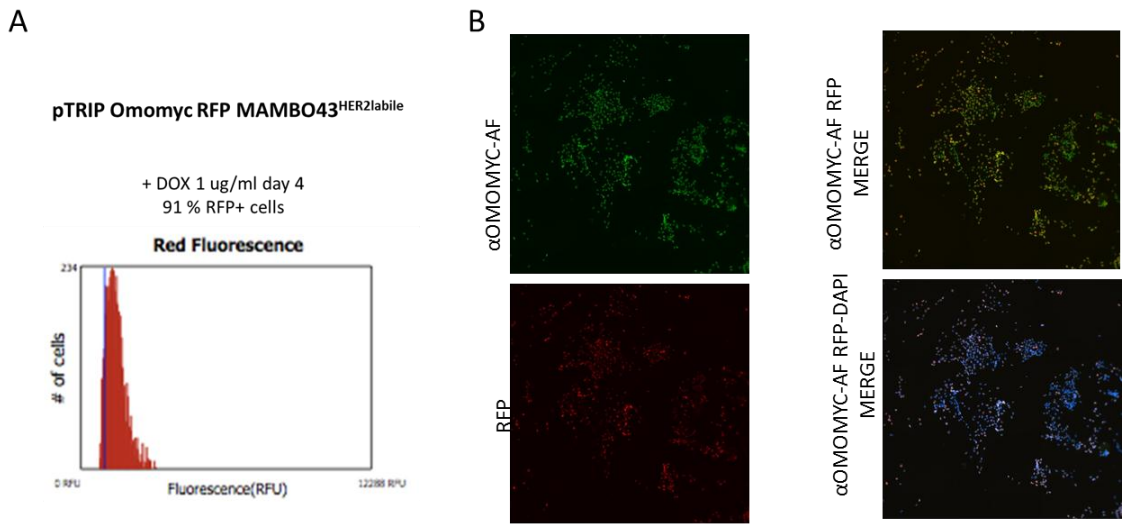

Figure 12: Omomyc induced expression MAMBO38^{HER2loss} pTripz-omomyc. (A) Intensity of RFP fluorescence measured by Invitrogen™ Tali™ Image-based Cytometer after 4 days of treatment with dox (1µg/ml). (B) Immunofluorescence assay, showing omomyc expression in green, RFP in red, DAPI in blue; detected by fluorescence microscopy after 4 days of treatment with dox (1µg/ml).

Omomyc expression was analyzed by immunofluorescence as well, using an anti-omomyc antibody (OMOMYC IG-1325) and compared with RFP expression (Figure 11B-12B). Both for MAMBO43^{HER2labile} and MAMBO38^{HER2loss} nearly 100% of cells were expressing omomyc. The RFP signal correlated with high specificity with anti-omomyc alexafluor signal, confirming the reliability of the gene reporter system. MAMBO89^{HER2stabile} was, however, much more challenging to infect, due to its high sensitivity to the infection process alone. Despite all the attempts, it was not possible to obtain the latter cell line with high and stable levels of omomyc expression.

The efficacy of transgenic omomyc expression upon dox addition (1µg/ml) was evaluated *in vitro* in MAMBO38^{HER2loss} and MAMBO 43^{HER2labile} infected cell lines by colony formation assay in 3 independent experiments (Figure 13-14).

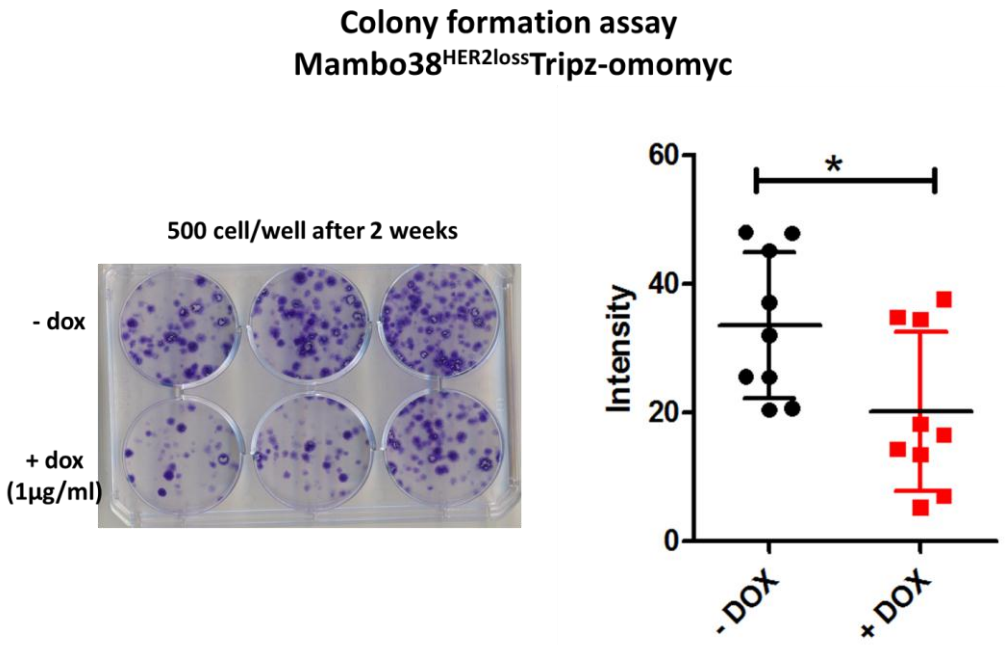

Figure 13: The suppressive effect of Omomyc on proliferation of MAMBO38^{HER2loss} infected cell line. Representative images of colony-formation assay of MAMBO38^{HER2loss} pTripz-omo untreated or treated with doxycycline and the corresponding quantification. Data are represented as means ± SD of three independent experiments. Statistical analysis was done using the Student's t test:*p < 0.05 vs. control group.

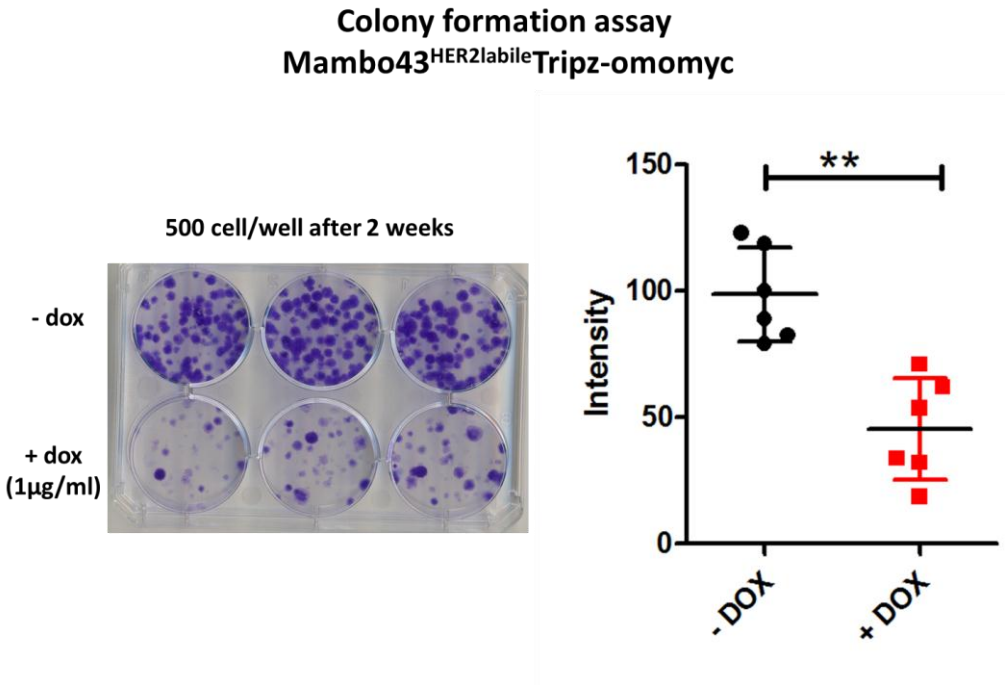

Figure 14: The suppressive effect of omomyc on proliferation of MAMBO43^{HER2labile} infected cell line. Representative images of colony-formation assay of MAMBO43^{HER2labile} pTripz-omo untreated or treated with doxycycline and the corresponding quantification. Data are represented as means ± SD of three independent experiments. Statistical analysis was done using the Student's t test:**p < 0.001 vs. control group.

Both cell lines resulted to be sensitive to omomyc. The effect of Myc inhibition was statistically significant in the colony formation assay. After treatment, there was a reduction of 80% in MAMBO38^{HER2loss} cells growth compared to the control, in contrast with a 55% reduction of MAMBO43^{HER2labile}.

The effect of omomyc on cell proliferation was further investigated by BrdU Incorporation assay (Figure 11).

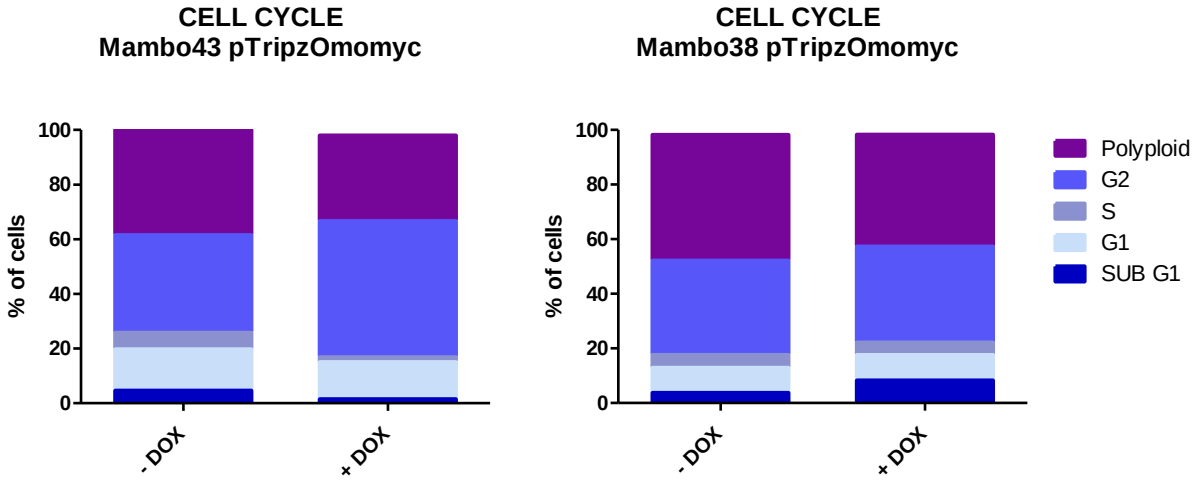

Figure 15: Cytometric Analyses of BrdU incorporation assay. Cell proliferation was measured by BrdU incorporation assay MAMBO38^{HER2loss} infected with PTripz-OMO -/+ DOX (1ug/ml) and MAMBO43^{HER2labile} infected with PTRIPZ-OMO -/+ DOX (1ug/ml) 72 hours after treatment. Analysis of the subpopulations of cells in cell cycle phases G1, S, sub G1, Polyploid and G2. Statistical comparisons were made by Student's t-test. Mambo43^{HER2labile}: S phase untreated vs treated ***p<0.0001; G2 phase untreated vs treated *p<0.05; Sub G1 phase untreated vs treated **p<0.001; Polyploid phase untreated vs treated **p<0.001; Mambo38^{HER2loss} Polyploid phase untreated vs treated * p<0.05.

After treatment, omomyc expressing MAMBO43^{HER2labile} cells were not able to proliferate as demonstrated by a significantly lesser percentage of cells in S phase compared to the control (Figure 15). A similar reduction can also be seen in sub G1 and in polyploid phases. Instead, there were more cells in G2 phase. This profile resembles that one of a cell population which does not proliferate anymore (less cells in S phase compared to the control), and that, perhaps, became senescent (more cells in G2 phase compared to the control). MAMBO38^{HER2loss} treated with omomyc upon dox subministration stopped proliferating, as shown by a blockage in Sub G1 phase, possibly meaning that cells are dying by apoptosis (Figure 15). The percentage of cells in G1, S and G2 phases did not change significantly after the treatment, while the number of treated polyploids cells was significantly lower compared to the control.

The therapeutic efficacy of omomyc alone (dox 1μg/ml) or in combination with lapatinib (1μM) was tested *in vitro* on MAMBO43^{HER2labile} and MAMBO38^{HER2loss}

omomyc inducible cell lines. As control we used the HER2 positive cell lines JIMT-1 pSlik-omomyc, already available in the host laboratory. Drugs' efficacy was assessed in three independent experiments (Figure 16).

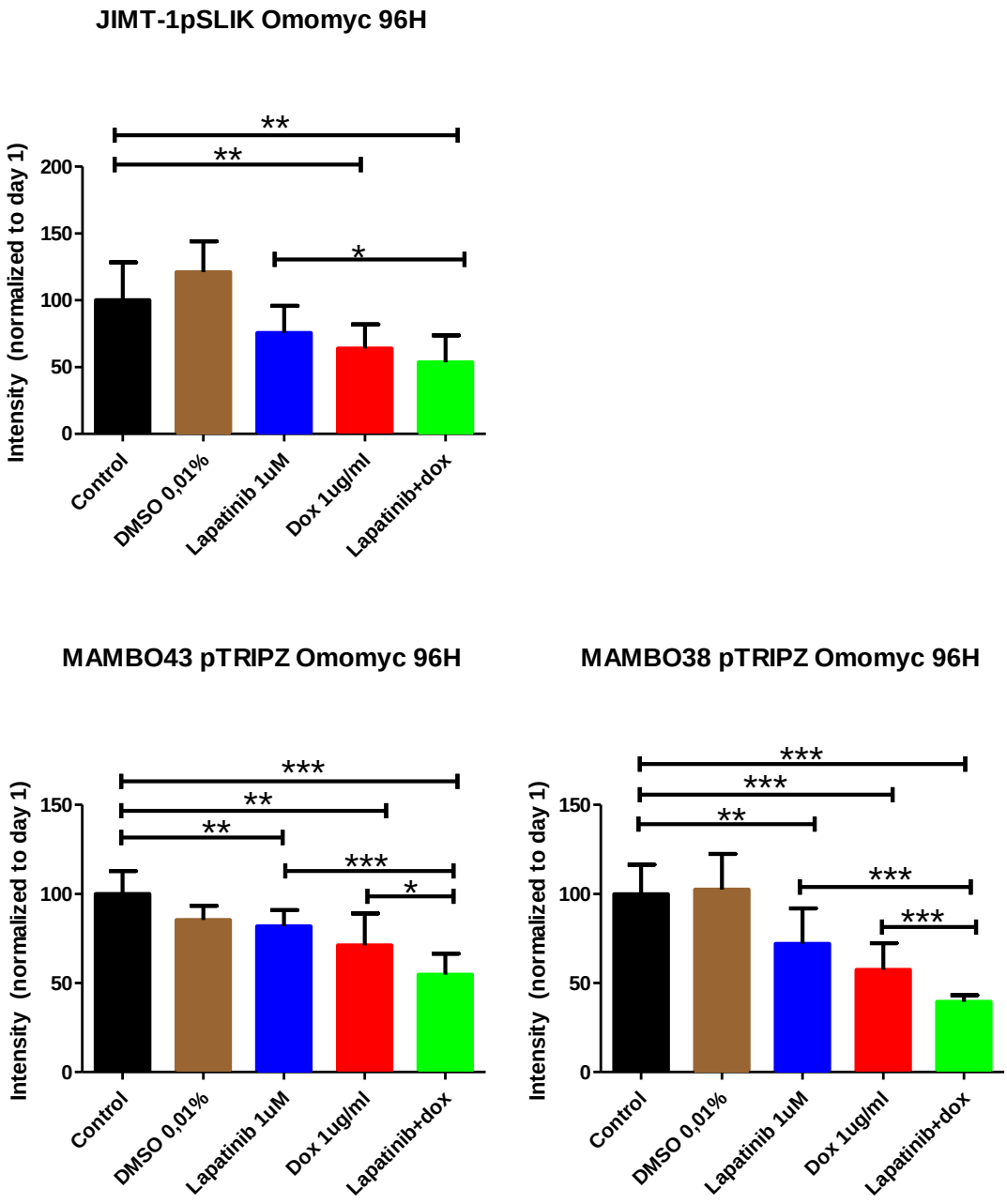

Figure 16: Sensitivity to Lapatinib alone or in combination with omomyc. *In vitro* (continuous culture) sensitivity to Lapatinib (1µM) alone or in combination with Doxycycline (1µg/ml) after 96h of treatment. Each bar represents the mean ± standard error of three independent experiments. Statistical significances among cell lines (Student's t test.): *p<0,05; **p<0,01; ***p<0,001.

In MAMBO38^{HER2loss} cell growth was significantly inhibited by omomyc expression upon dox treatment with 57% growth over control and by the combined therapy (40%). MAMBO43^{HER2labile} resulted resistant to lapatinib (82%) and quite sensitive to dox (70%). Interestingly, the combination of the two drugs was more effective compared to the control with 54% of cells proliferating. JIMT-1 pSLIK-OMO showed a significant inhibition of cell growth when treated with dox (64%) and with the combination of the two compounds (53%).

Determinated the efficacy of the treatments *in vitro*, we investigated their effect on the expression of HER2 and on the signaling pathways activated immediately downstream of the receptor. By western blot we tested on cells lysates, treated as described above, the expression of the total and phosphorylated amount of protein factors that mediate the intracellular signaling of huHER2 in FVBhuHER2 lines (Figure 17). In detail, Mambo43^{HER2labile} lost HER2 and pHER2 expression after infection independently from treatments. The amount of total AKT and total MAPK was lower in omomyc expressing cells compared to the control. This decrease was more evident when lapatinib is combined with dox; instead the levels of expression of the phosphorylated form of the proteins had an opposite trend: pAKT did not change after any treatment, pMAPK expression was up-regulated by lapatinib and by lapatinib+dox but showed a slight decrease (-32%) when treated with dox alone.

Mambo38^{HER2loss} did not express neither HER2 nor pHER2 but the expression of Akt, MAPK and their phosphorylated counterparts were already higher in basal conditions compared to Mambo43^{HER2labile}, as expected. The expression of total AKT, pAkt, total MAPK and pMAPK after Lapatinib treatment were increased. Omomyc expression upon dox treatment stimulated the level of expression of total AKT but its phosphorylated form was down-regulated by the treatment. MAPK expression was up-regulated but dox treatment didn't significantly change the expression of pMAPK. A higher amount of activated Akt and MAPK was detected after combining lapatinib with dox at the same time.

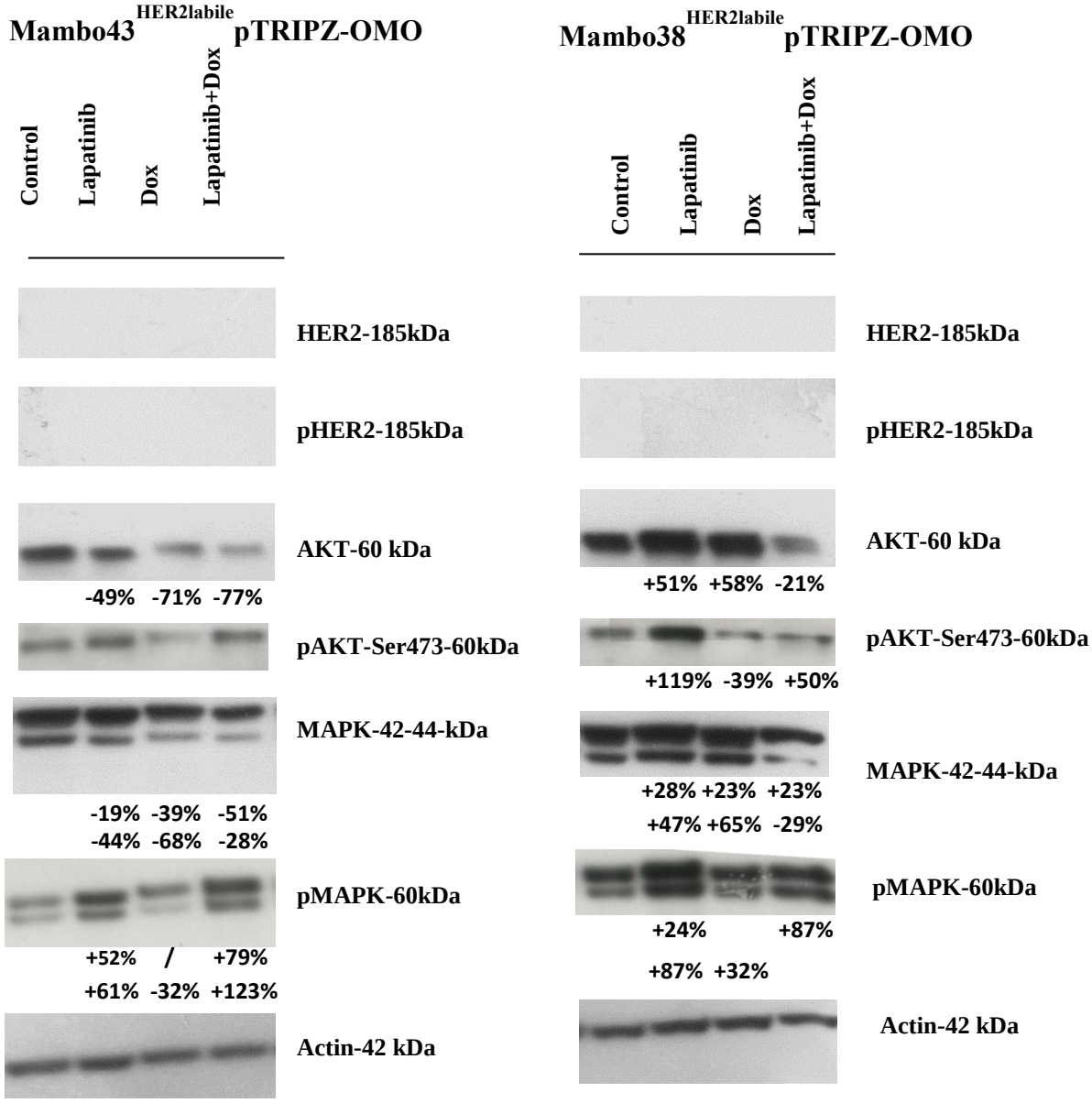

Figure 17: Modulation of the expression of second messengers downstream of HER2 after treatment with doxycycline alone or in combination with lapatinib. The western blot images show, for each cell line, the protein expression of HER2, of the main transducers of the downstream signal of HER2, and their phosphorylated forms in MAMBO43^{HER2labile} and MAMBO38^{HER2loss} cell lines infected with pTRIPZ-omomycRFP 96h from treatment with dox, lapatinib and their combination. Next to the name of each protein is reported the molecular weight in kDa. Band intensity was detected by densitometric analysis, normalized first over actin then over control. The percentage of decrease/increase between control and each treatment is shown when ≥ +20% or ≥-20%.

2. Co-expression of HER2 full-length and Delta16 in F1 mice

Human HER2-positive breast cancer cells co-express the full-length HER2 gene product p185 and various shorter isoforms, resulting from alternative splicing, proteolytic cleavage and other modifications. Some isoforms are definitely more oncogenic than full-length HER2 (Scaltriti et al., 2007; Pedersen et al., 2009; Angelini et al., 2013), whereas others inhibit carcinogenesis (Morancho et al., 2013). The Delta16 splice variant, lacking exon 16, has the properties of an activated oncogene, but it could also play beneficial roles (Alajati et al., 2013; Turpin et al., 2016; Castagnoli et al., 2014).

Full-length HER2 oncoprotein and splice variant Delta16 are co-expressed in human breast cancer. In order to analyze their interaction in a model that mirrors human co-expression, we have studied F1 hybrid transgenic mice bearing heterozygous copies of human HER2 and Delta16 (F1). From pre-existing analysis performed in our laboratory, we found that the presence of Delta16 causes the anticipation of tumor onset in mice. Furthermore, the simultaneous expression of Delta16 and HER2 does not determine any difference in F1 tumor latency compared to that of Delta16 mice, suggesting a dominant role of the splice variant in F1 phenotype (Lollini et al., AACR 2014; Palladini et al., EACR 2014).

In light of these findings, in this thesis the contribute of wild-type full-length HER2 and of its splice variant Delta16 to mammary HER2-positive carcinogenesis and to HER2 target therapy efficacy was studied.

2.1 Expression of full-length HER2 and Delta16 in F1 HER2/Delta16 mammary carcinomas

In order to demonstrate if Delta16 is mainly involved in neoplastic transformation and in the early phases of mammary carcinogenesis rather than in advanced tumor progression, we have analyzed the expression levels of the two isoforms in preneoplastic and in neoplastic mammary glands of F1 HER2/Delta16 mice, compared to HER2 full-length and Delta16-driven carcinomas.

The expression/coexistence of HER2 and Delta16 transcripts was analyzed by Real-time PCR, using specific primers for each isoform (Figure 18). Preneoplastic mammary glands of F1 HER2/Delta16 mice co-expressed both isoforms at homogeneous,

intermediate levels in comparison to mammary carcinomas of either full-length HER2 or Delta16 transgenic mice (Figure 18A).

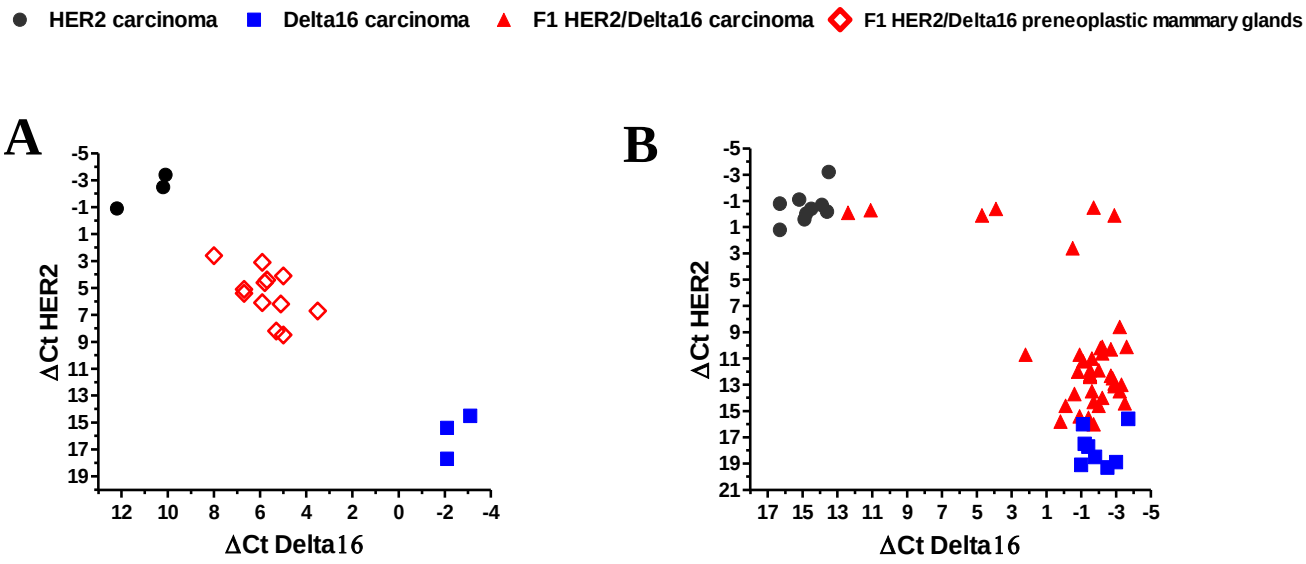

Figure 18: Expression of HER2 and Delta16 transcripts in mammary glands and primary mammary carcinomas ΔCt represents the difference in PCR between the indicated HER2 isoform and reference housekeeping gene GAPDH. (A) Each solid point represents one tumor of HER2 or Delta16 mice; each open diamond represents one preneoplastic mammary gland of F1 HER2/Delta16 mice. (B) Each point represents one tumor.

Mammary carcinomas of F1 mice exhibited three alternative patterns of expression (Figure 18B). The greatest part of tumors (~80%) expressed high levels of Delta16 and low levels of full length HER2, a few (~5%) expressed full-length HER2 and little Delta16, and the remainder (~15%) co-expressed at high level both isoforms. Thus, neoplastic progression to mammary carcinoma in F1 mice required the activation of both transgenes with a strong inclination toward Delta16. Moreover, individual tumors exhibiting different patterns of transgene expression can simultaneously develop within the same host.

2.2 HER2/Delta16 expression tunes tumor sensivity to trastuzumab in prevention and therapy

F1 HER2/Delta16 mice were treated with trastuzumab in order to study how HER2 full-length/Delta16 expression tunes the sensitivity of nascent and established tumors to HER2 targeted therapies. Trastuzumab was administrated in prevention to young F1 HER2/Delta16 mice and to the parental strains FVBhuHER2 and FVBDelta16. HER2 mice, Delta16 mice and F1 HER2/Delta16 mice were treated twice

weekly intraperitoneally with trastuzumab (4 mg/kg) starting from 17 weeks of age for HER2 mice and from 5-8 weeks of age for Delta16 and F1 HER2/Delta16 mice. Control mice were treated with physiological solution.

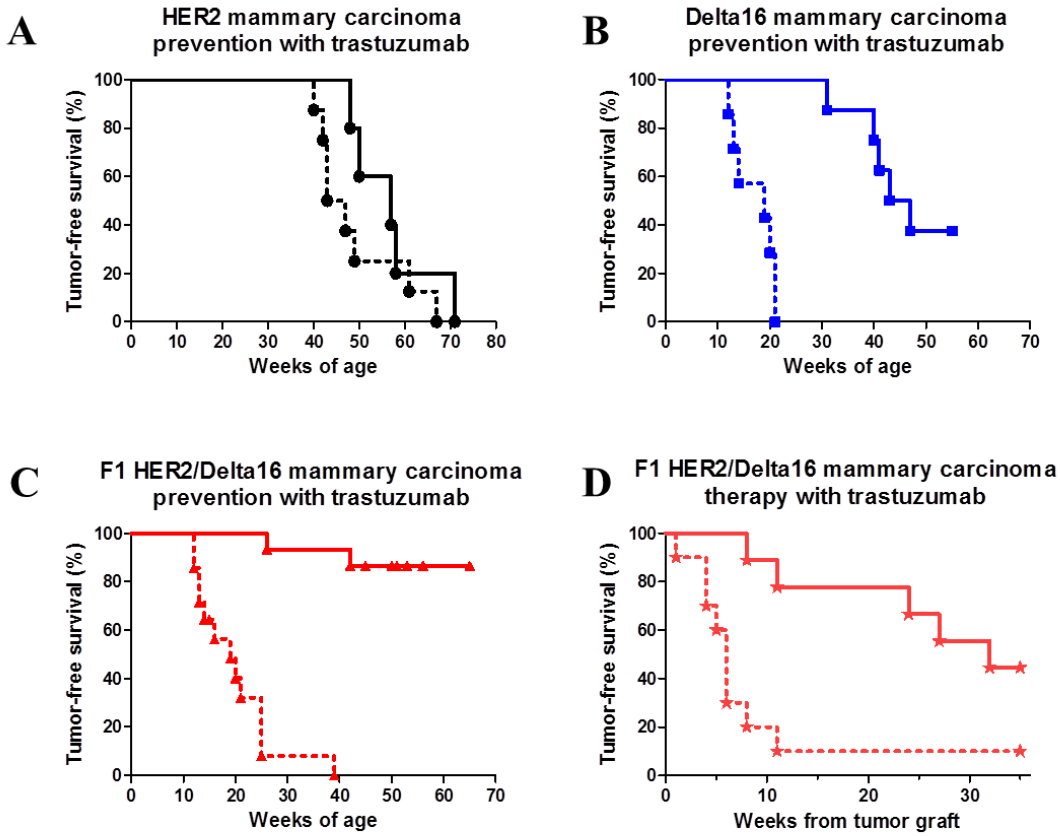

Figure 19: Response to trastuzumab treatment *in vivo*. Prevention of autochthonous mammary carcinogenesis by trastuzumab treatment (A-C): Kaplan-Meier tumor-free survival curves of transgenic mice treated i.p. with vehicle (dashed line) or trastuzumab (solid line); statistical comparisons were made by Mantel-Haenszel's test. (A) HER2 mice (vehicle n=8, trastuzumab n=5); no significant difference. (B) Delta16 mice (vehicle n=7, trastuzumab n=8); $p<0.001$. (C) F1 HER2/Delta16 mice (vehicle n=14, trastuzumab n=15); $p<0.001$. (D) Therapy of F1 HER2/Delta16 tumors implanted in the fourth left mammary fatpad of non-transgenic FVB mice treated with vehicle (dashed line) (n=10) or trastuzumab (solid line) (n=9); $p<0.01$ by the Student's t test.

At one year of age more than 85% of F1 HER2/Delta16 treated mice were tumor-free, whereas none of the untreated mice was tumor-free by 40 weeks of age (Figure 19 C). The preventive effect of trastuzumab was stronger in F1 HER2/Delta16 mice than in the two parental strains. A long delay in mammary carcinogenesis was obtained with trastuzumab in Delta16 mice (Figure 19 B), however more than 50% of mice already developed carcinoma by the first year of age. Trastuzumab also delayed tumor onset in full-length HER2 transgenic mice but statistical significance was not reached (Figure

19 A). The efficacy of trastuzumab was also confirmed in a therapeutical setting against homogeneous established tumors. Fragments of F1 HER2/Delta16 mammary tumors were implanted orthotopically into non-transgenic FVB mice. Intraperitoneal treatment (twice/week) started at positivity and lasted for one month. After the treatment with trastuzumab tumor growth was strongly inhibited, with more than 40% mice still tumor-free five months after the end of the treatment (Figure 19 D).

We further decided to compare the therapeutic effect obtained with trastuzumab to buparlisib treatment, in the same experimental conditions described above. After one month of treatment with buparlisib tumor growth was not as strongly inhibited as with trastuzumab, with only 20% of mice still alive five months after the end of the treatment (Figure 20).

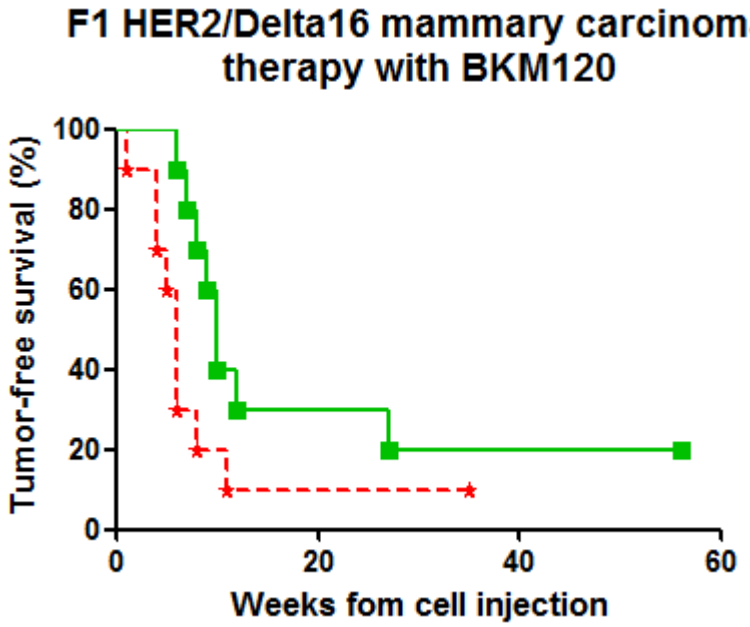

Figure 20: Response to Buparlisib treatment *in vivo*. Therapy of F1 HER2/Delta16 tumors implanted in the fourth left mammary fat pad of non-transgenic FVB mice treated with vehicle (dashed line) (n=10) or buparlisib (solid line) (n=10); Statistical comparisons were made by Student's t test: no significant difference.

With the aim to analyze the intrinsic sensitivity of F1 HER2/Delta16 mammary carcinoma cells to anti-HER2 monoclonal antibodies, a system of cell lines representative of the three isoform ratios (F1 HER2low/Delta16high, F1 HER2high/Delta16low, F1 HER2high/Delta16high) was previously established in the Laboratory of Immunology and Biology of Metastasis and exposed to trastuzumab in 3D (agar) cultures. A strong inhibition of 3D cell growth was obtained only when cells

expressed high levels of Delta16 either alone or together with a low level of full-length HER2. In contrast, all cell lines expressing high levels of full-length HER2 alone or together with Delta16, were not inhibited regardless of the level of Delta16 expression.

After the treatment with trastuzumab, in F1 HER2 high/Delta16high cell line 302-IVD and in F1 HER2low/Delta16high cell line 156-IS, we re-analyzed the expression of the two isoforms in order to detect variations in isoform ratios and in expression levels. The expression of HER2 and Delta16 transcripts was analyzed by Real-time PCR, using specific primers for each isoform.

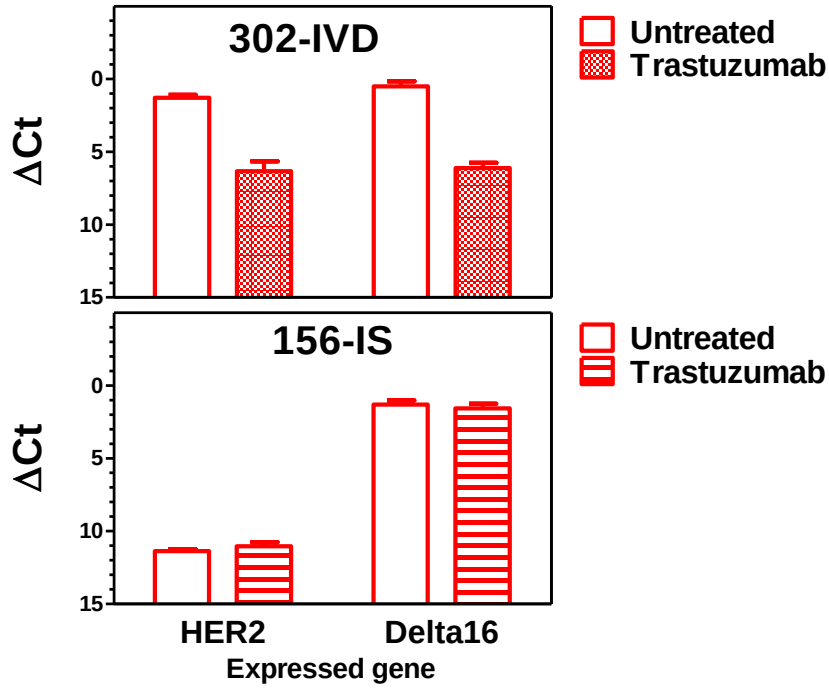

Figure 21: Response to trastuzumab treatment *in vitro*. Expression of HER2 and Delta16 transcripts in 302-IVD **(**F1HER2 high/Delta16high) (upper graph) and 156-IS **(**F1HER2low/Delta16high) (lower graph) cells after trastuzumab treatment in 3D culture. Each bar represents the mean and SEM of 2-6 independent determinations. ΔCt represents the difference in PCR threshold cycle between the indicated gene and reference housekeeping gene GAPDH. A significant ($p<0.01$ by the Student's t test) inhibition of both transcripts was observed only in 302-IVD cells.

Trastuzumab treatment did not affect the isoform ratios, either in trastuzumab-sensitive 156-IS cells or in resistant 302-IVD cells, even though the latter showed a significant decrease of both isoform levels (Figure 21).

2.3 HER2 isoforms long-term stability

In order to verify whether the isoform ratios were stable *in vivo* in the long term, we studied serial transplants of two F1 mouse tumors in syngeneic immunocompetent hosts. Serial *in vivo* passages of two F1 tumors (one with a high expression of both isoforms, the other with a higher expression of Delta16) were analyzed for each isoform expression by Real-Time PCR and for the total protein level by cytofluorometric analysis. A primary antibody that binds both HER2 isoforms was used, because specific antibodies for each isoform have not been developed yet. Delta16 levels were stable over all passages (which took more than 11 months *in vivo*), whereas the levels of full-length HER2 showed strong variations, including both increase and decrease over time (Figure 22).

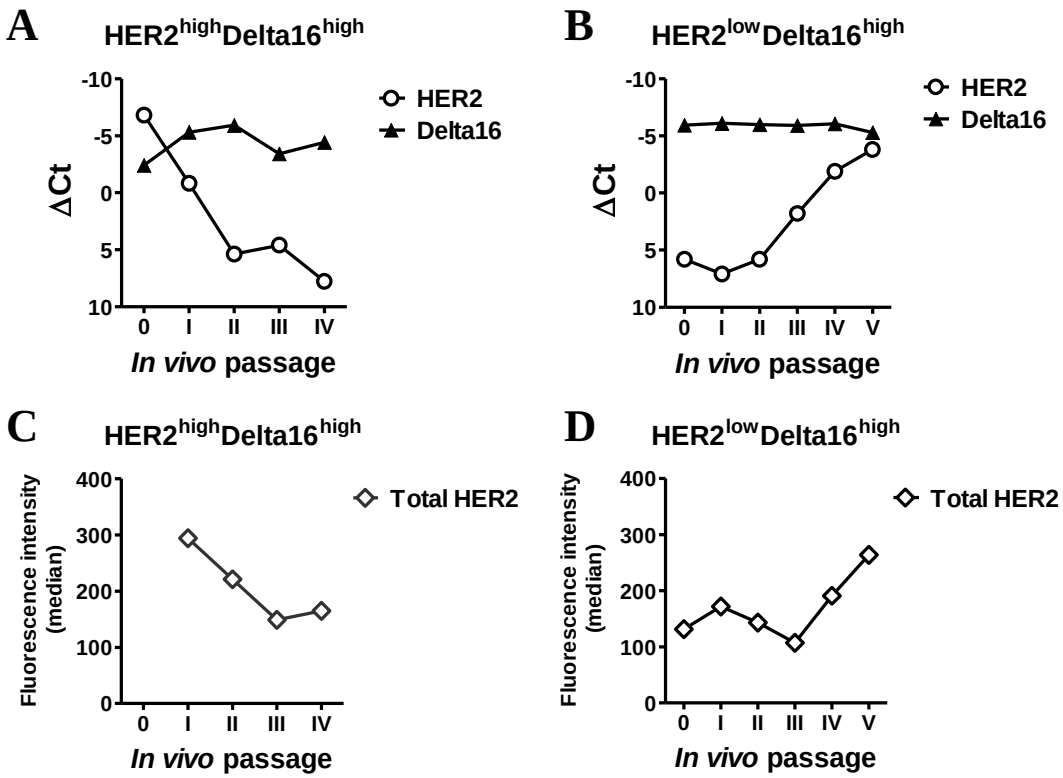

Figure 22: Kinetics of HER2 and Delta16 expression in serial transplants (mouse-derived isografts, MDI) of F1 HER2/Delta16 mammary carcinomas. (A-B) Expression of HER2 and Delta16 transcripts by qPCR; ΔCt represents the difference in PCR threshold cycle between the indicated HER2 isoform and reference housekeeping gene mTBP; (C-D) total surface HER2 protein by FACS analysis.

3. Patient Derived Xenografts

Despite improvements in therapies, HER2-positive breast cancer patients still display poor prognosis. Patient-derived tumor xenografts (PDX) are reported to better represent tumor heterogeneity than cell-based tumor xenografts. Here we show the generation of a collection of PDXs that portray the main subtypes of breast cancer, obtained thanks to the collaboration with Sant'Orsola-Malpighi Hospital, Bologna (Prof. Mario Taffurelli, Prof Donatella Santini, Dr. Claudio Ceccarelli) and Bellaria Hospital, Bologna (Prof. Maria Pia Foschini, Dr. Enrico Di Oto, Dr. Sofia Asioli). We focused on HER2-positive breast PDX models for the evaluation of molecular stability of selected biomarkers during prolonged *in vivo* transplantation. In order to select variants similar to those responsible for disease progression in patients, an HER2-positive breast PDX was treated with HER2-targeted therapies.

3.1 A panel of Breast Cancer Xenograft Models

Fresh surgically resected patient-derived specimens were implanted orthotopically into immunodeficient mice (RGKO or NSG). We chose an orthotopic tumor xenograft implantation since it provides a more biologically relevant context, ideal for tumor-host interactions and development of disease-related metastases. Each sample was classified by its histological and clinical features. Invasive ductal carcinomas (IDC) were more frequent than invasive lobular carcinomas (ILC), 86% and 9% respectively, reflecting their different frequency in the general population. More than the half of the specimens were classified as high grade (52%), considered to be the most aggressive ones. Expression of Estrogen/Progesterone receptors was very diffused, detected in the 85% of the tumor samples. Proliferation, evaluated as Ki67 expression, was high in the 40% of the tumors. HER2 overexpression and/or HER2 gene amplification, determined by FISH analysis, was observed in the 23% of tumors.

We established 7 transplantable PDXs out of 65 primary breast cancer specimens implanted, (11% tumor take-rate). The highest rate of PDX stabilization was obtained from HER2-positive carcinomas (40%) followed by Triple negative (20%), Luminal B (14%) and Luminal A (6%) subtypes (Table 6-7).

Table 6. Clinical features of primary tumors implanted			
Parameter		Cases	(%)
Histology			
	IDC	56	86
	ILC	6	9
Grade			
	III	34	52
	II	20	31
	I	10	15
AJCC Staging			
Hormon receptors			
	ER+ and/or PR+	55	85
	ER- and PR-	10	15
HER2 expression			
	HER2 overexpression or amplification	15	23
Proliferation			
	Ki67 high	26	40
	Ki67 intermediate	15	23
	Ki67 low	24	37
Intrinsic subtypes			
	Luminal A	31	48
	Luminal B	14	22
	Triple positive	10	15
	HER2	5	8
	Triple negative/basal like	5	8

Table 7. Charateristics and in vivo passages of each established PDX model

Tumor TAG	Histology	Grade	ER	PR	Proliferation	HER2	Intrinsic subtypes
FO4	IDC	III	ER−	PR−	High	HER2+	HER2+
FO15	IDC	III	ER+	PR+	Inter	HER2−	Luminal A
TA7	IDC	III	mixed		High	HER2−	Luminal B
TA18	IDC	III	ER+	PR−	High	HER2−	Luminal B
TA38	IDC	III	ER+	PR+	High	HER2−	Luminal A
TA45	IDC	III	ER−	PR−	High	HER2+	HER2+
TA51	IDC	III	ER−	PR−	High	HER2−	TN

IDC = Invasive ductal carcinomas, ER = Estrogen Receptor, PR = progesteron Receptor, HER2 TP = HER2 triple positive.

Tumor growth curves of engrafted PDXs at the first passage are reported in figure 23. Growth rate of the first passage of each tumor was representative of tumor growth in the later passages and was independent from the intrinsic subtype.

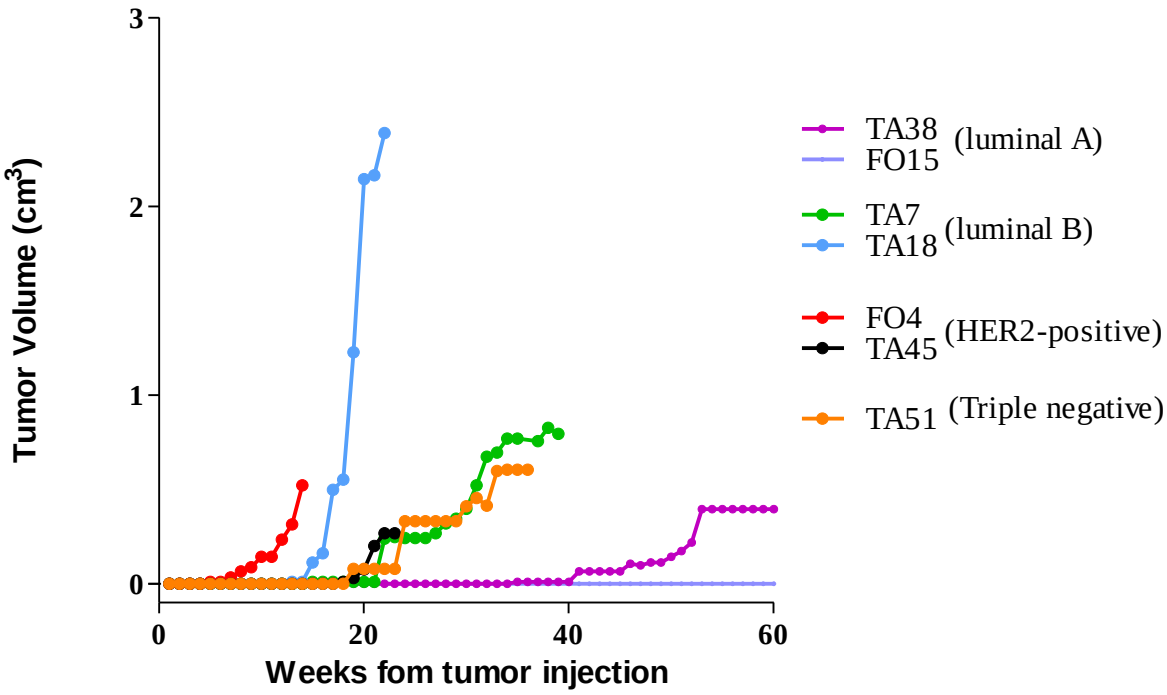

Figure 23: Kinetic of the growth of engrafted tumor at the first passage. Each point rapresents the tumor volume. X-axis shows the weeks after injection of patient-derived specimens. Y-axis shows tumor volume expressed in cm^3.

3.2 HER2-positive FOT4 PDX

Among the engrafted PDX, two were classified as HER2-positive, FO4 and TA45. FO4 was studied more in detail and characterized through several passages.

FO4 tumor is an invasive ductal carcinomas of grade III, with a high rate of proliferation, negative for the expression of Estrogen/Progesterone receptors, positive for HER2 amplification (2+). The tumor has been propagated *in vivo* for serial consecutive passages, here we show the results including the first seven generations of FO4. The parameters for the evaluation of FO4 *in vivo* growth are summarized in Table 8.

Table 8. Parameters for the evaluation of PDX FO4 in vivo growth

Passage	% engraftment #	Latency (weeks from injection)			Time to a tumor's volume of 1 cm^3 (weeks from injection)			
		Range	Mean	Median	Mice at volume / mice injected	Range	Mean	Median
I	1/1 (100%)	5	5	5	0/1			
II	5/5 (100%)	1-1	1	1	3/5	14-16	15	15
III	6/6 (100%)	1-2	1	1	6/6	10-15	12	11
IV	10/10 (100%)	1-11	3	1	10/10	7-16	11	11
V	13/13 (100%)	1-6	3	3	13/13	6-24	11	10
VI	16/16 (100%)	1-7	3	3	16/16	4-17	10	9
VII	13/13 (100%)	0-9	3	1	11/13	4-13	9	9

% Engraftment measured as number of positive mice/number of injected mice
Statistical comparison, Average latency: VII vs II ($p<0.05$, test *t* di Student). Mean time to reach a volume of 1 cm^3, VII vs II ($p<0.05$, test *t* di Student). Percentage of engraftment: no significant. test X^2 Fisher's exact test.

The average latency increased slightly but significantly in the VII passage in respect to the II ($p < 0.05$, Student's t test). The average time needed by the tumor to reach a volume of 1 cm^3 decreased in all steps compared to the II passage but a significant difference was observed only vs the VII ($p < 0.05$, Student's t test). All comparisons evaluated from the III passage on were similar, since the differences were not statistically significant. Therefore FO4 growth characteristics were stable. The percentage of engraftment of subsequent *in vivo* passages was of 100% among all the passages.

In order to validate FO4 as a preclinical model for translational research, we studied the molecular stability of selected biomarkers during prolonged *in vivo*

transplantation, and the expression ratio between HER2 full-length and Delta16 isoform, which is supposed to have a role in cancer aggressiveness. We selected a representative sample for each passage (I-VII) of FO4 PDX model. Histologic and immunohistochemistry analysis showed that FO4 PDXs recapitulated the morphologic and structural patterns, as well as HER2 expression, of patient tumor among several passages *in vivo* (II-VII) (Figure 24).

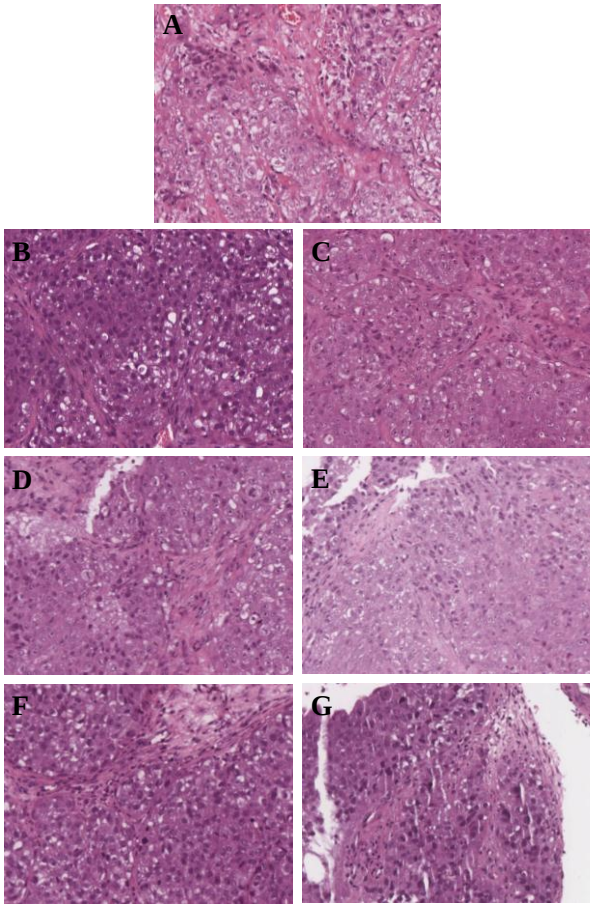

Figure 24: Hematoxylin and eosin staining. Staining of histological specimens from the original patient tumor (A), FO4 PDX model II (B), III (C), IV (D), V (E), VI (F), VII (G) at 10 × magnification. Staining and images provided by Prof. Foschini. and Dr. di Oto, Department of Pathology, Bellaria Hospital, Bologna.

FO4 maintained a stable gene expression of HER2 and Delta16 isoforms over time, analyzed by Real-time PCR, with specific primers for each isoform (Figure 25).

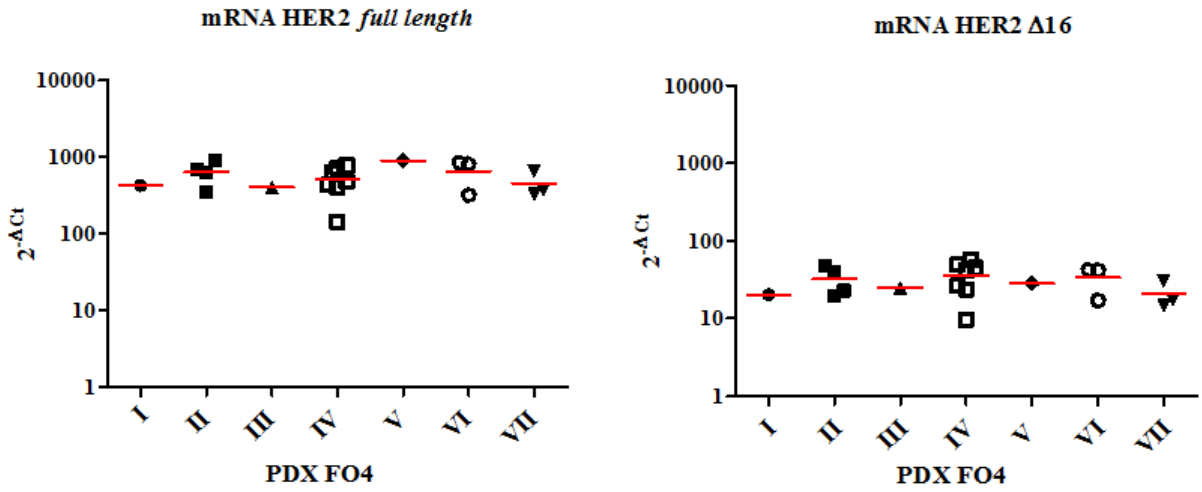

Figure 25: Real-time PCR expression of HER2 full length (A) and HER2Δ16 isoform (B) in PDX FO4 tumors from I to VII passage. In the abscissa the *in vivo* passages analyzed are reported and in ordinate the $2^{-\Delta Ct}$ value. Each symbol corresponds to the average of two replicas of real-time PCR carried out for each individual tumor. The red line is the average value of each passage. There were no statistically significant differences between passages (Student t test).

HER2 expression stability was also confirmed by Western blot and Flow Cytometry techniques (Figure 26-27). In western blot, the levels of HER2 and its phosphorylated form expression were high and stable, with values oscillating between 0.5 and 0.8 without association to the propagation passage (Figure 26).

Figure 26 HER2 and pHER2 expression. Western blot analysis of HER2 and pHER2 (Tyr 1248) expression in subsequent passages of PDX FO4 from the I to the VII. Western blots were performed on tumor lysates. Actin was employed as house-keeping protein.

Flow cytometry data showed high levels of expression of HER2 in the membrane, with a slight decrease trough the subsequent *in vivo* passages, statistically significat between the IV-V-VI-VII passages compared to the II. However, overall protein expression of HER2 can be considered constant through passages (Figure 27).

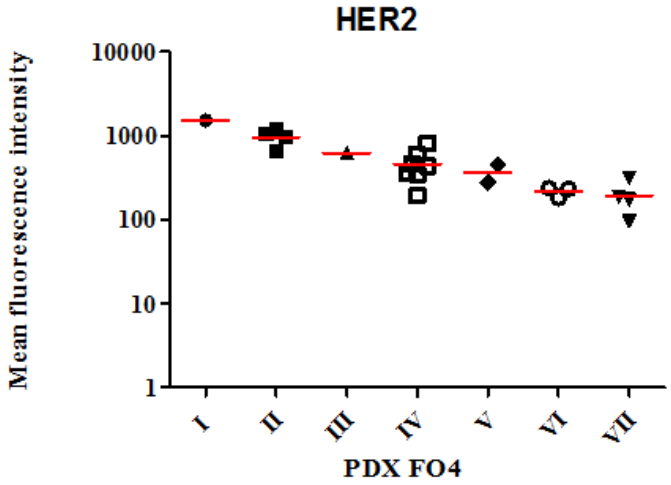

Figure 27 Expression of total HER-2 protein on cell membrane by Cytofluorimetry. Each point represents a FO4 PDX tumor among consecutive passages I-VII. The x-axis shows PDX FO4 passages from I to VII, the y-axis shows the mean of fluorescence intensity expressed in arbitrary units, on a logarithmic scale. The red line is the mean fluorescence intensity of each passage. Statistical significance: Student's t test. $p < 0.05$ between IV-V-VI-VII passages compared to the II passage, $p < 0.05$ between VII and IV passages.

Immunohistochemical analysis on same samples, performed at the Department of Pathology of Bellaria Hospital of Bologna, showed that the expression of the HER2 in membrane did not change by increasing the number of passages *in vivo*. However, a tendency to a progressive increase in the cytoplasmic component was observed (Figure 28).

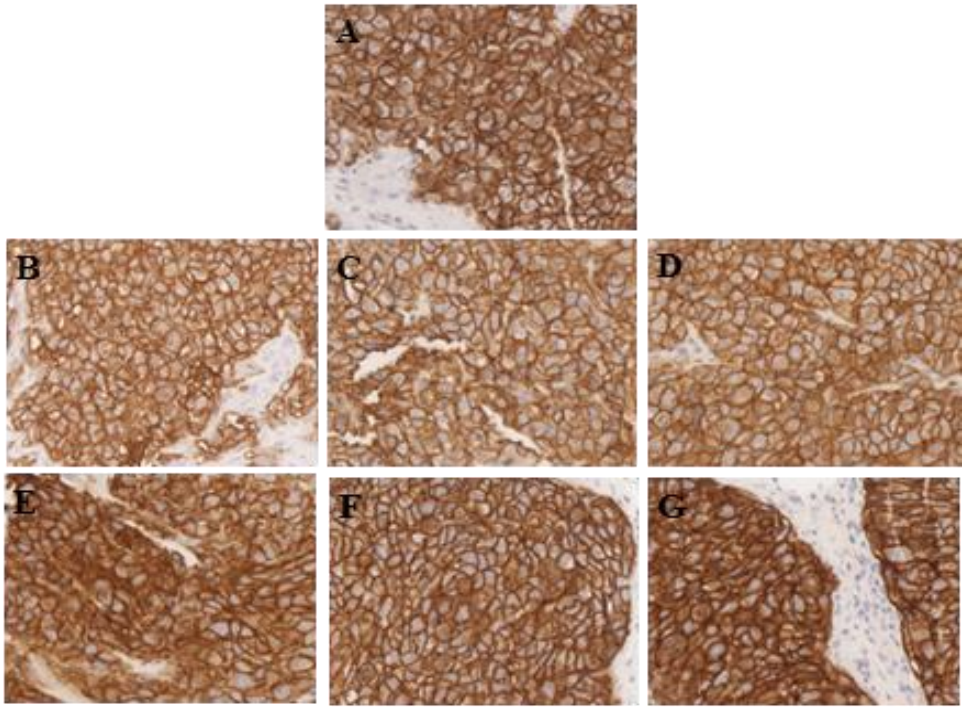

Figure 28: Representative Immunohistochemical (IHC) images of HER2 protein expression in tumor tissues. Analysis of HER2 of the original tumor derived from the patient (A) and the PDX FO4 passage II (B), III (C), IV (D), V (E), VI (F), VII (G) at 20 × magnification. Staining and images provided by Prof. Foschini. and Dr. di Oto, Department of Pathology, Bellaria Hospital, Bologna.

To complete the characterization of FO4, we investigated the expression of two other members of the ERBB family, HER1 (epidermal growth factor receptor, EGFR) and HER3; of IGFR tyrosine kinase receptor (insulin-like growth factor 1 receptor) and of the epithelial marker CD24.

Figure 29 A and 29 B show the profiles of these markers, respectively, relative to a representative sample of FO4 (V) and to the primary culture cells derived from a FO4 (VII) tumor.

FO4 was characterized by high expression of HER2 receptor, whereas the expression of HER1, HER3 and IGFR was very low, barely positivity. The expression of human CD24 on primary culture cells as well was detectable, which indicates their epithelial nature. This result suggests the lack of dependence from the signaling pathways mediated by these receptors in FO4 PDX tumor.

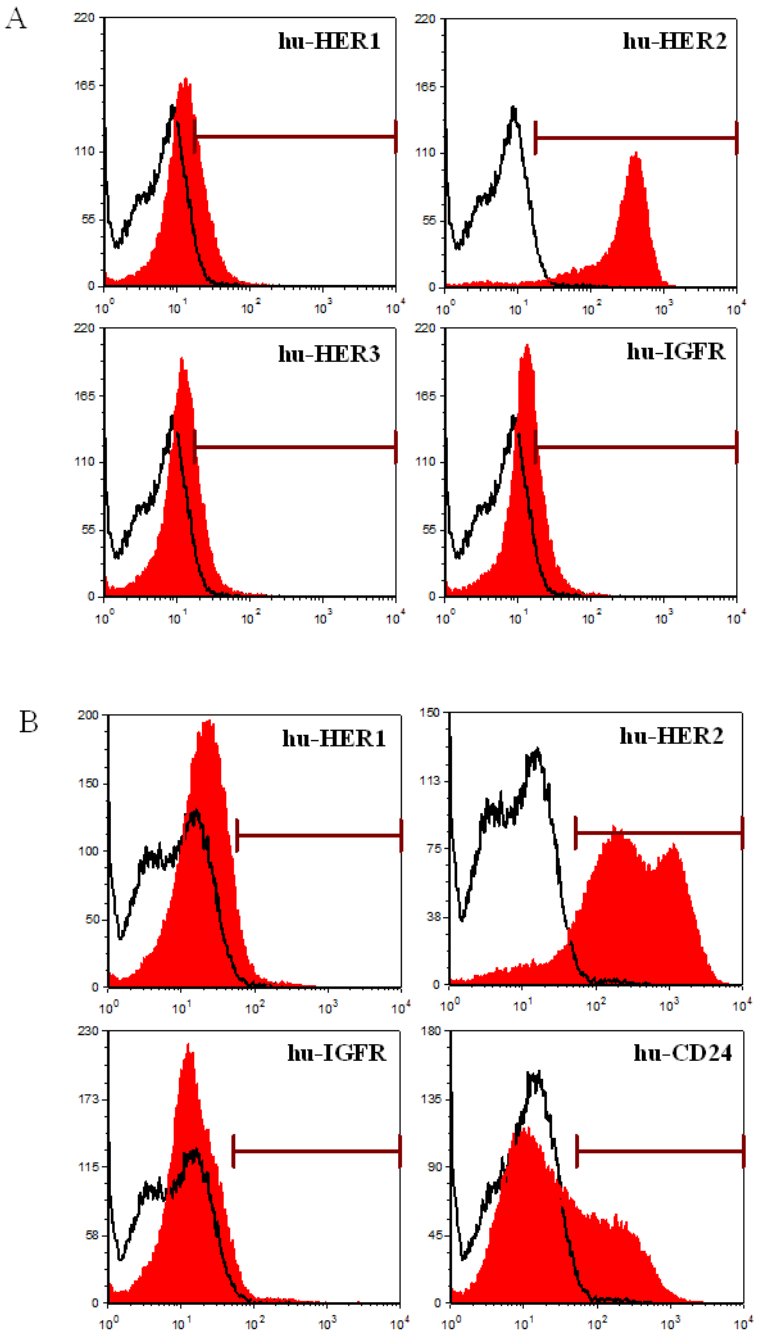

Figure 29: Flow cytometry analysis of HER1, HER2, HER3, and IGFR in FO4 tumors. Representative tumor sample of (A) FO4 PDX V passage *in vivo* and (B) primary cell culture derived from FO4 tumor at VII passage *in vivo*. The panels represent the histograms profiles: the x-axis shows the intensity of fluorescence in a logarithmic scale, expressed in arbitrary units along; the y-axis shows the number of cells.

3.3 Sensitivity to targeted therapies

Demonstrated FO4 molecular stability during prolonged *in vivo* transplantation, this model was therefore used to test treatments against HER2 (trastuzumab and neratinib). Palpable FO4 PDX bearing mice (IV-V-VI passage) were treated with trastuzumab 4mg/kg, twice a week by intraperitoneal injection (ip) till sacrifice, or with neratinib 40mg/kg, 5 times a week by oral administration (os), for 35 weeks; the control group did not receive any treatment.

Both treatments were able to inhibit tumor growth compared to untreated mice (Figure 30).

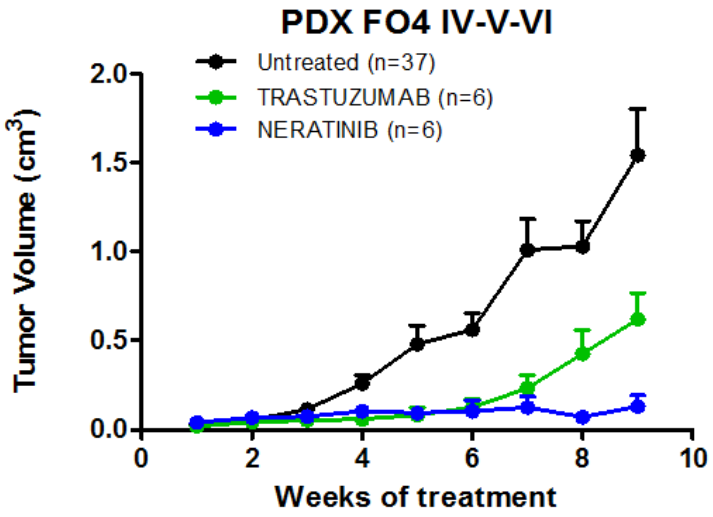

Figure 30: Responsiveness to neratinib and trastuzumab treatment *in vivo* in serial transplants (patient-derived xenografts, PDX) of human breast cancers FO4. Therapy of FO4 tumors (IV-V-VI passages) untreated (n=37), treated with neratinib (n=6) or trastuzumab (n=6); The curve shows the first 9 weeks of treatment. The values of neratinib curve are statistically lower than those of the control curve at weeks 6-7-8-9, the difference is statistical significant as well for neratinib compared to trastuzumab at weeks 8-9. Other comparisons did not reach statistical significance (Student's t test, $p < 0.05$).

Neratinib inhibited tumor growth, with a statistical significant difference from the sixth week of treatment ($p < 0.05$ Student's t test). Trastuzumab had also influence on growth, although without reaching statistical significance. The percentages of inhibition of tumor growth for neratinib and trastuzumab were respectively 92% and 60% at 9 weeks of treatment (Figure 30). The survival analysis of Kaplan-Meier curves (Figure 31) reflected what observed in tumor growth curves (Figure 30) ($p < 0.001$ for neratinib and $p < 0.05$ for trastuzumab, log-rank test Mantel-Haenszel's test).

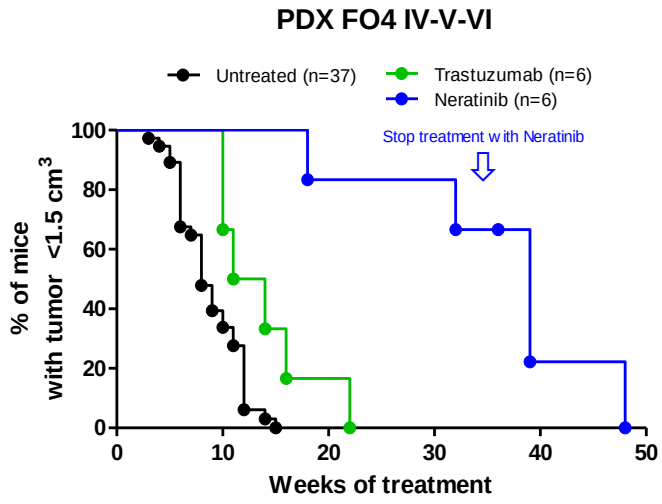

Figure 31: Responsiveness to neratinib and trastuzumab treatment *in vivo* in serial transplants (patient-derived xenografts, PDX) of human breast cancers FO4. Kaplan-Meier curves of FO4 tumors (IV-V-VI passages) untreated (n=37), treated with Neratinib (n=6) or Trastuzumab (n=6); Treatments started at positivity and continued up to sacrifice. In the graph the x-axis shows the weeks of treatment, the y-axis shows the percentage of animals in each group with a tumor volume lower than 1.5 cm3. The statistical comparisons were made by the Mantel-Haenszel's test: Neratinib vs Control: $p < 0.001$; Trastuzumab vs Control: $p < 0.05$. Other comparisons did not reach statistical significance.

After 30 weeks of treatment with neratinib, for the 80% of FO4 PDX mice tumor growth was stopped, whereas none of the untreated mice was alive later than 15 weeks from positivity. The therapeutic effect of trastuzumab on tumor growth was less strong compared to neratinib, with only 20% of mice with a tumor volume < 1,5 cm^3 after 15 weeks of treatment. In order to evaluate the real effect of neratinib on tumor growth and survival, in 4 animals the treatment was suspended after 35 weeks. In these mice the tumor started to re-grow, demonstrating the crucial role of the drug in controlling tumor proliferation.

We therefore investigated the effect of treatments on the expression of HER2 and on the signaling pathways activated immediately downstream of the receptor by real-time PCR and flow cytometry (Figure 32-33). All the molecular analyses were performed on tumor samples belonging to the IV-V-VI passage untreated or treated with trastuzumab or neratinib. None of the treatments altered the expression ratio of HER2 full-length and Delta16 isoform or led to the selection of HER2-negative variants. Figure 28 shows the values of $2^{-\Delta Ct}$ for the two isoforms, none of the comparisons reached statistical significance and, therefore, the expression of HER2 at the transcriptional level did not appear modified by any treatment.

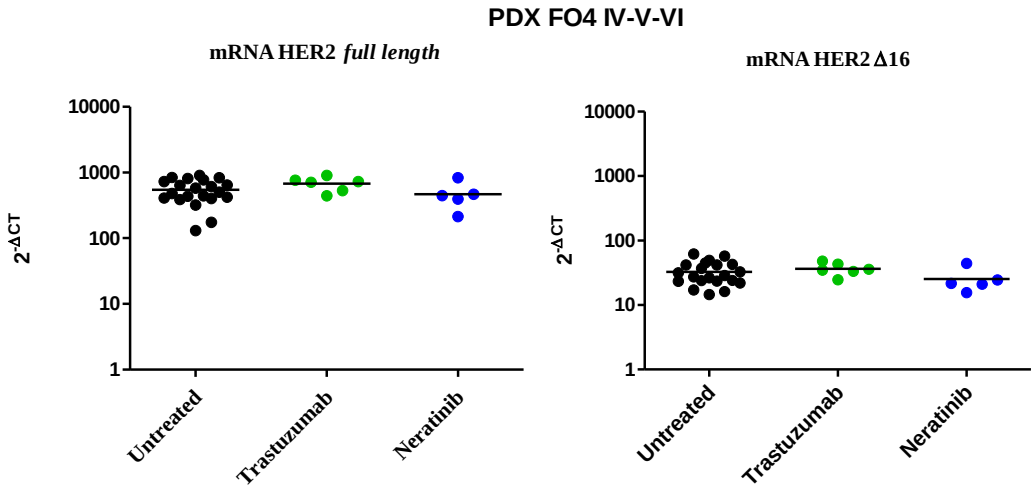

Figure 32: Expression of HER2 and Delta16 transcripts in PDX FO4 mammary carcinomas. ΔCt represents the difference in PCR threshold cycle between the indicated HER2 isoform and reference housekeeping gene human TBP. Each solid point represents the average of two replicas of real-time PCR carried out for each individual tumor of PDX FO4 belonging to the IV-V-VI passage *in vivo*, treated with Trastuzumab, Neratinib or untreated.; The line represents the average value in each group. Statistical significance not reached (Student's t test).

Even the HER2 protein level analysis revealed no statistical significant differences in treated groups compared to the control (Figure 33).

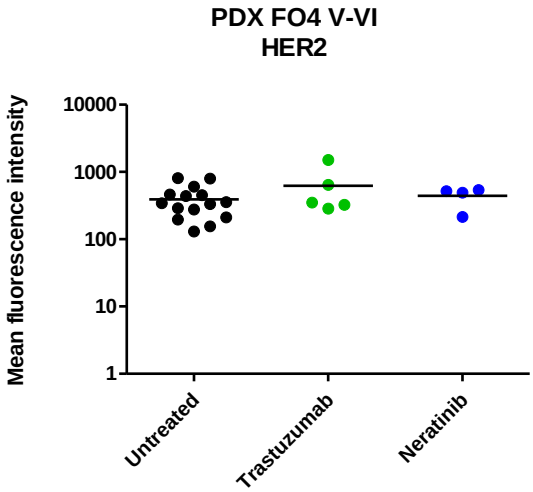

Figure 33: Kinetics of HER2 expression in serial transplants of FO4 PDX mammary carcinomas. Total surface HER2 protein by FACS analysis. Each point represents the median fluorescence intensity (MFI) of dissociated cells from PDX FO4 tumors belonging to the IV-V-VI serial transplants *in vivo*, treated with Trastuzumab, Neratinib or untreated; horizontal bars represent the median value of all tumors; In each graph the x-axis shows the groups of treatment, the y-axis shows the mean of fluorescence intensity expressed in arbitrary units, on a logarithmic scale. Statistical significance not reached (Student's t test).

Primary cultures established from a FO4 tumor sample showed aepithelial morphology and the ability of forming spheres (Figure 34).

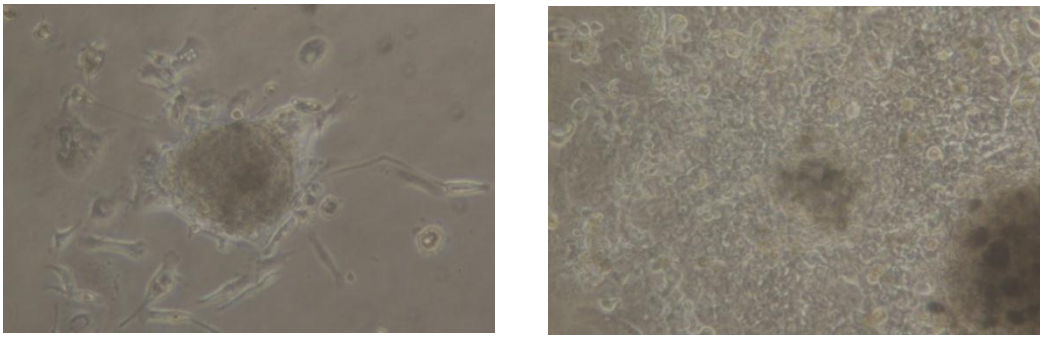

Figure 34: Primary cultures derived from tumor tissue of PDX FO4 VII passage. The images are representative of (A) cell spheres adherent to the culture substrate and (B) cells with markedly stretched epithelial morphology. Images were assessed by phase contrast microscopy. Magnification was 125×.

After 5 days from seeding, cells were treated with Neratinib (40 nM) or, as control, with DMSO (0.01%) (diluent of the drug). The treatment was maintained for 24 hours, then cells were harvested and the proteins obtained from the pellet were extracted for Western blot analysis (Figure 35).

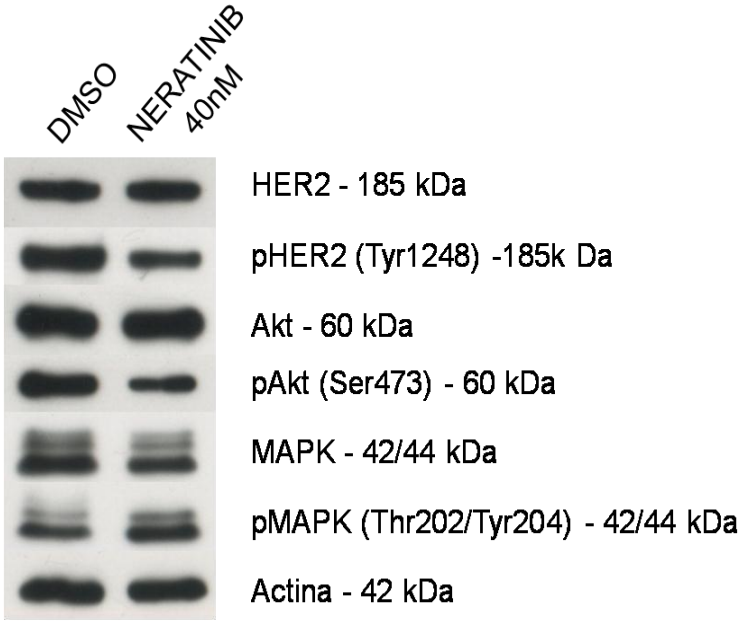

Figure 35: Modulation of the expression of second messengers downstream of HER2 after treatment Neratinib. Western blot analysis of proteins extracted from primary cultures of PDX FO4 VII passage, treated *in vitro* with Neratinib (40 nM) or with DMSO (control). The image shows the expression of total HER2, pHER2 (Tyr 1248), total Akt, pAkt (ser473), total MAPK (ERK1/2), pMAPK (pERK1 / 2) (Thr202 / Try204). Actin was employed as house-keeping protein.

Total HER2 and Akt levels were similar in the control and in the treated spheres, whereas after the treatment, a clear reduction of phosphorylated proteins was observed after treatment, with an inhibition of 37% and 38% respectively. Concerning MAPK pathway, while in the control these proteins appeared only partially activated, after treatment their activation was complete and the phosphorylated protein levels were increased compared to the control. This experiment seems to indicate that neratinib acts as an inhibitor of the activity of HER2 mainly through inhibiting PI3K-Akt signaling. The increased activation level of p-MAPK was probably due to a compensatory mechanism, which leads to the activation of other receptors that converge on MAPK pathway.

DISCUSSION

Overexpression of huHER2 occurs in nearly 15–20% of breast cancers, and it is generally associated with poor patient survival. Existing therapies such as trastuzumab and lapatinib are currently used in the treatment of HER2-positive cancers, although issues with high recurrence and acquired resistance still remain (Schroeder et al., 2014).

Elucidation of the molecular mechanisms underlying resistance is leading to the identification of therapies and strategies to manage resistance to HER2-targeted therapies. In addition to intrinsic and acquired resistance associated to HER2 oncogene, the induction of bypass pathways that reactivate growth factor-dependent signalling upon oncogene inhibition is likely pervasive across cancers and should be anticipated. Together, these findings underscore that many resistance mechanisms fall into predictable and therapeutically tractable themes, and can be effectively targeted with rationally designed combined therapies (Pagliarini et al., 2015). It is, therefore, necessary to come back to dissect HER2 pathway and unravel key features contributing to its transforming capacity (Sasso et al., 2011).

The present thesis, is focused on the role played by HER2-loss variants and Delta16 isoform in mediating HER2 oncogenic activity and in conditioning the response to HER2 therapies in breast cancer. These HER2 phenotypes can drive differential drug responses of the tumor and of distant metastases. Thus, recent investigations on drug resistance and on tumor biology converged to the development of preclinical cancer models representative of cancer heterogeneity and able to mimic all possible scenarios observed in human tumors.

In the laboratory of Immunology and Biology of Metastatis several preclinical mice models are currently available, including transgenic mice for huHER2, for Delta16 and a double transgenic model coexpressing both huHER2-full length and Delta16, obtained by crossing female FVBhuHER2 and male FVBDelta16 mice. Moreover, a panel of cell lines expressing different levels of HER2 was previously established, in order to study the mechanism of HER2 loss.

In this project, thanks to the availability of these preclinical models, it was studied the contribute of HER2 and of its variants to cancer development and drug resistance. In addition, with the purpose of obtaining preclinical models that could best recapitulate human tumor heterogeneity a panel of breast cancer PDX was developed.

1. HER2-loss

Besides the expression of high levels of the oncogene, cell lines grown from HER2-positive spontaneous mammary carcinomas can undergo to a progressive loss of HER2 expression. In the Laboratory of Immunology and Biology of Metastasis a panel of cell lines expressing a different pattern of HER2 levels was established; it represents the first model available to study HER2 loss mechanism. In fact, even though the down-regulation of HER2 expression can be studied by using other approaches (e.g. siRNA and lysozimes), the ensuing loss of tumorigenic capability does not reflect what happens in patients. In our model, Mambo38^{HER2loss} completely lost the expression of HER2, but showed either increased tumorigenic capacity or higher metastatic ability, in particular for what concerns the metastatic load in the lungs, when compared to Mambo89^{HER2stable}.

1.1 Stemness of FVBHUHER2 cell lines and EMT associated to HER2 loss

The experiments reported in this thesis underline that Mambo89^{HER2stable}, Mambo43^{HER2labile} and Mambo38^{HER2loss} cell lines differ between each other not only for HER2 expression. Indeed, they showed different morphology, stemness and expression of genes associated to Epithelial-to-Mesenchymal Transition (EMT).

Confirming the finding of Al-Haji and colleagues (Al-Haji et al., 2003) a connection between tumorigenity and stemness was observed. Mambo38^{HER2loss} showed the most expressed stem-like profile and the expression of stem surface markers correlated with their ability to form mammospheres. Moreover, it was found that Mambo38^{HER2loss} displayed a reprogrammed gene expression of EMT genes compared to Mambo89^{HER2stable}. In light of these findings Mambo38^{HER2loss} showed the core signature of EMT.

1.2 Sensivity to anti-cancer therapies

HER2 loss may be due either to the heterogeneity inherent in cancer cells or to clonal selection promoted by targeted therapies against HER2 with the consequent loss of oncogene addiction. Many studies assessing receptor discordance between primary

and metastatic breast cancers have been published. From meta-analysis studies a negative conversion in 13-24% metastasis was reported (Aurilio et al., 2014). However, it remains unclear what could be the clinical and prognostic effect of the expression of HER2 discordance between primary tumors and metastases. (Turner and Di Leo, 2013).

FVBhuHER2 cell lines sensivity to HER2 targeted therapies and to small molecule inhibitors of related pathways was investigated. MAMBO89^{HER2stable} resulted to be resistant to continuous treatment with trastuzumab and showed high and stable levels of HER2. On the other hand, MAMBO43^{HER2labile} was sensitive to trastuzumab. However, after 30 days of treatment emerging resistant clones did not express anymore HER2, even after the recovery period, and changed morphology from a typical epithelial to a fusiform shape. These results confirmed what described in literature, where several *in vitro* and *in vivo* studies have shown that resistance to lapatinib and trastuzumab is associated with HER2-loss and EMT induction (Creedon et al., 2014; Kim et al., 2013; Korkaya et al., 2014; Creedon et al., 2016).

As expected, HER2 loss was accompanied by resistance to HER2 targeted therapy in 3-D culture (lapatinib). MAMBO38^{HER2loss} was resistant also to dasatinib, whereas buparlisib was highly effective regardless of HER2 expression, highlighting the importance of targeting effectors belonging to PI3K-AKT signalling cascade.

It has been widely demonstrated that the presence of a HER2-PI3K crosstalk allows continued cancer cell growth and their survival (Carnero et al., 2008). In addition, these data are in agreement with *in vitro* studies that implicated the PI3K pathway in EMT (Xue et al., 2012; Wallin et al., 2012) and stem cell maintenance in breast cancer (Zhou et al., 2007; Korkaya et al., 2009; Hardt et al., 2012; Hanker et al., 2013).

1.3 Molecular mechanisms regulated by HER2 targeted therapies

In Mambo89^{HER2stable} and Mambo43^{HER2labile} cell lines 96h of pharmacological treatments did not significantly change the expression of HER2 and phosphoHER2. Notably, phospho-Akt was detectable only in the samples treated with buparlisib 1uM.

Published data show that Akt maximal enzymatic activation requires the phosphorylation of Thr308, located in the activation loop, and the phosphorylation of

Ser473, located in the C-terminal hydrophobic motif (Garcia- Echeverria & Sellers, 2008). The antibody used in this project for western blot detection is specific for Ser473 residue. The higher pAKT-Ser473 expression observed after buparlisib treatment could be due to a compensatory mechanism adopted by the cells in order to balance the inhibition effect of buparlisib on PI3K-PDK1.

The high expression of pAkt and pMAPK in Mambo38^{HER2loss} cells remarks their independence from huHER2 signalling and the induction of a bypass pathways, as demonstrated by the *in vitro* sensivity to buparlisib and confirmed as well by GNE-317 inhibition effect *in vivo*.

Hanker and colleagues generated a genetically engineered mouse model of mammary tumor harbouring both huHER2 and mutant PIK3CA. They showed that the coexpression of both oncogenes in the mouse mammary gland accelerated tumor formation and displayed a high metastatic propensity to lungs. Moreover, these tumors were histologically heterogeneous and exhibited features of EMT and stem-like cells and were able to form mammospheres. huHER2+PIK3CA tumors were also resistant to trastuzumab as a single agent and in combination with lapatinib or with pertuzumab. Drug resistance was partially reversed by the PI3K inhibitor buparlisib (Hanker et al., 2013). Our model of HER2 loss resembles that one described by Hanker and colleagues, confirming that the aberrant activation of the PI3K pathway is the mechanism of resistance to anti-HER2 therapies adopted by MAMBO38^{HER2loss} cells.

In summary, HER2 and PI3K cooperate in order to promote HER2 mammary tumor establishment and metastatic progression. These results suggest that combining anti-HER2 therapies with PI3K inhibitors may be beneficial for the clinical treatment of HER2-loss breast cancers.

In light of these findings the FVBhuHER2 model could be a valuable tool to investigate the underlying biology of HER2-loss breast cancers and for preclinical testing of alternative therapeutic strategies against this subtype of breast cancer.

2. Myc inhibition

The involvement of c-Myc, another key transcription factor involved in breast cancer, was studied in this model.

2.1 Omomyc action

Omomyc action, tested in MAMBO43^{HERlabile} and MAMBO38^{HER2loss} cell lines, determined a decrease in proliferation, confirming the findings of earlier studies developed on different types of cancers. In fact, Soucek and colleagues widely demonstrated the efficacy of omomyc, a dominant negative c-Myc inhibitor, *in vitro* and *in vivo*. They showed that c-Myc inhibition is a promising strategy for eradicating lung cancer (Soucek et al., 2008, Soucek et al. 2013), insulinoma (Sodir et al., 2011) and glioma (Annibali et al., 2014) inducing profound regression of tumours, eliciting only very mild side effects in normal tissues and circumventing the resistance mechanisms encountered with other targeted therapies.

Here, a new preclinical model was obtained in order to extend those previous studies, showing that c-Myc inhibition has a similar effective therapeutic potential for treating HER2-positive breast cancer.

An inducible stable system of cell lines was generated, using a doxycycline-switchable lentiviral vector to drive the expression of omomyc.

MAMBO43^{HERlabile} and MAMBO38^{HER2loss} were sensitive to omomyc effect, demonstrating that the regulation of Myc gene, whose aberrantly elevated and/or deregulated activity is associated with the majority of human cancers, could offer the opportunity to develop more effective therapeutic approaches to be applied to HER2-positive and HER-loss tumors that are unresponsive to current therapies.

Moreover omomyc appears to act in different ways in the two cell lines tested.

After treatment, omomyc expressing MAMBO43^{HER2labile} cells stopped proliferating, with a decrease of cells in S phase. Instead, there were more cells in G2 phase. Originally, cellular senescence was defined as an irreversible arrest in the G1 phase of the cell cycle. The idea that the senescence program can also be launched after G2 arrest has gained support from several recent publications, including evidence for its existence *in vivo* (Gire and Dulić, 2015). In agreement with this hypothesis, omomyc seems to drive MAMBO43^{HER2labile} cells through G2 exit program in senescence.

MAMBO38^{HER2loss} treated with omomyc upon doxycycline (dox) subministration arrested in Sub G1 phase, meaning that cells were dying by apoptosis.
These results confirmed what previously observed with other Myc inhibitors. The anti-proliferative effects of BET inhibitors (associated with a block in the transcription of Myc, followed by genome-wide suppression of c-Myc-dependent target genes) induced growth inhibition and undergo G0/G1 cell-cycle arrest, apoptosis and cellular senescence (Tolani et al., 2014).

In summary, it was demonstrated that Myc inhibition reduces proliferation, increases apoptosis and probably senescence. The pleiotropic nature of Myc is reflected in the way of action of its inhibitor—in our case omomyc—that can vary with the context-specific role of Myc, whose function ramifies throughout all aspects of tumorigenesis, either at the intracellular or at the extracellular levels.

2.2 Myc inhibition in combined targeted therapy of HER2-positive breast cancer

2.2.1 Cell proliferation

Whereas the HER2/PI3K/AKT pathway is frequently mutated in a wide range of cancers, thus driving tumorigenesis, inhibitors of this pathway such as lapatinib yield only limited success, because the cancer cells adapt quickly. Matkar and collegues (Matkar et al. Cancer Cell 2015) demonstrated that the MLL2/FOXO/c-Myc axis is inactivated by lapatinib, reducing sensivity to the drug, and that BRD4 inhibitor and lapatinib synergistically suppress HER2-positive breast cancer cells *in vitro* and *in vivo*. Taking this into account, the purpose of this project was to test omomyc efficacy in combination with lapatinib, an approved HER2-targeted therapy, to demonstrate that inhibiting Myc is a possible strategy to overcome drug resistance.

In MAMBO38^{HER2loss}, resistant to lapatinib because of the loss of HER2, cell growth was significantly inhibited by omomyc expression upon dox treatment and by the combined therapy. Notably, MAMBO43^{HER2labile} resulted resistant to lapatinib (82%) and quite sensitive to dox (70%). Interestingly, the combination of the two drugs resulted effective compared to the control.

These data confirmed what showed by Matkar and collegues, suggesting a potential role of Myc inhibition in combined targeted therapy of HER2-positive breast cancer and of its resistant variants, thus supporting the notion that combinatorial

regimens targeting different "layers" of the intracellular signaling may be more effective than single-agent treatments (Yarden and Pines, 2012; Arteaga and Engelman, 2014).

2.2.2 Cell signalling

At the proteic level it was detected that Mambo43^{HER2labile} lost HER2 and pHER2 expression after the infection with omomyc, independently from treatments. This could explain why this cell line was resitant to lapatinib *in vitro*. The causes of HER2 loss are unknown, since it does not depend on the treatment, as previously discussed for trastuzumab. Probably, the lentiviral infection and the antibody selection process together can induce a change in the cell line already described as "labile" for HER2 expression; not being anymore in confluent condition thus, losing cell-to-cell contacts, is a condition that can affect cell phenotype. In fact, Mambo43^{HER2labile} have been found to exhibit the EMT-like changes found in MAMBO38^{HER2loss} when grown at low cell density, in the specific fusiform morphology and HER2 loss.

These data agree with the cell density pattern described for MCF10A (Cichon et al., 2015). MCF10A cell line are known to show differential expression of EMT marker genes depending on whether the cells are cultured under sparse or confluent conditions. This cell line showed progressively increasing mRNA levels of the epithelial marker E-cadherin and progressively decreasing mRNA levels of the mesenchymal markers N-cadherin and vimentin at higher cell densities throughout the density range (Cichon et al., 2015).

In Mambo43^{HER2labile} the amount of total Akt and total MAPK was lower after omomyc expression alone or in combination with lapatinib compared to the control, suggesting a correlation between these pathways, c-Myc and EGFR inhibition. However, a lower effect was observed after the treatment with lapatinib alone too. Reduction of c-Myc expression in literature is closely associated with deregulated ERK, JNK, MAPK and AKT activity. Furthermore, lapatinib is demonstrated to effectively inhibit the transactivation of EGFR and HER2 by IGF-1 signalling (Nahta et al., 2007).

Instead, in Mambo38^{HER2loss} the expression of Akt and MAPK proteins either at the basal or at the activated level increased after lapatinib treatment, suggesting the presence of a compensatory mechanism driven by EGFR inhibition. On the contrary, omomyc expression upon dox treatment did not clearly change the expression of the activated proteins, proposing that inhibiting Myc the compensatory mechanism switched on by lapatinib was partially inhibited. In both cell lines after the combined

treatment, it was observed a clear increase of MAPK phosphorylated protein levels compared to lapatinib alone and to the control, that could be due to the activation of a compensatory mechanism, which leads to the activation of other receptors of the convergence on MAPK pathway

In literature many examples of negative feedback induced by small molecules inhibitors are available. In particular, Turke and colleagues demonstrated that the treatment of BT-474 with a MEK inhibitor (AZD6244) was able to activate ErbB receptors (including HER2) by releasing a negative feedback on ErbB dimerization. As a consequence, the impaired MAPK cascade was compensated by the strong activation of PI3K-AKT pathway (Turke *et al.,* 2012). Similarly, two studies showed that the inhibition of PI3K-AKT cascade in the same cell line caused the potent activation of HER receptors and of MAPK pathway (Chandarlapaty *et al.,* 2011; Serra *et al.,* 2011).

In conclusion these data validated Myc inhibition as a therapeutic strategy in HER2-positive tumors where, in combination with HER2 targeted therapies, it could be very helpful to overcome drug resistance.

3. Co-expression of full-length HER2 and Delta16 in F1 mice

Most human HER2-positive breast cancers express the Delta16 splicing isoform (Wong 1998; Siegel 1999; Castiglioni 2006), involved in cancer aggressiveness and to targeted therapies responses (Mitra 2009; Marchini 2011; Alajiati 2013). Transgenic mice for each isoform (full-length human HER2 or Delta16) have been developed (Finkle 2004; Marchini 2011), but coexpressing murine models were never studied so far. To study mammary carcinogenesis in a mouse model that mimics the human situation, hybrid mice bearing heterozygous copies of both human transgenes (HER2/Delta16 mice) were produced and compared to parental mice (referred to as Delta16 and HER2 transgenic mice, respectively).

The aim of this part of the project was to analyze the contribute of wild-type full-lenght HER2 and of its splice variant Delta16 to mammary HER2-positive carcinogenesis and to HER2 targeted therapy efficacy.

3.1 Neoplastic progression to mammary carcinoma in F1 mice

Pre-existing analysis performed in the laboratory of Immunology and Biology of Metastatis confirmed the findings of Marchini and colleagues (Marchini et al., 2011) showing that the presence of Delta16 causes the anticipation of tumor onset in mice, and that the simultaneous presence of the two isoforms does not change tumor latency in respect to Delta16 isoform alone. Moreover, despite the enhanced transformation ability of Delta16, tumors in Delta16 and F1 mice grew slower than those of HER2-expressing mice. Thus, the expression of the splice variant seems significant for early carcinogenic events, but it may not be so relevant for later stages as progression and metastatic development. The analysis of the expression levels of the two isoforms in preneoplastic and neoplastic mammary glands of F1 mice, compared to HER2 full-length and Delta16-driven carcinomas, confirmed our hypothesis.

Homogeneous and intermediate levels of expression of both isoforms characterized F1 preneoplastic mammary glands, compared to either HER2 full-length or Delta16 mice, while F1 tumors were mostly expressing high levels of Delta16 isoform and low levels of full length HER2 (80%). Thus, neoplastic progression to mammary carcinoma in F1 mice requires the activation of both transgenes with a strong bias towards Delta16 probably due to its ability to form highly active homodimers (Castagnoli et al., 2015).

The coexistence of HER2 and Delta16 in mammary tumors arisen in the hybrid model was shown by the presence of the transcripts of both isoforms. In humans, HER2 and Delta16 transcripts coexist in nearly half HER2-positive breast cancers and in 90% of patients with locally advanced disease, i.e. with invasive cancer cells in the lymph nodes (Castiglioni *et al*., 2006; Mitra *et al*., 2009). Thus, if compared with HER2 and Delta16 models, F1 mice represent a further step in the attempt to mimic the human situation in preclinical models.

3.2 HER2 /Delta16 expression and tumor sensivity to therapies

The expression of the Delta16 isoform was initially thought to be involved in resistance to HER2 targeted therapies. However Delta16 expression in Delta16 transgenic mice is actually associated with increased trastuzumab sensitivity and in breast cancer patients with decreased risk of relapse after trastuzumab treatment (Castagnoli et al, 2015).

In this thesis sensitivity to trastuzumab was studied both in preventive and in therapeutic setup. Trastuzumab *in vivo* treatment delayed tumor onset showing the maximal efficacy in the prevention of Delta16-expressing tumors with respect to tumors expressing full length HER2 isoform only. Therefore the expression of the Delta16 isoform confers a higher sensitivity to trastuzumab even in tumor prevention.

Anti-HER2 and -PI3K treatment did not have the same efficacy in therapeutical setting against F1 homogeneous established tumors. After five months of trastuzumab 40% of mice were still tumor free, while buparlisib showed an inhibition of tumor growth just in 20% of mice. This result underline the sensivity of Delta16 isoform to only trastuzumab therapy, a very important challenge to consider in clinic.

Previous data obtained in our laboratory already demonstrated *in vitro* sensivity of Delta16 expressing cell lines to tratuzumab. In particular, as high was the expression of Delta16 variant as strong was the inhibitor effect of trastuzumab on 3D cell growth. Taking this into account, it was studied how trastuzumab treatment can modulate the levels of expression of the two isoform. Two cell lines were evaluated, 302-IVD (high HER-2, high Δ16) and 156-IS (low HER-2, high Δ16). It was found that trastuzumab treatment does not affect the isoform ratios, either in trastuzumab-sensitive 156Is cells or in resistant 302-IVD cells, even though the latter showed a significant decrease of both isoform levels.

3.3 HER2 isoforms long-term stability

Although HER2 overexpression is implicated in the pathogenesis of breast cancer, HER2 is more commonly overexpressed in patients with ductal carcinoma in situ (DCIS) when compared with invasive breast cancer (Park et al., 2006; Kato et al., 2016). Furthermore, discordance in HER2 expression and in drug susceptibility between primary tumors and metastases has been reported (Niikura et al., 2012), thus suggesting variation in HER2 expression during tumor progression.

F1 transgenic model is a useful tool for studying the effects on HER2 isoform expression of long-term *in vivo* host-tumor interaction. However, transgenic mice are, in general, not the best model to study the late stages of breast cancer and the biology of metastasis, because of the low incidence of metastases (Ottewell et al., 2006; Saxena and Christofori, 2013). To overcome this issue, syngenic transplantation models were employed. F1 HER2/Delta16 murine tumors were serially transplanted in

immunocompetent mice for five consecutive passages. Serial graft evidenced the long stability of Delta16 isoform and the variation in HER2 expression.
The tumors were analysed for the expression of HER2 and Delta16 transcript by quPCR and for the expression of total surface HER2 protein by FACS analysis.
The results obtained suggest that Delta16 maintains a stable expression because of its driver role in this tumor system, whereas full-length HER2 could freely change because it plays a lesser role. However, it is important to realize that the evaluation of the expression of total plasmatic HER2 protein on cells surface was hampered by the lack of an antibody that specifically target each isoform.

In conclusion, it was found that the coexpression of HER2 and Delta16 isoforms tunes tumor onset, growth and sensitivity to targeted therapy.

Furthermore, the heterogeneous expression of HER2 and Δ16 in the F1 model, enhances its preclinical value as a suitable tool for investigational studies on new therapeutic strategies against HER2.

4. PDX model

Molecular studies have revealed underlying complexity and molecular heterogeneity of breast cancer. Patient derived tumor xenografts (PDX) are reported to better recapitulate this complexity than cell-based tumor xenografts (Cassidy et al., 2015). With the aim to generate a collection of PDXs that represent the main subtypes of breast cancer, starting from 65 primary breast cancer specimens, 7 transplantable PDXs were established.

4.1 A panel of Breast Cancer Xenograft Models

Fresh surgically resected patient-derived specimens were obtained thanks to the collaboration with Sant'Orsola-Malpighi Hospital, Bologna (Prof. Mario Taffurelli, Prof. Donatella Santini, Dr. Claudio Ceccarelli) and Bellaria Hospital, Bologna (Prof. Maria Pia Foschini, Dr. Enrico Di Oto, Dr. Sofia Asioli).

Orthotopic tumor xenograft implantation and severe immunodepressed mice (RGKO or NSG) were chosen in order to improve the engraftment rate and to reduce tumor latency. The histological and molecular subdivision of the specimens received reflected their frequency documented in clinic.

7 transplantable PDXs out of 65 primary breast cancer specimens implanted were established, reaching a tumor take-rate of 11%. This low percentage of engraftment underlines what is documented in literature, where the variable engrafted rates are reported as one of the main challenges fronted when developing a panel of PDX (Siolas and Hannon, 2013).

In this panel of PDXs all the engrafted specimens were invasive ductal carcinomas, reflecting the clinical evidences supporting their higher rate of engraftment in respect to lobular carcinomas (Marangoni et al., 2007). Moreover, all of them were of histologic grade III and Ki67-high, confirming that higher engraftment rates are associated with more clinically aggressive tumors (Zhao et al., 2012, Beckhove et al., 2003; Marangoni et al., 2007; Kabos et al., 2012; Zhang et al., 2013; Bergamaschi et al., 2009). In addition, these results are as well consistent with ER-negative receptor guidelines, associated to a better growth of specimens *in vivo*, as it was observed in these PDXs. Considering the intrinsic subtype, De Rose and co-workers, as Kabos and co-workers, showed that Luminal B carcinoma can engraft better than Luminal A, thanks to its higher proliferative capability (De Rose et al., 2013; Kabos et al., 2012). This result was confirmed too. The highest rate of PDX stabilization was obtained for HER2-positive (40%) followed by Triple negative (20%), Luminal B (14%) and Luminal A (3%) subtype.

A long latency period after the engraftment can limit PDXs feasible employment (Siolas & Hannon, 2013; Ledford, 2016). In our data, tumor growth curves of engrafted PDXs at the first passage showed a latency range of 1- 62 weeks. This variability is probably due to the intrinsic characteristic of the specimen. Moreover, it could be affected by its condition at the moment of the inoculation, e.g. correct crio-conservation, freshness and time-efficiency from the surgery to the animal house. The kinetics of the growth was independent from the latency period. Each tumor was represented by the tumor growth in the later passages, and was independent from the intrinsic subtype. Furthermore, all engrafted PDXs maintained stabile features through the consecutive passages, regarding engraftment rate, latency period and growth fast rate.

4.2 HER2-positive FOT4 PDX

Among the engrafted PDX, two were classified as HER2-positive, the FO4 and TA45. In this thesis, FO4 was studied in more detail. FO4 tumor histologically is described as an invasive ductal carcinoma of grade III, with a high rate of proliferation, negative for the expression of Estrogen/Progesteron receptors and positive for HER2 proliferation. FO4 was propagated *in vivo* for more than XI generations. It represents a successful example of HER2-positive PDX, whose intrinsic characteristic resembles that of one of the most aggressive HER2 positive breast cancer found in clinic. FO4 *in vivo* growth was stable over all the consecutive passages, in terms of latency and growth fast rate. Moreover, we had 100% of the engraftment rate from the second passage on.

One of the key premises of developing PDX models for cancer research is the assumption that these models faithfully represent the original tumor from which they were developed and that this similarity is maintained across passages (Aparicio et al., 2015). In order to establish the degree of reliability of our PDX model, the expression ratio between HER2 full-length, Delta16 isoform and the molecular stability of selected biomarkers during prolonged vivo transplantation was investigated.

FO4 PDX recapitulated the morphologic and structural patterns, as well as HER2 expression of patient tumor among several passages *in vivo* (II-VII), which maintained a stable gene expression of HER2 full-length and Delta16 isoforms over time, and exhibited stable patterns of protein expression. Moreover, the high levels of HER2 phosphorylation among passages confirmed the essential role of the receptor and of its signalling pathway in the maintenance of tumor aggressiveness. While the analysis of other markers such as HER1, HER3 and IGFR have suggested the lack of dependence from the signalling pathways mediated by these receptors. In light of these findings, FO4 showed a high level of concordance with the profile of the tumor of origin. Hence, confirming FO4 as a good PDX model.

4.3 Sensitivity to targeted therapies

Supporting these conclusions, in order to validate FO4 PDX as preclinical tool for drug discovery, the susceptibility of this model to anti-HER2 drugs was tested *in vivo*. The inhibition of HER2 was investigated on 2 different levels: the extracellular

inhibition mediated by trastuzumab and the intracellular inhibition of neratinib, which specifically recognise the tyrosine-kinasic intracellular domain of HER2. Neratinib was able to inhibit FO4 tumor growth in a higher extent in respect to trastuzumab.

Data from *in vivo* experiments and clinical trials indicate that the efficacy of trastuzumab could be partly related to its induction of an immune response (Gennari et al. 2004; Carter et al. 1992; Cooley et al. 1999; Lewis et al. 1993; Stockmeyer et al. 2003). Cancer immunotherapies are designed to work in conjunction with a patient's immune system in order to increase native anti-tumor responses. In this field of study, conventional xenograft models lack relevance due to the animals' immunocompromised status. Indeed, trastuzumab partial efficacy could be due to the lack of an immune system in the mice strain used for the experiment. However, both drugs stopped tumor growth, confirming the HER2 driver role in the maintenance of the malignancy phenotype. In contrast, as observed from western blot and FACS analysis, none of the treatments led to alterations in the expression ratio between HER2 full-length and HER2 Delta16 isoform or selection of HER2-negative variants.

To further investigate the effect of neratinib treatment on HER2 activation pathway, the drug effect was tested as well on primary cultures established from a FO4 tumor sample by Western blot. After the treatment, a clear reduction of HER2 and Akt phosphorylation levels was observed, while MAPK phosphorylated protein levels increased compared to the control. This accumulation of activated MAPK could be the direct consequence of the decrease of phospho-HER2 and –Akt, suggesting the activation of a compensatory mechanism, which leads to the activation of other receptors of the convergence on MAPK pathway.

In conclusion, it was established a well-characterized panel of breast cancer xenograft models suitable as preclinical tools for translational studies.

CONCLUSION

Conclusion

In the present thesis, the functional role of HER2 and its isoforms in tumor progression and in drug resistance was investigated. Three breast cancer preclinical models representative of HER2 mammary carcinogenesis were developed and characterized.

Cell lines derived from human HER2 transgenic mammary carcinoma faithfully reproduced the dynamic of HER2 expression/loss in human breast cancer.

MAMBO38HER2loss cell line is a clear example of resistance with the consequent loss of oncogene addiction. This cell line escaped HER2 dependence by EMT and compensatory PI3K activation.

The therapeutic efficacy of buparlisib and GNE317 on MAMBO38^{HER2loss} cell line is the demonstration that HER2 and PI3K cooperate in order to promote HER2 mammary tumor establishment and metastatic progression. These results suggest that combining anti-HER2 therapies with PI3K inhibitors may be beneficial for the clinical treatment of HER2-loss breast cancers. Moreover, it was suggested a potential role of Myc inhibition in combined targeted therapy of HER2-positive breast cancer and of its resistant variants.

Indeed, the mouse model presented here could be a valuable tool in order to investigate the underlying biology of HER2-loss breast cancers and for preclinical testing of therapeutic strategies against this subtype of breast cancer

The study of the natural history of tumors in F1 mice showed that, even in genetically identical mice, a divergent evolution could occur, leading to tumors with a variable expression of HER2 isoforms, which reminds the human situation.

The coexpression of HER2 and Delta16 isoforms tunes tumor onset, growth and sensitivity to targeted therapy. Furthermore, the heterogeneous expression of HER2 and Delta16 in the F1 model enhances its preclinical value as a suitable tool for investigational studies on new therapeutic strategies against HER2.

Finally, a well-characterized panel of breast cancer xenograft models was established. Preservation of therapeutic targets across primary tumors and their matching PDXs over serial passaging, and effective responses to targeted therapies, validate them as preclinical tools for translational studies. However the low rate of appearance of variants related to disease progression suggest the opportunity to integrate data from PDX models obtained in immunodeficient mice with data from autochthonous tumors in immunocompetent transgenic mice.

SCIENTIFIC PUBLICATIONS DURING PHD PERIOD

Related to the PhD project

Landuzzi L, Palladini A, Ianzano ML, **Laranga R**, D'Intino G, Nanni P, Lollini P-L. Evaluation of metastatic burden and recovery of human metastatic cells from a mouse model, «MACS & MORE», 2016, 17, pp. 17 – 19

Palladini A, Nicoletti G, Lamolinara A, Dall'Ora M, Balboni T, Ianzano ML, **Laranga R**, Landuzzi L, Giusti V, Ceccarelli C, Santini D, Taffurelli M, Di Oto E, Asioli S, Amici A, Pupa S.M , De Giovanni C., Tagliabue E, Iezzi M, Nanni P,. Lollini P-L. HER2 isoform co-expression tunes mammary carcinoma onset and progression. *Submitted.*

Other

De Giovanni C, Nicoletti G, Quaglino E, Landuzzi L, Palladini A, Ianzano ML, Dall'Ora M, Grosso V, Ranieri D, **Laranga R**, Croci S, Amici A, Penichet ML, Iezzi M, Cavallo F, Nanni P and Lollini PL. (2014) Vaccines against human HER2 prevent mammary carcinoma in mice transgenic for human HER2. Breast Cancer Res; 16: R10.

Landuzzi L, Ianzano ML, Nicoletti G, Palladini A, Grosso V, Ranieri D, Dall'Ora M, Raschi E, **Laranga R**, Gambarotti M, Picci P, De Giovanni C, Nanni P, Lollini P-L. (2014) Genetic prevention of lymphoma in p53 knockout mice allows the early development of p53 related sarcomas. Oncotarget; 5(23):11924-38.

REFERENCES

References

Agus DB, Akita RW, Fox WD, Lewis GD, Higgins B, Pisacane PI, Lofgren JA, Tindell C, Evans DP, Maiese K, Scher HI, Sliwkowski MX. 2002. Targeting ligand-activated ErbB2 signaling inhibits breast and prostate tumor growth. Cancer Cell 2(2): 127-137.

Ahmadi L, Kamkari S, Mokarram P, et al. HER-2/neu and E-cadherin Expression and Microsatellite Instability in Gastric Dysplasia. Middle East Journal of Digestive Diseases. 2011;3(1):20-27.

Alajati A, Sausgruber N, Aceto N, Duss S, Sarret S, Voshol H, et al. Mammary tumor formation and metastasis evoked by a HER2 splice variant. Cancer Res 2013;73:5320-7.

Al-Hajj M, Wicha MS, Benito-Hernandez A, Morrison SJ, and Clarke MF. (2003). "Prospective Identification of Tumorigenic Breast Cancer Cells." Proceedings of the National Academy of Sciences of the United States of America 100: 3983–3988

Altomare DA, Testa JR. Perturbations of the AKT signaling pathway in human cancer. Oncogene (2005) 24(50):7455–64.10.1038/sj.onc.1209085

Angelini PD, Zacarias Fluck MF, Pedersen K, Parra-Palau JL, Guiu M, Bernado MC, et al. Constitutive HER2 signaling promotes breast cancer metastasis through cellular senescence. Cancer Res 2013;73:450-8.

Annibali D, Whitfield JR, Favuzzi E, Jauset T, Serrano E, Cuartas I, Redondo-Campos S, Folch G, Gonzàlez-Juncà A, Sodir NM, Massó-Vallés D, Beaulieu ME,. Swigart LB, Mc Gee MM, Somma MP, Nasi S, Seoane J, Evan JI, Soucek L. Myc inhibition is effective against glioma and reveals a role for Myc in proficient mitosis. Nat Commun. 2014 Aug 18; 5: 4632. Published online 2014 Aug 18. doi: 10.1038/ncomms5632

Aparicio S, Hidalgo M and Kung AL. (2015). "Examing the utility of patient-derived xenograft mouse models." Nature Reviews Cancer Viewpoint 15: 311-316.

Arpino G, Gutierrez C, Weiss H, et al. 2007. Treatment of human epidermal growth factor receptor2–overexpressing breast cancer xenografts with multiagent HER-targeted therapy. J. Natl. Cancer Inst.99:694–705

Arpino G., Wiechmann L., Osborne C., Schiif R. (2008) Crosstalk between the estrogen receptor and the HER tyrosine kinase receptor family: molecular mechanism and clinical implications for endocrine therapy resistance. Endocr Rev 29: 217–233.

Arribas J, Baselga J, Pedersen K, Parra-Palau JL. 2011. p95HER2 and breast cancer. Cancer Res. 71:1515–19

Arteaga CL and Engelman JA. (2014) ERBB receptors: from oncogene discovery to basic science to mechanism-based cancer therapeutics. Cancer Cell; 25: 282-303.Baselga J et al. (2001) Mechanism of action of trastuzumab and scientific update. Semin Oncol 28 (Suppl 16): S4–S1119

Arteaga CL, Sliwkowski MX, Osborne CK, et al. 2012. Treatment of HER2-positive breast cancer:current status and future perspectives. Nat. Rev. Clin. Oncol. 9:16–32

Aurilio G, Disalvatore D, Pruneri G, Bagnardi V, Viale G, Curigliano G, Adamoli L, Munzone E, Sciandivasci A, De Vita F, Goldhirsch A, Nolè F. (2014). "A Meta-Analysis of Oestrogen Receptor, Progesterone Receptor and Human Epidermal Growth Factor Receptor 2 Discordance between Primary Breast Cancer and Metastases." European Journal of Cancer 50: 277–289

Ayyanan, A., Civenni, G., Ciarloni, L., Morel, C., Mueller, N., Lefort, K., … Brisken, C. (2006). Increased Wnt signaling triggers oncogenic conversion of human breast epithelial cells by a Notch-dependent mechanism. Proceedings of the National Academy of Sciences of the United States of America, 103(10), 3799–3804

Bachman KE, Argani P, Samuels Y, Silliman N, Ptak J, Szabo S, et al. The PIK3CA gene is mutated with high frequency in human breast cancers. Cancer Biol Ther. 2004;3:772–775.

Bailey TA, Luan H, Clubb RJ, Naramura M, Band V, Raja SM and Band H. Mechanisms of Trastuzumab resistance in ErbB2-driven breast cancer and newer opportunities to overcome therapy resistance. J Carcinog. 2011; 10:28.

Barok M, Balazs M, Lazar V, et al. Character- ization of a novel, trastuzumab resistant human breast cancer cell line. Front Biosci (Elite Ed) 2010;2:627-40).

Baselga J, Albanell J, Molina MA, Arribas J. Mechanism of action of trastuzumab and scientific update. Semin Oncol. 2001 Oct;28(5 Suppl 16):4-11.

Baselga J, Bradbury I, Eidtmann H, Di Cosimo S, de Azambuja E, Aura C, Gomez H, Dinh P, Fauria K, Van Dooren V, Aktan G, Goldhirsch A, Chang TW, Horvath Z, Coccia-Portugal M, Domont J, et al. Lapatinib with trastuzumab for HER2-positive early breast cancer (NeoALTTO): a randomised, open-label, multicentre, phase 3 trial. Lancet. 2012;379:633–64

Baselga J, J.Cortés, S.B. Kim, S.A. Im, R. Hegg, Y.H. Im, L. Roman, J.L. Pedrini, T. Pienkowski, A. Knott, CLEOPATRA Study Group, et al. Pertuzumab plus trastuzumab plus docetaxel for metastatic breast cancer. N. Engl. J. Med., 366 (2012), pp. 109–119.

Baselga J, Swain SM. Novel anticancer targets: revisiting ERBB2 and discovering ERBB3. Nat Rev Cancer 2009; 9: 463–475.

Beckhove P, Schutz F, Diel IJ, Solomayer EF, Bastert G, Foerster J, Feuerer M, Bai L, Sinn HP, Umansky V and Schirrmacher V. (2003). "Efficient engraftment of human primary breast cancer transplants in nonconditioned NOD/SCID mice." International Journal of Cancer 105: 444–453.

Bellacosa A, de Feo D, Godwin AK, Bell DW, Cheng JQ, Altomare DA, et al. Molecular alterations of the AKT2 oncogene in ovarian and breast carcinomas. Int J Cancer. 1995;64:280–285.

Bergamaschi A, Hjortland GO, Triulzi T, Sørlie T, Johnsen H, Ree AH, Russnes HG, Tronnes S, Mælandsmo GM, Fodstad O, Borresen-Dale AL and Engebraaten O. (2009). "Molecular profiling and characterization of luminal-like and basal-like *in vivo* breast cancer xenograft models." Molecular Oncology 3: 469-482.

Berns K, Horlings HM, Hennessy BT, et al. 2007. A functional genetic approach identifies the PI3K pathway as a major determinant of trastuzumab resistance in breast cancer. Cancer Cell 12:395–402

Bose P, Ozer H. Neratinib: an oral, irreversible dual EGFR/HER2 inhibitor for breast and non-small cell lung cancer. Expert Opin Investig Drugs. 2009;18:1735–1751.

Bose R, Kavuri SM, Searleman AC, ShenW, Shen D, et al. 2013. Activating HER2 mutations in HER2 gene amplification negative breast cancer. Cancer Discov. 3:224–37

Bottle A, Tsang C, Parsons C, Majeed A, Soljak M, Aylin P. Association between patient and general practice characteristics and unplanned first-time admissions for cancer: observational study. Br J Cancer.2012.

Bray SJ.. Notch signalling: a simple pathway becomes complex. Nat Rev Mol Cell Biol (2006) 7(9):678–89.10.1038/nrm2009

Breast cancer intrinsic subtype classification, clinical use and future trends. American Journal of Cancer Research, 5(10), 2929–2943.

Brenton JD, Carey LA, Ahmed AA, Caldas C. Molecular classification and molecular forecasting of breast cancer: ready for clinical application? J. Clin. Oncol. 2005;23:7350–7360

Burgess, A. W. et al. An open-and-shut case? Recent insights into the activation of EGF/ErbB receptors. Mol. Cell 12, 541–552 (2003).

Cameron DA, Stein S. Drug insight: intracellular inhibitors of her2--clinical development of lapatinib in breast cancer. Nat Clin Pract Oncol. 2008;5:512–20.

Campbell IG, Russell SE, Choong DY, Montgomery KG, Ciavarella ML, Hooi CS, et al. Mutation of the PIK3CA gene in ovarian and breast cancer. Cancer Res. 2004;64:7678–7681.

Canonici A, Gijsen M, Mullooly M, et al. Neratinib overcomes trastuzumab resistance in HER2 amplified breast cancer. Oncotarget. 2013;4(10):1592-1605.

Cao X, Shores EW, Hu-Li J, Anver MR, Kelsall BL, Russell SM, Drago J, Noguchi M, Grinberg A, Bloom ET and . (1995) Defective lymphoid development in mice lacking expression of the common cytokine receptor gamma chain. Immunity; 2: 223-238.

Cappuzzo, F., Bemis, L. & Varella-Garcia, M. HER2 mutation and response to trastuzumab therapy in non-small-cell lung cancer. N. Engl. J. Med. 354, 2619–2621 (2006).

Carey LA, Perou CM, Livasy CA, Dressler LG, Cowan D, Conway K, Karaca G, Troester MA, Tse CK, Edmiston S, et al. Race, breast cancer subtypes, and survival in the Carolina Breast Cancer Study. JAMA. 2006;295:2492–2502

Carey LA. Through a glass darkly: advances in understanding breast cancer biology, 2000-2010. Clin Breast Cancer. 2010;10:188–195.

Carnero A, Blanco-Aparicio C, Renner O, Link W, Leal JFM. (2008). The PTEN/PI3K/Akt signalling pathway in cancer, therapeutic implications. Curr Cancer Drug Targets 8: 187–198.

Carpten JD, Faber AL, Horn C, Donoho GP, Briggs SL, Robbins CM, et al. A transforming mutation in the pleckstrin homology domain of AKT1 in cancer. Nature. 2007;448:439–444.

Carter P et al. (1992) Humanization of an antip185her2 antibody for human cancer therapy. Proc Natl Acad Sci USA 89: 4285–428923

Cassidy JW, Caldas C and Bruna A. (2015). "Maintaining tumor heterogeneity in patient-derived tumor xenografts." Cancer Research 75: 2963-2968.

Castagnoli L, Iezzi M, Ghedini GC, Ciravolo V, Marzano G, Lamolinara A, et al. Activated d16HER2 homodimers and SRC kinase mediate optimal efficacy for trastuzumab. Cancer Res 2014;74:6248-59.

Castiglioni F, Tagliabue E, Campiglio M, et al. 2006. Role of exon-16-deleted HER2 in breast carcinomas.Endocrine-Related Cancer 13:221–32

Chandarlapaty S, Sawai A, Scaltriti M, Rodrik-Outmezguine V, Grbovic-Huezo O, Serra V, Majumder PK, Baselga J and Rosen N. (2011) AKT inhibition relieves feedback suppression of receptor tyrosine kinase expression and activity. Cancer Cell; 19: 58-71.

Cho, H. S. et al. Structure of the extracellular region of HER3 reveals an interdomain tether. Science 297, 1330–1333 (2002).

Cichon MA, Nelson CM, Radisky DC. Regulation of Epithelial-Mesenchymal Transition in Breast Cancer Cells by Cell Contact and Adhesion. Cancer Informatics. 2015;14(Suppl 3):1-13. doi:10.4137/CIN.S18965.

Citri A, Yarden Y. EGF-ERBB signalling: towards the systems level. Nat Rev Mol Cell Biol 2006; 7: 505–516.

Cobleigh MA, Vogel CL, Tripathy D et al (1999) Multinational study of the efficacy and safety of humanized anti-HER2 monoclonal antibody in women who have HER2-overexpressing metastatic breast cancer that has progressed after chemotherapy for metastatic disease. J Clin Oncol 17(9):2639–2648

Cooley S et al. (1999) Natural killer cell cytotoxicity of breast cancer targets is enhanced by two distinct mechanisms of antibody-dependent cellular cytotoxicity against LFA-3 and HER2/neu. Exp Hematol 27: 1533–154124

Cornolti, G. et al. Amplification and overexpression of HER2/neu gene and HER2/neu protein in salivary duct carcinoma of the parotid gland. Arch. Otolaryngol. Head Neck Surg. 133, 1031–1036 (2007).

Creedon H, Balderstone LA, Muir M, et al. Use of a genetically engineered mouse model as a preclinical tool for HER2 breast cancer. Disease Models & Mechanisms. 2016;9(2):131-140. doi:10.1242/dmm.023143.

Creedon, H., Byron, A., Main, J., Hayward, L., Klinowska, T. and Brunton, V.G.(2014). Exploring mechanisms of acquired resistance to HER2 (human epidermal growth factor receptor 2)-targeted therapies in breast cancer.Biochem. Soc. Trans. 42, 822-830. doi:10.1042/BST20140109

Creighton CJ. The molecular profile of luminal B breast cancer. Biologics. 2012;6:289–297.

D. Slamon, et al. Adjuvant trastuzumab in HER2-positive breast cancer. N Engl J Med, 365 (2011), pp. 1273–1283

D.B. Agus, R.W. Akita, W.D. Fox, G.D. Lewis, B. Higgins, P.I. Pisacane, J.A. Lofgren, C. Tindell, D.P. Evans, K. Maiese, et al. Targeting ligand-activated ErbB2 signaling inhibits breast and prostate tumor growth Cancer Cell, 2 (2002), pp. 127–137

Dang CV. Enigmatic MYC Conducts an Unfolding Systems Biology Symphony. Van Dang C, ed. Genes & Cancer. 2010;1(6):526-531. doi:10.1177/1947601910378742.Soucek L, Helmer-Citterich M, Sacco A, Jucker R, Cesareni G, Nasi S 1998. Design and properties of a Myc derivative that efficiently homodimerizes. Oncogene 17: 2463–2472

Dawson SJ, Ruenda OM, Aparicio S and Caldas C. (2013). "A new genome-driven integrated classification of breast cancer and its implication." The EMBO Journal 32: 617-628.

Dawson, S. J., Duffy, S. W., Blows, F. M., Driver, K. E., Provenzano, E., LeQuesne, J., Wishart, G. C. (2009). Molecular characteristics of screen-detected vs symptomatic breast cancers and their impact on survival. British Journal of Cancer, 101(8), 1338–1344.

De Laurentiis M, Arpino G, Massarelli E, Ruggiero A, Carlomagno C, Ciardiello F,et al. A meta-analysis on the interaction between HER-2 expression and response to endocrine treatment in advanced breast cancer. Clin Cancer Res 2005;11:4741–8.;

DeRose YS, Wang G, Lin YC, Bernard PS, Buys SS, Ebbert MT, Factor R, Matsen C, Milash BA, Nelson E, Neumayer L, Randall RL, Stijleman IJ, Welm BE and Welm AL. (2013). "Tumor grafts derived from women with breast cancer authentically reflect tumor pathology, growth, metastasis and disease outcomes." Nature Medicine 17: 1514–1520.

Dowsett M, Allred C, Knox J, Quinn E, Salter J, Wale C, et al. Relationship between quantitative estrogen and progesterone receptor expression and human epidermal growth factor receptor 2 (HER-2) status with recurrence in the arimidex, tamoxifen, alone or in combination trial. J Clin Oncol 2008;26:1059–65;

E.A. Perez, et al. Trastuzumab plus adjuvant chemotherapy for human epidermal growth factor receptor 2-positive breast cancer: planned joint analysis of overall survival from NSABP B-31 and NCCTG N9831. J Clin Oncol, 32 (2014), pp. 3744–3752

Eccles SA. The epidermal growth factor receptor/Erb-B/HER family in normal and malignant breast biology. Int J Dev Biol. 2011;55(7-9):685-96:

Eceles SA (2001) The role of c-erbB-2/HER2/neu in breast cancer progression and metastasis. J Mamm Gland Biol Neoplasia 6: 393–40614

Ellis IO, Schnitt SJ, Sastre-Garau X, Bussolati G, Tavassoli FA, Eusebi V, Peterse JL, Mukai K, Tabar L, Jacquemier J, Cornelisse CJ, Sasco AJ, Kaaks R, Pisani P, Goldgar DE, Devilee P, Cleton-Jansen MJ, Børrensen-Dale AL, Van't Veer L, Sapino A. In: Tumors of the Breast and Female Genital Organs. Tavassoli FA, Devilee P, editor. Lyon: IARC; 2003. Invasive breast carcinoma; pp. 30–48.

Ellis MJ, Tao Y, Luo J, A'Hern R, Evans DB, Bhatnagar AS, Chaudri Ross HA, von Kameke A, Miller WR, Smith I, et al. Outcome prediction for estrogen receptor-positive breast cancer based

on postneoadjuvant endocrine therapy tumor characteristics. J Natl Cancer Inst. 2008;100:1380–1388.

Elston, C.W., Ellis I.O. and Pinder S.E. (1999) Pathological prognostic factors in breast cancer. Crit Rev Oncol Hematol, 31, 209-23.

Emde A, Kostler WJ and Yarden Y. (2012) Therapeutic strategies and mechanisms of tumorigenesis of HER2-overexpressing breast cancer. Crit Rev Oncol Hematol; 84 Suppl 1: e49-e57.

English DP, Roque DM, Santin AD. HER2 Expression Beyond Breast Cancer: Therapeutic Implications for Gynecologic Malignancies. Molecular diagnosis & therapy. 2013;17(2):85-99. doi:10.1007/s40291-013-0024-9.

Estevez LG, Garcia E and Hidalgo M. (2015). "Inhibiting the PI3K signling pathway: buparlisib as a new targeted option in breast carcinoma." Clinical and Traslational Oncology, DOI 10.1007/s12094-015-1410-z.

Fan C, Oh DS, Wessels L, Weigelt B, Nuyten DS, Nobel AB, van't Veer LJ, Perou CM. Concordance among gene-expression-based predictors for breast cancer. N Engl J Med. 2006;355:560–569.

Ferguson, K. M. et al. EGF activates its receptor by removing interactions that autoinhibit ectodomain dimerization. Mol. Cell 11, 507–517 (2003).

Finkle D, Quan ZR, Asghari V, Kloss J, Ghaboosi N, Mai E, Wong WL, Hollingshead P, Schwall R, Koeppen H and Erickson S. (2004) HER2-targeted therapy reduces incidence and progression of midlife mammary tumors in female murine mammary tumor virus huHER2-transgenic mice. Clin Cancer Res; 10: 2499-2511

Franklin M.C., Carey K.D., Vajdos F.F., Leahy D.J., de Vos A.M, Sliwkowski M.X. Insights into ErbB signaling from the structure of the ErbB2-pertuzumab complex Cancer Cell, 5 (4) (2004), pp. 317–328

Garcia-Echeverria C, and Sellers WR. (2008). "Drug Discovery Approaches Targeting the PI3K/Akt Pathway in Cancer." Oncogene 27: 5511–5526.

Garrett, J. T., & Arteaga, C. L. (2011). Resistance to HER2-directed antibodies and tyrosine kinase inhibitors: Mechanisms and clinical implications. Cancer Biology & Therapy, 11(9), 793–800.

Gennari R *et al*. (2004) Pilot study of the mechanism of action of preoperative trastuzumab in patients with primary operable breast tumors overexpressing HER2. *Clin Cancer Res* **10:** 5650–565522

Gewinner C, Wang ZC, Richardson A, Teruya-Feldstein J, Etemadmoghadam D, Bowtell D, et al. Evidence that inositol polyphosphate-4-phosphatase type II is a tumor suppressor that inhibits PI3K signaling. Cancer Cell. 2009;16:115–125.

Geyer CE, Forster J, Lindquist D, Chan S, Romieu CG, Pienkowski T, Jagiello-Gruszfeld A, Crown J, Chan A, Kaufman B, Skarlos D, Campone M, Davidson N, Berger M, Oliva C, Rubin

SD, et al. Lapatinib plus capecitabine for HER2-positive advanced breast cancer. N Engl J Med. 2006;355:2733–2743

Ghosh R., Narasanna A., Wang S.E., Liu S., Chakrabarty A., Balko J.M.,. González-Angulo A.M, Mills G.B., Penuel E., Winslow J., et al. Trastuzumab has preferential activity against breast cancers driven by HER2 homodimers. Cancer Res., 71 (2011), pp. 1871–1882

Gianni L, Pienkowski T, Im YH, Roman L, Tseng LM, Liu MC, et al. Efficacy and safety of neoadjuvant pertuzumab and trastuzumab in women with locally advanced, inflammatory, or early HER2-positive breast cancer (NeoSphere): a randomised multicentre, open-label, phase 2 trial. LancetOncol. 2012;13(1):25–32.

Giordano Sharon H., Temin S, Kirshner JJ., Chandarlapaty S., Crews JR., Davidson NE., Esteva FJ., Gonzalez-Angulo AM., Krop I, Levinson J., Lin NU., Modi S, Patt, Edith A. Perez DA., Perlmutter J, Ramakrishna N, and Winer EP. Systemic Therapy for Patients With Advanced Human MEpidermal Growth Factor Receptor 2–Positive Breast Cancer: American Society of Clinical Oncology Clinical Practice Guideline. Journal of Clinical Oncology 2014 32:19, 2078-2099

Gire V, Dulić V. Senescence from G2 arrest, revisited. Cell Cycle. 2015;14(3):297-304. doi:10.1080/15384101.2014.1000134.

Goldhirsch A, Gelber RD, Piccart-Gebhart MJ, de Azambuja E, Procter M, Suter TM, Jackisch C, Cameron D, Weber HA, Heinzmann D, et al. 2 years versus 1 year of adjuvant trastuzumab for HER2-positive breast cancer (HERA): An open-label, randomised controlled trial. Lancet. 2013;382:1021–1028. doi: 10.1016/S0140-6736(13)61094-6

Goldhirsch A., et al. 2 years versus 1 year of adjuvant trastuzumab for HER2-positive breast cancer (HERA): an open-label, randomised controlled trial. Lancet, 382 (2013), pp. 1021–1028

Goldman JP, Blundell MP, Lopes L, Kinnon C, Di Santo JP and Thrasher AJ. (1998) Enhanced human cell engraftment in mice deficient in RAG2 and the common cytokine receptor gamma chain. Br J Haematol; 103: 335-342.

Guy CT, Webster MA, Schaller M, Parsons TJ, Cardiff RD and Muller WJ. (1992) Expression of the neu protooncogene in the mammary epithelium of transgenic mice induces metastatic disease. Proc Natl Acad Sci U S A; 89: 10578-10582.

Guy CT, Webster MA, Schaller M, Parsons TJ, Cardiff RD and Muller WJ. (1992) Expression of the neu protooncogene in the mammary epithelium of transgenic mice induces metastatic disease. Proc Natl Acad Sci U S A; 89: 10578-10582.

Hanker AB, Pfefferle AD, Balko JM, et al. Mutant PIK3CA accelerates HER2-driven transgenic mammary tumors and induces resistance to combinations of anti-HER2 therapies. Proceedings of the National Academy of Sciences of the United States of America. 2013;110(35):14372-14377. doi:10.1073/pnas.1303204110.

Hardt O, et al. Highly sensitive profiling of CD44+/CD24- breast cancer stem cells by combining global mRNA amplification and next generation sequencing: Evidence for a hyperactive PI3K pathway. Cancer Lett. 2012;325(2):165–174.

Harris L, Fritsche H, Mennel R, Norton L, Ravdin P, Taube S, Somerfield MR, Hayes DF, Bast RC Jr. (2007) American Society of Clinical Oncology 2007 update of recommendations for the use of tumor markers in breast cancer. J Clin Oncol 25: 5287–5312

Herter-Sprie GS, Greulich H, Wong K-K. Activating Mutations in ERBB2 and Their Impact on Diagnostics and Treatment. Frontiers in Oncology. 2013;3:86. doi:10.3389/fonc.2013.00086.

Hirasawa T, Yamashita H and Makino S. (1998) Genetic typing of the mouse and rat nude mutations by PCR and restriction enzyme analysis. Exp Anim; 47: 63-67.

Ho-Yen C, Bowen RL, Jones J. Characterization of basal-like breast cancer: an update. Diagnostic Histopathology. 2012;18:104–111.40.

http://www.myccancergene.org

Hurvitz S, Hu Y, O'Brien N, Finn RS. Current approaches and future directions in the treatment of HER2-positive breast cancer. Cancer treatment reviews. 2013;39(3):10.1016/j.ctrv.2012.04.008. doi:10.1016/j.ctrv.2012.04.008.

Hynes NE, Lane HA.. ERBB receptors and cancer: the complexity of targeted inhibitors. Nat Rev Cancer (2005) 5(5):341–54.10.1038/nrc166

Ishizawar, R. & Parsons, S. J. c-Src and cooperating partners in human cancer. Cancer Cell 6, 209–214 (2004).

Jaehne, J. et al. Expression of Her2/neu oncogene product p185 in correlation to clinicopathological and prognostic factors of gastric carcinoma. J. Cancer Res. Clin. Oncol. 118, 474–479 (1992).

Jonkers J and Derksen PW. (2007) Modeling metastatic breast cancer in mice. J Mammary Gland Biol Neoplasia; 12: 191-203.

Junttila TT., Akita RW., Parsons K., Fields C, Lewis Phillips GD, Friedman LS, Sampath D, Sliwkowski MX. Ligand-independent HER2/HER3/PI3K complex is disrupted by trastuzumab and is effectively inhibited by the PI3K inhibitor GDC-0941. Cancer Cell, 15 (2009), pp. 429–440

Kabos P, Finlay-Schultz J, Li C, Kline E, Finlayson C, Wisell J, Manuel CA, Edgerton SM, Harrell JC, Elias A and Sartorius CA. (2012). "Patient-derived luminal breast cancer xenografts retain hormone receptor heterogeneity and help define unique estrogen dependent gene signatures." Breast Cancer Research and Treatment 135 doi:10.1007/s10549-012-2164-8.

Kato S, Lippman SM, Flaherty KT, Kurzrock R. The Conundrum of Genetic "Drivers" in Benign Conditions. J Natl Cancer Inst 2016;108.

Khanna C and Hunter K. (2005) Modeling metastasis *in vivo*. Carcinogenesis; 26: 513-523

Kim, H.-P., Han, S.-W., Song, S.-H., Jeong, E.-G., Lee, M.-Y., Hwang, D., Im, S.-A., Bang, Y.-J. and Kim, T.-Y. (2013).Testican-1-mediated epithelial-mesenchymal transition signaling confers acquired resistance to lapatinib in HER2-positive gastric cancer. Oncogene 33, 3334-3341. doi:10.1038/onc.2013.285

Konecny G, Wilson C, Slamon D. Is there a role for epidermal growth factor receptor inhibitors in breast cancer prevention. J Natl Cancer Inst. 2003;95:1813–1815.

Korkaya H, et al. Regulation of mammary stem/progenitor cells by PTEN/Akt/beta-catenin signaling. PLoS Biol. 2009;7(6):e1000121.

Korkaya, H., Kim, G.I., Davis, A., Malik, F., Henry, N.L., Ithimakin, S., Quraishi, A., Tawakkol, N., D'Angelo, R.,Paulson, A. K. et al. (2012). Activation of an IL6 inflammatory loop mediates trastuzumab resistance in HER2+ breast cancer by expanding the cancer stem cell population. Mol. Cell 47, 570-584.doi:10.1016/j.molcel.2012.06.014

Kovanen PE and Leonard WJ. (2004) Cytokines and immunodeficiency diseases: critical roles of the gamma(c)-dependent cytokines interleukins 2, 4, 7, 9, 15, and 21, and their signaling pathways. Immunol Rev; 202: 67-83.

Kwong KY and Hung MC. (1998) A novel splice variant of HER2 with increased transformation activity. Mol Carcinog; 23: 62-68.

Lane HA et al. (2001) Modulation of p27/Cdk2 complex formation through 4D5-mediated inhibition of HER2 receptor signaling. Ann Oncol 12: 21–22

Larsson LG, Henriksson MA 2010. The Yin and Yang functions of the Myc oncoprotein in cancer development and as targets for therapy. Exp Cell Res 316: 1429–1437

Ledford H. (2016). “US Cancer Institute overhauls cell lines.” Nature 530:391.

Lewis GD et al. (1993) Differential responses of human tumor cell lines to anti-p185HER2 monoclonal antibodies. Cancer Immunol Immunother 37: 255–26325

Li J, Yen C, Liaw D, Podsypanina K, Bose S, Wang SI, et al. PTEN, a putative protein tyrosine phosphatase gene mutated in human brain, breast and prostate cancer. Science. 1997;275:1943–1947.

Lin NU, Guo H, Yap JT, et al. Phase II Study of Lapatinib in Combination With Trastuzumab in Patients With Human Epidermal Growth Factor Receptor 2–Positive Metastatic Breast Cancer: Clinical Outcomes and Predictive Value of Early [18F]Fluorodeoxyglucose Positron Emission Tomography Imaging (TBCRC 003). Journal of Clinical Oncology. 2015;33(24):2623-2631. doi:10.1200/JCO.2014.60.0353.

Lipton A, Ali SM, Leitzel K, Demers L, Chinchilli V, Engle L, et al. Elevated serum Her-2/neu level predicts decreased response to hormone therapy in metastatic breast cancer. J Clin Oncol 2002;20:1467–72

Liu S, Cong Y, Wang D, Sun Y, Deng L, Liu Y, Martin- Trevino R, Shang L, McDermott Sean P, Landis Melissa D, Hong S, Adams A, D’Angelo R, Ginestier C, Charafe- Jauffret E, Clouthier Shawn G, et al. Breast Cancer Stem Cells Transition between Epithelial and Mesenchymal States Reflective of their Normal Counterparts. Stem Cell Reports. 2014; 2:78-91.

Liu, E. et al. The HER2 (c-erbB-2) oncogene is frequently amplified in in situ carcinomas of the breast. Oncogene 7, 1027–1032 (1992).

Lollini PL, Cavallo F, Nanni P and Forni G. (2006) Vaccines for tumour prevention. Nat Rev Cancer; 6: 204-216.

Lollini PL, Grosso V, Ranieri D, Palladini A, Ianzano M, Dall'Ora M, Landuzzi L, Nicoletti G, Balboni T, Laranga R, De Giovanni C, Amici A, Pupa SM, Iezzi M, Nanni P. Coexpression of Delta16 isoform and full-length HER-2 in F1 hybrid transgenic mice: effects on tumor growth and malignancy. AACR 2014, San Diego, 5-9 April 2014 Abstract number 2774;

Lousberg L, Collignon J, Jerusalem G. Resistance to therapy in estrogen receptor positive and human epidermal growth factor 2 positive breast cancers: progress with latest therapeutic strategies. Therapeutic Advances in Medical Oncology. 2016;8(6):429-449.

Lv, Q., Meng, Z., Yu, Y., Jiang, F., Guan, D., Liang, C., … Zhang, G. (2016). Molecular Mechanisms and Translational Therapies for Human Epidermal Receptor 2 Positive Breast Cancer. International Journal of Molecular Sciences, 17(12), 2095.

Maira SM, Pecchi S, Huang A, Burger M, Knapp M, Sterker D, Schnell C, Guthy D, Nagel T, Wiesmann M, Brachmann S, Fritsch C, Dorsch M, Chène P, Shoemaker K, De Pover A, Menezes D, Martiny-Baron G, Fabbro D, Wilson CJ, Schlegel R, Hofmann F, García-Echeverría C, Sellers WR and Voliva CF. (2012). "Identification and characterization of buparlisib, an orally available pan-class I PI3-kinase inhibitor." Molecular Cancer Therapeutics. 11: 317-328.

Makhoul I, Klimberg VS, Korourian S, et al. Combined neoadjuvant chemotherapy with bevacizumab improves pathologic complete response in patients with hormone receptor negative operable or locally advanced breast cancer. Am J Clin Oncol. 2015;38(1):74–79.

Malaney, P., Nicosia, S. V., & Davé, V. (2014). One mouse, one patient paradigm: new avatars of personalized cancer therapy. Cancer Letters, 344(1), 1–12.

Mallini P, Lennard T, Kirby J, Meeson A. Epithelial-to-Mesenchymal transition: what is the impact on breast cancer stem cells and drug resistance. Cancer Treat Rev. 2014; 40:341–348.

Mani, S.A., Guo, W., Liao, M.J., Eaton, E.N., Ayyanan, A., Zhou, A.Y., Brooks, M., Reinhard, F., Zhang, C.C., Shipitsin, M., et al. (2008). The epithelial-mesenchymal transition generates cells with properties of stem cells. Cell 133,704–715.

Marangoni E and Poupon MF. (2014). "Patient-derivd tumor xenografts as models for breast cancer drug development." Current Opinion in Oncology 26: 556-561.

Marangoni E, Vincent-Salomon A, Auger N, Degeorges A, Assayag F, De Cremoux P, De Plater L, Guyader C, De Pinieux G, Judde JG, Rebucci M, Tran-Perennou C, Sastre-Garau X, Sigal-Zafrani B, Delattre O, Dieras V and Poupon MF. (2007). "A new model of patient tumor-derived breast cancer xenografts for preclinical assays." Clinical Cancer Research 13: 3989–3998.

Marchini C, Gabrielli F, Iezzi M, Zenobi S, Montani M, Pietrella L, Kalogris C, Rossini A, Ciravolo V, Castagnoli L, Tagliabue E, Pupa SM, Musiani P, Monaci P, Menard S and Amici A. (2011) The human splice variant Delta16HER2 induces rapid tumor onset in a reporter transgenic mouse. PLoS One; 6: e18727.

Marinas MC, Mogos G, Ciurea R, Mogos DG. EGFR, HER2/neu and Ki67 immunoexpression in serous ovarian tumors. Romanian journal of morphology and embryology = Revue roumaine de morphologie et embryologie. 2012;53(3):563–7. Epub 2012/09/20

Maroun CR, Rowlands T. 2014. The Met receptor tyrosine kinase: a key player in oncogenesis and drug resistance. Pharmacol. Ther. 142:316–38

Massarweh S., Schiff R. (2007) Unraveling the mechanisms of endocrine resistance in breast cancer: new therapeutic opportunities. Clin Cancer Res 13: 1950–1954

Matkar S, Sharma P, Gao S, et al. An Epigenetic Pathway Regulates Sensitivity of Breast Cancer Cells to HER2 Inhibition via FOXO/c-Myc Axis. Cancer cell. 2015;28(4):472-485. doi:10.1016/j.ccell.2015.09.005.

Mendelsohn, J. & Baselga, J. Status of epidermal growth factor receptor antagonists in the biology and treatment of cancer. J. Clin. Oncol. 21, 2787–2799 (2003).

Mitra D, Brumlik MJ, Okamgba SU, Zhu Y, Duplessis TT, Parvani JG, Lesko SM, Brogi E and Jones FE. (2009) An oncogenic isoform of HER2 associated with locally disseminated breast cancer and trastuzumab resistance. Mol Cancer Ther; 8: 2152-2162.

Molina MA et al. (2001) Trastuzumab (Herceptin), a humanized anti-HER2 receptor monoclonal antibody, inhibits basal and activated HER2 ectodomain cleavage in breast cancer cells. Cancer Res 61:4744–4749

Moon HG, Oh K, Lee J, Lee M, Kim JY, Yoo TK, Seo MW, Park AK, Ryu HS, Jung EJ, Kim N, Jeong S, Han W, Lee DS and Noh DY. (2015). "Prognostic and functional importance of the engrafment-associated genes in the patient-derived xenograft models of triple-negative breast cancer." Breast Cancer Research and Treatment 154: 13-22.

Morancho B, Parra-Palau JL, Ibrahim YH, Bernado MC, Peg V, Bech-Serra JJ, et al. A dominant-negative N-terminal fragment of HER2 frequently expressed in breast cancers. Oncogene 2013;32:1452-9.

Morel, A.-P., Lièvre, M., Thomas, C., Hinkal, G., Ansieau, S., and Puisieux, A.(2008). Generation of breast cancer stem cells through epithelial-mesenchymaltransition. PLoS ONE 3, e2888.

Morton JJ., Bird G, Refaeli J. and Jimeno A. Humanized Mouse Xenograft Models: Narrowing the Tumor–Microenvironment Gap. Cancer Res November 1 2016 (76) (21) 6153-6158; DOI: 10.1158/0008-5472.CAN-16-1260

Mulholland DJ, Kobayashi N, Ruscetti M, Zhi A, Tran LM, Huang J, Gleave M and Wu H. Pten loss and RAS/MAPK activation cooperate to promote EMT and metastasis initiated from prostate cancer stem/progenitor cells. Cancer Res. 2012; 72:1878-1889.

Muller WJ, Sinn E, Pattengale PK, Wallace R and Leder P. (1988) Single-step induction of mammary adenocarcinoma in transgenic mice bearing the activated c-neu oncogene. Cell; 54: 105-115.

Munzone E., Curigliano G., Rocca A., Bonizzi G., Renne G., Goldhirsch A., et al. (2006) Reverting estrogen-receptor-negative phenotype in HER-2-overexpressing advanced breast cancer patients exposed to trastuzumab plus chemotherapy. Breast Cancer Res 8: 4

Nagata Y, Lan K-H, Zhou X, Tan M, Esteva FJ, Sahin AA, Klos KS, Li P, Monia BP, Nguyen NT, Hortobagyi GN, Hung M-C and Yu D. PTEN activation contributes to tumor inhibition by trastuzumab, and loss of PTEN predicts trastuzumab resistance in patients. Cancer Cell. 2004; 6:117-127.

Nahta R and Esteva FJ (2003) HER-2-targeted therapy: lessons learned and future directions. Clin Cancer Res 9: 5078–508417

Nahta R and Esteva FJ (2006) Herceptin: mechanisms of action and resistance. Cancer Lett 232: 123–138.

Nahta R, Shabaya S, Ozbay T, Rowe DL. 2009. Personalizing HER2-targeted therapy in metastatic breast cancer beyond HER2 status: What we have learned from clinical specimens? Curr. Pharmacogenomics Personalized Med. 7:263–74

Nahta R, Yuan LX, Du Y, Esteva FJ. Lapatinib induces apoptosis in trastuzumab-resistant breast cancer cells: effects on insulin-like growth factor I signaling. Mol Cancer Ther. 2007;6(2):667–74

Nahta R, Yuan LX, Zhang B, et al. 2005. Insulin-like growth factor-I receptor/human epidermal growth of the HER-2/neu oncogene. Science 235: 177–1823

Nair R, Roden DL, Teo WS, McFarland A, Junankar S, Ye S, Nguyen A, Yang J, Nikolic I, Hui M, et al. c-Myc and Her2 cooperate to drive a stem-like phenotype with poor prognosis in breast cancer. Oncogene. 2014;33:3992–4002.

Nanni P, Nicoletti G, Palladini A, Croci S, Murgo A, Ianzano ML, Grosso V, Stivani V, Antognoli A, Lamolinara A, Landuzzi L, Di Tomaso E, Iezzi M, De Giovanni C and Lollini PL. (2012). "Multiorgan Metastasis of Human HER-2+ Breast Cancer in Rag2-/-;Il2rg-/- Mice and Treatment with PI3K Inhibitor." Plos One 7:e39626. doi:10.1371/journal.pone.0039626.

Nanni P, Palladini A, Landuzzi L, Dall'Ora M, Ianzano M, Grosso V, Ranieri D, Nicoletti G, Laranga R, De Giovanni C, Iezzi M, Lollini PL. Dynamics of HER-2 loss in mammary carcinoma of human HER-2 trangenic mice AACR 2014, San Diego, 5-9 April 2014 Abstract number 1820

Niehans GA et al. (1993) Stability of HER-2/neu expression over time and at multiple metastatic sites. J Natl Cancer Inst 85: 1230–1235

Niikura N, Liu J, Hayashi N, Mittendorf EA, Gong Y, Palla SL, et al. Loss of human epidermal growth factor receptor 2 (HER2) expression in metastatic sites of HER2-overexpressing primary breast tumors. J Clin Oncol 2012;30:593-9.

Nishimura R, Osako T, Okumura Y, Hayashi M, Toyozumi Y, Arima N. Ki-67 as a prognostic marker according to breast cancer subtype and a predictor of recurrence time in primary breast cancer. Exp Ther Med. 2010;1:747–754

Oettinger MA, Schatz DG, Gorka C and Baltimore D. (1990) RAG-1 and RAG-2, adjacent genes that synergistically activate V(D)J recombination. Science; 248: 1517-1523.

Ogiso, H. et al. Crystal structure of the complex of human epidermal growth factor and receptor extracellular domains. Cell 110, 775–787 (2002).

Olayioye, M. A., Neve, R. M., Lane, H. A. & Hynes, N. E. The ErbB signaling network: receptor heterodimerization in development and cancer. EMBO J. 19, 3159–3167 (2000).

Osborne CK, Schiff R. Mechanisms of endocrine resistance in breast cancer.Annu Rev Med 2011;62:233–47.; Shou J, Massarweh S, Osborne CK, Wakeling AE, Ali S, Weiss H, et al. Mechanisms of tamoxifen resistance: increased estrogen receptor-HER2/neu cross-talk in ER/HER2-positive breast cancer. J Natl Cancer Inst 2004;96:926–35.;

Osipo C, Patel P, Rizzo P, Clementz AG, Hao L, Golde TE, et al. ErbB-2 inhibition activates Notch-1 and sensitizes breast cancer cells to a γ-secretase inhibitor. Oncogene (2008) 27(37):5019–32.10.1038/onc. 2008.149

Oswald F, Liptay S, Adler G, Schmid RM.. NF-kB2 is a putative target gene of activated Notch-1 via RBP-Jk. Mol Cell Biol (1998) 18(4):2077–88.

Ottewell PD, Coleman RE and Holen I. (2006) From genetic abnormality to metastases: murine models of breast cancer and their use in the development of anticancer therapies. Breast Cancer Res Treat; 96: 101-113.

Owens, M. A. et al. HER2 amplification ratios by fluorescence in situ hybridization and correlation with immunohistochemistry in a cohort of 6556 breast cancer tissues. Clin. Breast Cancer 5, 63–69 (2004).

Pagliarini, R., Shao, W., & Sellers, W. R. (2015). Oncogene addiction: pathways of therapeutic response, resistance, and road maps toward a cure. EMBO Reports, 16(3), 280–296. http://doi.org/10.15252/embr.201439949

Paik S et al. (1990). Pathologic findings from the National Surgical Adjuvant Breast and Bowel Project: prognostic significance of erbB-2 protein overexpression in primary breast cancer. J ClinOncol 8: 103–11215

Palladini A, Dall'Ora M, Grosso V, Ianzano ML, Ranieri D, Balboni T, Iezzi M, De Giovanni C, Lollini P-L, Nanni P. HER2 isoforms in mammary carcinogenesis and targeted therapy susceptibility. EACR 23, Munich, 5-8 July 2014. Abstract number 662.

Park, K., Han, S., Kim, H. J., Kim, J. & Shin, E. HER2 status in pure ductal carcinoma in situ and in the intraductal and invasive components of invasive ductal carcinoma determined by fluorescence in situ hybridization and immunohistochemistry. Histopathology 8, 702–707 (2006).

Parra-Palau JL, Morancho B, Peg V, Escorihuela M, Scaltriti M, Vicario R, Zacarias-Fluck M, Pedersen K, Pandiella A, Nuciforo P, Serra V, Cortes J, Baselga J, Perou CM, Prat A, Rubio IT and Arribas J. (2014) Effect of p95HER2/611CTF on the response to trastuzumab and chemotherapy. J Natl Cancer Inst; 106

Pedersen K, Angelini PD, Laos S, Bach-Faig A, Cunningham MP, Ferrer-Ramon C, et al. A naturally occurring HER2 carboxy-terminal fragment promotes mammary tumor growth and metastasis. Mol Cell Biol 2009;29:3319-31

Pegram M, Hsu S, Lewis G, et al. 1999. Inhibitory effects of combinations of HER-2/neu antibody and chemotherapeutic agents used for treatment of human breast cancers. Oncogene 18:2241–51

Perou CM, Sorlie T, Eisen MB, van de Rijn M, Jeffrey SS, Rees CA, Pollack JR, Ross DT, Johnsen H, Akslen LA, Fluge O, Pergamenschikov A, Williams C, Zhu SX, Lonning PE, Borresen-Dale AL, Brown PO, Botstein D. Molecular portraits of human breast tumours. Nature. 2000;406:747–752.16

Petrelli F, Borgonovo K, Cabiddu M, Ghilardi M, Barni S (2011) Neoadjuvant chemotherapy and concomitant trastuzumab in breast cancer: a pooled analysis of two randomized trials. Anticancer Drugs 22(2):128–135

Pietras RJ, Pegram MD, Finn RS, et al. 1998. Remission of human breast cancer xenografts on therapy with humanized monoclonal antibody to HER-2 receptor andDNA-reactive drugs. Oncogene 17:2235–49

Prat A, Bianchini G, Thomas M et al. Research-based PAM50 subtype predictor identifies higher responses and improved survival outcomes in HER2-positive breast cancer in the NOAH study. Clin Cancer Res 2014; 20: 511–521.

Prempree T, Wongpaksa C. 2006. Mutations ofHER2 gene inHER2-positive metastatic breast cancer.J. Clin. Oncol. 24(18S):Abstr. 13118

Rabindran SK, Discafani CM, Rosfjord EC, Baxter M, Floyd MB, Golas J, Hallett WA, Johnson BD, Nilakantan R, Overbeek E, Reich MF, Shen R, Shi X, Tsou HR, Wang YF, Wissner A. Antitumor activity of HKI-272, an orally active, irreversible inhibitor of the HER-2 tyrosine kinase. Cancer Res.2004;64:3958–3965.

Rachel Schiff, Suleiman A. Massarweh, Jiang Shou, Lavina Bharwani, Syed K. Mohsin and C. Kent Osborn. Cross-Talk between Estrogen Receptor and Growth Factor Pathways as a Molecular Target for Overcoming Endocrine Resistance. Clin Cancer Res January 1 2004 (10) (1) 331s-336s;

Rakha EA, Putti TC, Abd El-Rehim DM, Paish C, Green AR, Powe DG, Lee AH, Robertson JF, Ellis IO. Morphological and immunophenotypic analysis of breast carcinomas with basal and myoepithelial differentiation. J Pathol. 2006;208:495–506.Dai, X., Li, T., Bai, Z., Yang, Y., Liu, X., Zhan, J., & Shi, B. (2015).

Rakha, E. A., Reis-Filho, J. S., Baehner, F., Dabbs, D. J., Decker, T., Eusebi, V., … Ellis, I. O. (2010). Breast cancer prognostic classification in the molecular era: the role of histological grade. Breast Cancer Research : BCR, 12(4), 207.

Rexer BN, Arteaga CL. 2012. Intrinsic and acquired resistance to HER2-targeted therapies in HER2gene-amplified breast cancer: mechanisms and clinical implications. Crit. Rev. Oncol. 17:1–16

Rimawi M. F., De Angelis C. & Schiff R. Resistance to Anti-HER2 Therapies in Breast Cancer. American Society of Clinical Oncology educational book/ASCO. American Society of Clinical Oncology. Meeting , e157–164, (2015).10.14694/EdBook_AM.2015.35.e157

Rimm D, Ballman KV, Cheng H, et al. 2012. EGFR expression measured by quantitative immunofluorescense is associated with decreased benefit from trastuzumab in the adjuvant setting in the NCCTG (Alliance) N9831 trial. Proc. Thirty-Fifth Annual CTRC-AACR San Antonio Breast Cancer Symp., Cancer Res. 72(Suppl.):Abstr. S5–4

Rita Nahta, Dihua Yu, Mien-Chie Hung, Gabriel N Hortobagyi and Francisco J Esteva. Mechanisms of Disease: understanding resistance to HER2-targeted therapy in human breast canceNature Clinical Practice Oncology (2006) 3, 269-280doi:10.1038/ncponc0509

Robinson AG, Turbin D, Thomson T et al (2006) Molecular predictive factors in patients receiving trastuzumab-based chemotherapy for metastatic disease. CLBC 7(3):254–261

Rosfjord E, Lucas J, Li G and Gerber HP. (2014). "Advances in patient-derived tumor xenografts: from target identification to predicting clinical response rates in oncology." Biochemical Pharmacology 91: 135-143.

Ross JS1, Fletcher JA, Bloom KJ, Linette GP, Stec J, Symmans WF, Pusztai L, Hortobagyi GN. Targeted therapy in breast cancer: the HER-2/neu gene and protein. Mol Cell Proteomics. 2004 Apr;3(4):379-98. Epub 2004 Feb 3.

Ruggeri BA, Camp F, Miknyoczki S. Animal models of disease: pre-clinical animal models of cancer and their applications and utility in drug discovery. Biochem Pharmacol. 2014;87(1):150–161

Saal LH, Johansson P, Holm K, Gruvberger-Saal SK, She QB, Maurer M, et al. Poor prognosis in carcinoma is associated with a gene expression signature of aberrant PTEN tumor suppressor pathway activity. Proc Natl Acad Sci USA. 2007;104:7564–7569

Saini K.S., Loi S., de Azambuja E., Metzger-Filho O., Saini M.L., Ignatiadis M., Dancey J.E., Piccart-Gebhart M.J. Targeting the PI3K/AKT/mTOR and Raf/MEK/ERK pathways in the treatment of breast cancer. Cancer Treat. Rev. 2013;39:935–946.

Salphati L, Heffron TP, Alicke B , Nishimura M, Barck K, Carano RA, Cheong J, Edgar KA, Greve J, Kharbanda S, Koeppen H, Lau S, Lee LB., Pang J, Plise EG., Pokorny J L., Hani Bou Reslan, Sarkaria JN., Wallin JJ., Zhang X, Gould SE., Olivero AG and Phillips HS. Targeting the PI3K Pathway in the Brain—Efficacy of a PI3K Inhibitor Optimized to Cross the Blood–Brain Barrier. Clin Cancer Res November 15 2012 (18) (22) 6239-6248; DOI: 10.1158/1078-0432.CCR-12-0720

Sasso M, Bianchi F, Ciravolo V, Tagliabue E, and Campiglio M, "HER2 splice variants and their relevance in breast cancer," Journal of Nucleic Acids Investigation, vol. 2, no. 1, pp. 52–59, 2011.

Savino M, Annibali D, Carucci N, Favuzzi E, Cole MD, Evan GI, Soucek L, Nasi S 2011. The action mechanism of the Myc inhibitor termed Omomyc may give clues on how to target Myc for cancer therapy. PLoS ONE 6: e22284.

Saxena M and Christofori G. (2013) Rebuilding cancer metastasis in the mouse. Mol Oncol; 7: 283-296.

Scaltriti M, Nuciforo P, Bradbury I, Sperinde J, Agbor-Tarh D, Campbell C, Chenna A, Winslow J, Serra V, Parra JL, Prudkin L, Jimenez J, Aura C, Harbeck N, Pusztai L, Ellis CE, Eidtmann H, Arribas J, Cortes J, De AE, Piccart M and Baselga J. (2014) High HER2 expression correlates with response to the combination of lapatinib and trastuzumab. Clin Cancer Res;

Scaltriti M, Rojo F, Ocana A, Anido J, Guzman M, Cortes J, et al. Expression of p95HER2, a truncated form of the HER2 receptor, and response to anti-HER2 therapies in breast cancer. J Natl Cancer Inst 2007;99:628-38.

Scheuer W, Friess T, Burtscher H, Bossenmaier B, Endl J, Hasmann M. Strongly enhanced antitumor activity of trastuzumab and pertuzumab combination treatment on HER2-positive human xenograft tumor models. Cancer Res., 69 (2009), pp. 9330–9336.

Schlessinger, J. Common and distinct elements in cellular signaling via EGF and FGF receptors. Science 306, 1506–1507 (2004).

Schroeder RL, Stevens CL, Sridhar J. (2014). "Small molecule tyrosine kinase inhibitors of ErbB2/HER2/Neu in the treatment of aggressive breast cancer". Molecules. 19:15196-15212.

Sergina, N. V., & Moasser, M. M. (2007). The HER family and cancer: emerging molecular mechanisms and therapeutic targets. Trends in Molecular Medicine, 13(12), 527–534. http://doi.org/10.1016/j.molmed.2007.10.002

Serra, V., Scaltriti, M., Prudkin, L., Eichhorn, P. J. A., Ibrahim, Y. H., Chandarlapaty, S., … Baselga, J. (2011). PI3K inhibition results in enhanced HER signaling and acquired ERK dependency in HER2-overexpressing breast cancer. Oncogene, 30(22), 2547–2557. http://doi.org/10.1038/onc.2010.626

Shinkai Y, Rathbun G, Lam KP, Oltz EM, Stewart V, Mendelsohn M, Charron J, Datta M, Young F, Stall AM and . (1992) RAG-2-deficient mice lack mature lymphocytes owing to inability to initiate V(D)J rearrangement. Cell; 68: 855-867.

Sibilia M, Kroismayr R, Lichtenberger BM, Natarajan A, Hecking M, Holcmann M.The epidermal growth factor receptor: from development to tumorigenesis.Differentiation 2007; 75: 770–787.

Siegel PM, Dankort DL, Hardy WR and Muller WJ. (1994) Novel activating mutations in the neu proto-oncogene involved in induction of mammary tumors. Mol Cell Biol; 14: 7068-7077.

Siegel, R. L., Miller, K. D. and Jemal, A. (2015), Cancer statistics, 2015. CA: A Cancer Journal for Clinicians, 65: 5–29. doi:10.3322/caac.21254

Singh, A. and Settleman, J. (2010). EMT, cancer stem cells and drug resistance: an emerging axis of evil in the war on cancer. Oncogene 29, 4741-4751. doi:10.1038/onc.2010.215

Siolas D and Hannon GJ. (2013). "Patient-derived tumor xenografts: transforming clinical samples into mouse models." Cancer Research 73: 5315-5319.

Slamon DJ et al. (1989) Studies of the HER-2/neu proto-oncogene in human breast and ovarian cancer.Science 244: 707–712

Slamon DJ, Leyland-Jones B, Shak S et al (2001) Use of chemotherapy plus a monoclonal antibody against HER2 for metastatic breast cancer that overexpresses HER2. N Engl J Med 344(11):783–792

Slamon, D. J. et al. Human breast cancer: correlation of relapse and survival with amplification of the HER-2/neu oncogene. Science 235, 177–182 (1987).

Sliwkowski M et al. (1999) Nonclinical studies addressing the mechanism of action of trastuzumab (Herceptin). Semin Oncol 26 (Suppl 12): S60–S70

Sodir NM, Swigart LB, Karnezis AN, Hanahan D, Evan GI, Soucek L 2011. Endogenous Myc maintains the tumor microenvironment. Genes Dev 25: 907–916.

Sørlie T, Tibshirani R, Parker J, Hastie T, Marron JS, Nobel A, Deng S, Johnsen H, Pesich R, Geisler S, Demeter J, Perou CM, Lønning PE, Brown PO, Børresen-Dale A, Botstein D. Repeated observation of breast tumor subtypes in independent gene expression data sets. PNAS. 2003;100:8418–8423

Soucek L, Helmer-Citterich M, Sacco A, Jucker R, Cesareni G, Nasi S. Design and properties of a Myc derivative that efficiently homodimerizes. Oncogene. 1998;17:2463–2472.

Soucek L, Jucker R, Panacchia L, Ricordy R, Tatò F, Nasi S. Omomyc, a potential Myc dominant negative, enhances Myc-induced apoptosis. Cancer Res. 2002 Jun 15; 62(12):3507-10.

Soucek L, Nasi S, Evan GI. Omomyc expression in skin prevents Myc-induced papillomatosis. Cell Death Differ. 2004 Sep; 11(9):1038-45.

Soucek L, Whitfield J, Martins CP, Finch AJ, Murphy DJ, Sodir NM, Karnezis AN, Swigart LB, Nasi S, Evan GI 2008. Modelling Myc inhibition as a cancer therapy. Nature 455: 679–683

Soucek L. et al. . Inhibition of Myc family proteins eradicates KRas-driven lung cancer in mice. Genes Dev. 27, 504–513 (2013)

Stockmeyer B *et al*. (2003) Polymorphonuclear granulocytes induce antibody-dependent apoptosis in human breast cancer cells. *J Immunol* **171:**5124–5129

Straussman R, Morikawa T, Shee K et al (2012) Tumour micro-environment elicits innate resistance to RAF inhibitors through HGF secretion. Nature 487(7408):500–504

Sun, L., Burnett, J., Gasparyan, M., Xu, F., Jiang, H., Lin, C., Myers, I., Korkaya, H., Liu, Y., Connarn, J., He, H., Zhang, N., Wicha, M., & Sun, D. (2016). Novel cancer stem cell targets during epithelial to mesenchymal transition in PTEN-deficient trastuzumab-resistant breast cancer. Oncotarget, 7(32), 51408-51422.

Swain SM, Kim S-B, Cortés J et al (2013) Pertuzumab, trastuzumab, and docetaxel for HER2-positive metastatic breast cancer (CLEOPATRA study): overall survival results from a randomised, double-blind, placebo-controlled, phase 3 study. Lancet Oncol 14(6):461–471

Swanton C, Futreal A, Eisen T. Her2-targeted therapies in non-small cell lung cancer. Clin Cancer Res 2006; 12: 4377s–83s.

Swenson RR, Rizzo CJ, Brown LK, Payne N, Di-Clemente RJ, Salazar LF, Vanable PA, Carey MP, Valois RF, Romer D, Hennessy M. Prevalence and correlates of HIV testing among sexually active African American adolescents in 4 US cities. Sex Transm Dis. 2009;36:584–591.

Systemic Therapy for Patients With Advanced Human Epidermal Growth Factor Receptor 2–Positive Breast Cancer: American Society of Clinical Oncology Clinical Practice Guideline

T.T. Junttila, R.W. Akita, K. Parsons, C. Fields, G.D. Lewis Phillips, L.S. Friedman, D. Sampath, M.X. Sliwkowski. Ligand-independent HER2/HER3/PI3K complex is disrupted by trastuzumab and is effectively inhibited by the PI3K inhibitor GDC-0941Cancer Cell, 15 (2009), pp. 429–440

The Cancer Genome Atlas Network. 2012. Comprehensive molecular portraits of human breast tumours. Nature 490:61–70

Thiery JP, Acloque H, Huang RY, Nieto MA. Epithelial mesenchymal transitions in development and disease. Cell. 2009

Thomsen M, Galvani S, Canivet C, Kamar N and Bohler T. (2008) Reconstitution of immunodeficient SCID/beige mice with human cells: applications in preclinical studies. Toxicology; 246: 18-23.

Tolani B, Gopalakrishnan R, Punj V, Matta H, Chaudhary PM. Targeting Myc in KSHV-associated primary effusion lymphoma with BET bromodomain inhibitors. Oncogene. 2014;33(22):2928-2937. doi:10.1038/onc.2013.242.

Turke AB, Song Y, Costa C, Cook R, Arteaga CL, Asara JM and Engelman JA. (2012) MEK inhibition leads to PI3K/AKT activation by relieving a negative feedback on ERBB receptors. Cancer Res; 72: 3228-3237.

Turner NH., and Di Leo A. (2013). "HER2 Discordance between Primary and Metastatic Breast Cancer: Assessing the Clinical Impact." Cancer Treatment Reviews 39: 947-957.

Turpin J, Ling C, Crosby EJ, Hartman ZC, Simond AM, Chodosh LA, et al. The ErbB2DeltaEx16 splice variant is a major oncogenic driver in breast cancer that promotes a pro-metastatic tumor microenvironment. Oncogene 2016. Epub ahead of print.

Untch M, Loibl S, Bischoff J, Eidtmann H, Kaufmann M, Blohmer JU, Hilfrich J, Strumberg D, Fasching PA, Kreienberg R, Tesch H, Hanusch C, Gerber B, Rezai M, Jackisch C, Huober J, et al. Lapatinib versus trastuzumab in combination with neoadjuvant anthracycline-taxane-based chemotherapy (GeparQuinto, GBG 44): a randomised phase 3 trial. Lancet Oncol. 2012;13:135–144.

Vermeij, J. et al. Genomic activation of the EGFR and HER2-neu genes in a significant proportion of invasive epithelial ovarian cancers. BMC Cancer 8, 3 (2008).

Vici, P., Crispo, A., Giordano, A., Lauro, L. D., Sperati, F., Terrenato, I., Pizzuti, L., Sergi, D., Mottolese, M., Botti, C., Grimaldi, M., Capasso, I., D'Aiuto, G., Bonito, M. D., Paola, F. D., Maugeri-Saccà, M., Montella, M. and Barba, M. (2015), Anthropometric, Metabolic and

Molecular Determinants of Human Epidermal Growth Factor Receptor 2 Expression in Luminal B Breast Cancer. J. Cell. Physiol., 230: 1708–1712.

Wallin JJ, et al. Active PI3K pathway causes an invasive phenotype which can be reversed or promoted by blocking the pathway at divergent nodes. PLoS ONE. 2012;7(5):e36402.

Wang SE, Xiang B, Guix M et al (2008) Transforming growth factor beta engages TACE and ErbB3 to activate phosphatidylinositol-3 kinase/Akt in ErbB2-overexpressing breast cancer and desensitizes cells to trastuzumab. Mol Cell Biol 28(18):5605–5620

Wang YC, Morrison G, Gillihan R, et al. 2011. Different mechanisms for resistance to trastuzumabversus lapatinib in HER2-positive breast cancers—role of estrogen receptor and HER2 reactivation. Breast Cancer Res. 13:R121, 1–19

Wang, S E. et al. HER2 kinase domain mutation results in constitutive phosphorylation and activation of HER2 and EGFR and resistance to EGFR tyrosine kinase inhibitors. Cancer Cell 10, 25–38 (2006).

Weinstein IB, Joe A. 2008. Oncogene addiction. Cancer Res. 68:3077–80

Wheeler DL, Iida M, Dunn EF (2009) The role of Src in solid tumors. Oncologist 14(7):667–678

Whittle JR, Lewis MT, Lindeman GJ and Visvader JE. (2015). "Patient-derived xenografts models of breast cancer and their predictive power." Breast Cancer Research 17: 17. DOI 10.1186/s13058-015-0523-1.

Williams SA, Anderson WC, Santaguida MT and Dylla SJ. (2013). "Patient-derived xenografts, the cancer stem cell paradigm, and cancer pathobiology in the 21st century." Laboratory Investigation 93: 970-982.

Wissner A, Mansour TS. The development of HKI-272 and related compounds for the treatment of cancer. Arch Pharm (Weinheim) 2008;341:465–477.

Wolff AC, Hammond ME, Hicks DG, et al. Recommendations for human epidermal growth factor receptor 2 testing in breast cancer: American Society of Clinical Oncology/College of American Pathologists clinical practice guideline update. J Clin Oncol. 2013;31(31):3997–4013.

Xia W., Bacus S., Hegde P., Husain I., Strum J., Liu L., et al. (2006) A model of acquired autoresistance to a potent ErbB2 tyrosine kinase inhibitor and a therapeutic strategy to prevent its onset in breast cancer. Proc Natl Acad Sci U S A 103: 7795–7800

Xue G, et al. (2012) Akt/PKB-mediated phosphorylation of Twist1 promotes tumor metastasis via mediating cross-talk between PI3K/Akt and TGF-beta signaling axes. Cancer Discov 2(3):248–259.

Yamaguchi N, Oyama T, Ito E, Satoh H, Azuma S, Hayashi M, et al. NOTCH3 signaling pathway plays crucial roles in the proliferation of ErbB2-negative human breast cancer cells. Cancer Res (2008) 68(6):1881–8.10.1158/0008-5472.CAN-07-1597

Yamamoto H, Higasa K, Sakaguchi M et al Novel germline mutation in the transmembrane domain of HER2 in familial lung adenocarcinomas. J Natl Cancer Inst 2014; 106: djt338.

Yan M, Parker BA, Schwab R and Kurzrock R. (2014) HER2 aberrations in cancer: implications for therapy. Cancer Treat Rev; 40: 770-780.

Yarden Y and Pines G. (2012) The ERBB network: at last, cancer therapy meets systems biology. Nat Rev Cancer; 12: 553-563.

Yarden, Y. & Sliwkowski, M. X. Untangling the ErbB signalling network. Nature Rev. Mol. Cell Biol. 2, 127–137 (2001).

Yaziji, H. et al. HER-2 testing in breast cancer using parallel tissue-based methods. J. Am. Med. Assoc. 291, 1972–1977 (2004).

Yersal, O., & Barutca, S. (2014). Biological subtypes of breast cancer: Prognostic and therapeutic implications. World Journal of Clinical Oncology, 5(3), 412–424.

Yu, H. & Jove, R. The STATs of cancer — new molecular targets come of age. Nature Rev. Cancer 4, 97–105 (2004).

Zhang X, Claerhout S, Prat A, Dobrolecki LE, Petrovic I, Lai Q, Landis MD, Wiechmann L, Schiff R, Giuliano M, Wong H, Fuqua SW, Contreras A, Gutierrex C, Huang J, Mao S, Pavlick AC, Froehlich AM, Wu MF, Tsimelzon A, Hilsenbeck SG, Chen ES, Zuloaga P, Shaw CA, Rimawi M, Perou CM, Mills GB, Chang JC and Lewis MT. (2013). "A renewable tissue resource of phenotypically stable, biologically and ethnically diverse, patient-derived human breast cancer xenograft models." Cancer Research 73: 4885–4897.

Zhou J, et al. Activation of the PTEN/mTOR/STAT3 pathway in breast cancer stem-like cells is required for viability and maintenance. Proc Natl Acad Sci USA. 2007;104(41):16158–16163.

Zuo, T. et al. FOXP3 is an X-linked breast cancer suppressor gene and an important repressor of the HER-2/ErbB2 oncogene. Cell 129, 1275–1286 (2007).